IMAGING OF THE ANAL SPHINCTER COMPLEX

CIP-DATA KONINKLIJKE BIBLIOTHEEK, DEN HAAG

Hussain, Shahid Mahmood

Imaging of the anal sphincter complex /
Shahid Mahmood Hussain ; [ill.: A.W. Zwamborn]. - [S.l.:s.n.].-Ill.
Thesis Erasmus University Rotterdam. - With ref. - With summary in Dutch.
ISBN 90-9009360-5
Subject headings: Anorectal / Radiology / Anatomy / Abnormalities

Cover designed by A.W. Zwamborn
Type-setting: A.W. Zwamborn
Photographs: T. Rijsdijk

Printed by: Ridderprint B.V., Ridderkerk.

IMAGING OF THE ANAL SPHINCTER COMPLEX

Afbeelding van het anale sfinctercomplex

PROEFSCHRIFT

ter verkrijging van de graad van doctor

aan de Erasmus Universiteit Rotterdam

op gezag van de rector magnificus

Prof. Dr. P.W.C. Akkermans M.A.

en volgens besluit van het College voor Promoties.

De openbare verdediging zal plaatsvinden op

woensdag 5 juni 1996 om 13.45 uur

door

SHAHID MAHMOOD HUSSAIN

Geboren te Guliana, Pakistan

Promotiecommissie:

Promotores:	Prof. Dr. J.S. Laméris Prof. Dr. H.E. Schütte
Overige leden:	Prof. Dr. J. Jeekel Prof. Dr. Th. H. van der Kwast Prof. Dr. A.C. Drogendijk

Opgedragen aan Ellen en Emma

CONTENTS

Chapter 1

GENERAL INTRODUCTION

1.1 Introduction

The ano-rectum, with a length of about 15 cm and located extraperitoneally, is the most distal part of the colon (Fig. 1.1) [1-2]. This relatively short segment of the colon is of paramount importance because it is responsible for the mechanism of faecal continence. In addition it is prone to many diseases such as faecal incontinence [3-17], which can result from defects of the anal sphincters, perianal fistulae [18-32], and malignant tumours [33-45]. For proper management of disease in this area, understanding of the normal anatomy [46-51] is important. The normal ano-rectal anatomy, though, has been controversial in the literature [46].

To improve the diagnostic possibilities, cross-sectional imaging of the ano-rectum with ultrasound [52] and MRI [53] can play an important role in displaying the normal anatomy and pathology of this region. Before treatment, the exact relationship of the normal anatomical structures and abnormalities must be appreciated. For understanding imaging data properly, knowledge of the previous anatomical concepts is essential. Therefore a historical review of the different concepts of the ano-rectal anatomy will be provided.

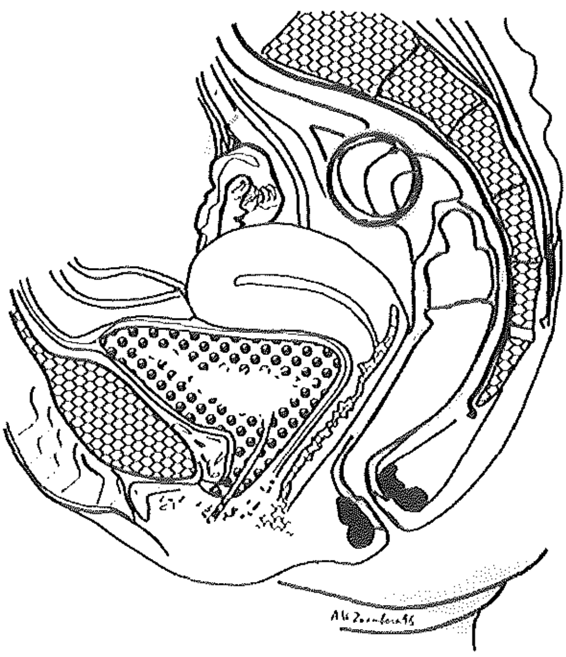

Fig. 1.1 Lateral view of the pelvis in a female showing the rectum and other organs.

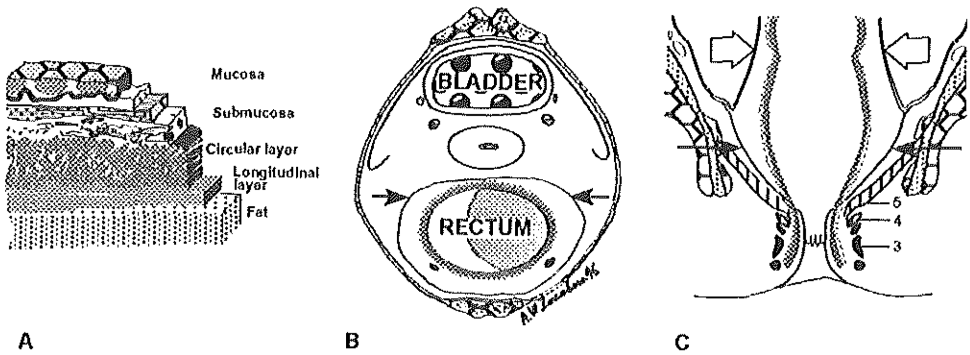

Fig. 1.2 *The anatomy of the rectum.* The layers of the rectal wall are shown (A). The circular and the longitudinal layers form the muscularis propria. Note the perirectal fascia (arrows) in the axial view of the rectum (B). The coronal view of the ano-rectum (C). The two layers of the muscularis propria extend into the anal canal. Note the position of the peritoneum (open arrows), the perirectal fascia (arrows), the levator ani muscle (5), the puborectal muscle (4), and the external anal sphincter (3).

1.2 Anorectal anatomy in a historical perspective

The anatomy of the rectum is well established [1-2]. The layers of the rectal wall consist of the mucosa, the submucosa, the circular (inner) and longitudinal (outer) layer of the muscularis propria (Fig. 1.2). The rectum is surrounded by perirectal fat and the perirectal fascia (Fig. 1.2). This anatomical concept of the rectum and its perirectal tissue is widely accepted [2].

The anatomy of the anal canal is more controversial [46]. The anal canal begins at the level of attachment of the levator ani muscle to the rectum. The inner, circular layer of the muscularis propria of the rectum extends into the anal canal and becomes the internal anal sphincter, while the longitudinal component of the muscularis propria becomes the longitudinal layer of the anal canal. Around these two muscular layers, the external anal sphincter, the puborectalis muscle, and the levator ani muscle can be found. Unclarity about the relationship among these three muscles has been the major source of controversy [46-50].

The anal sphincter anatomy has puzzled gross anatomists, human physiologists, surgeons and other clinicians for decades. Since the days of Galen (2nd century AD), there have been many, often contradictory and confusing, views on the anatomy of the external anal sphincter and its relation to the puborectalis muscle [48-50]. Based on anatomic and histologic studies, and strengthened by surgical experience, the external anal sphincter was described to consist of one [49], two [48] or three [47] parts. Vesalius (1543) was the first to illustrate a one-part external sphincter (Fig. 1.3) [46]. Milligan and Morgan [47] (1934) have perhaps been the most influential authors with their description of a trilaminar configuration of the external anal sphincter. In this view, the external sphincter consists of subcutaneous, superficial and profundus part (Fig. 1.3). However, according to them, this

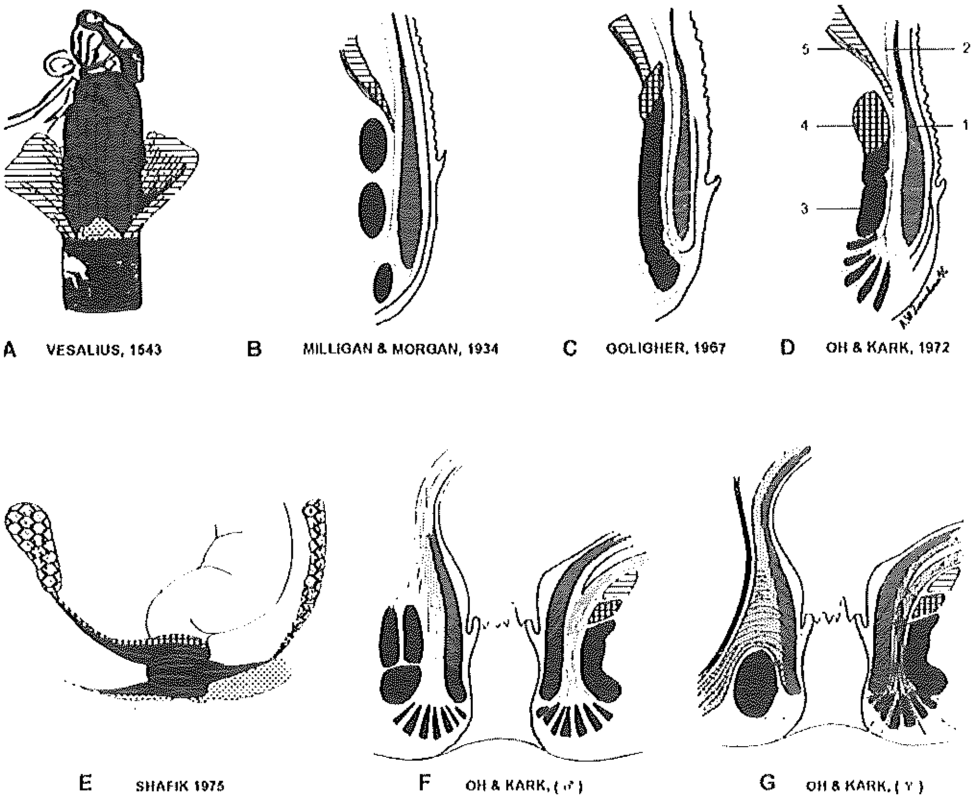

Fig. 1.3 *The anatomy of the anal canal.* Note the simple concept of Vesalius (A). Compare the interrelationship of the external sphincter (3), the puborectal muscle (4) and the levator ani muscle (5) in Milligan and Morgan (B), Goligher (C), and Oh and Kark's (D) concepts. Shafik's triple-loop view (E) seems to be inspired by Milligan and Morgan (B). According to Oh and Kark, the anterior part of the external sphincter is different in men (F) and women (G). Internal anal sphincter (1). Longitudinal layer (2).

configuration was not a constant finding. Contrary to Milligan and Morgan, Goligher et al[49] (1967) described the external sphincter as a one continuous muscle (Fig. 1.3).
The lower part or the subcutaneous portion, traversed by a fan-shaped expansion of the longitudinal muscle, did though, differ from the rest of the external sphincter. At its upper end the external sphincter was fused with the puborectalis part of the levator ani[5].
Oh and Kark[48] (1972) stressed the distinct differences in the arrangement in the anterior, lateral and posterior aspect of the external sphincter. They found either a bilaminar or a trilaminar arrangement and felt that it was more accurate to describe the external sphincter as being composed of a deep compartment (deep sphincter and puborectalis) and a superficial compartment (subcutaneous and superficial sphincter) (Fig. 1.3). Later, Shafik[50] (1975) proposed a new triple-loop concept of the external anal sphincter (Fig.

1.3). The external sphincter was arranged into three U-shaped loops. The top loop comprised the deep portion of the external sphincter as well as puborectalis, the intermediate loop the midportion of the external sphincter, and the base loop the lower portion of the external sphincter (Fig. 1.3). Ayoub [51] (1979) observed a large variation between the external sphincter of different anatomic specimens. No two specimens presented exactly the same arrangement of fibres. The external anal sphincter demonstrated no separate parts. Oh and Kark [48] are the only authors who have stressed the sex-dependent differences in the anatomy of the anal sphincters (Fig. 1.3).

In spite, or perhaps because, of these findings, there is no consensus on the anatomy of the anal sphincter complex [46]. Recently, in a well-known surgical textbook [1] (1992), all illustrations of the anal canal were based on the trilaminar concept of Milligan and Morgan. Almost all of the outlined concepts of the sphincter anatomy are based on the dissection studies, often supplemented with the surgical findings. The mechanism of faecal continence is still obscure [17,46]. Unfamiliarity with the exact anatomy, accompanied by the many controversies may be responsible for this obscurity.

It remains to be seen which, if any, of the previous anatomical views will be able to explain the imaging findings of the sphincters in vivo.

1.3 Importance of imaging the anorectal diseases

Faecal incontinence is a common problem in the elderly, although, the incidence is unknown [1]. The prevalence in the community has been estimated as 4-10 per 1000 men and 2-13 per 1000 in women; the prevalence increases with age [1]. Most common causes of faecal incontinence are obstetric injury and previous surgical procedures, such as lateral internal sphincterotomy, fistula surgery, hemorrhoidectomy, manual dilatation of the anus and sphincter saving procedures. Less common causes, apart from aging, are congenital abnormalities, rectal prolapse, trauma, irradiation, neurogenic disease (for instance diabetic neuropathy), and primary disease such as ulcerative colitis [1]. Childbirth is considered the most common cause of incontinence in women [5-6]. Previous reports [8-9] conclude that incontinence results from denervation of the anal sphincters, and not from direct muscle damage. The introduction of anal endosonography [11-13] demonstrated structural damage to the sphincters in patients with faecal incontinence. This is an important finding, particularly in patients who may be treated surgically. The operative procedure in patients with denervation is postanal sphincter repair while in patients with sphincter defects the direct sphincter repair is performed [1]. Imaging of the anal sphincter complex therefore is essential to identify patients with sphincter defects in patients with faecal incontinence.

Fistula-in-ano is an abnormal communication between the anal canal and the perianal skin. The perianal abscess is the acute manifestation and fistula is the chronic condition of the same disease [1]. Anal fistulae have a prevalence of about 10 per 100 000 in the European population [1]. Numerous conditions can cause fistulae. These are classified as specific or nonspecific. Specific ones include Crohn's disease, ulcerative colitis, tuberculosis, presence of a foreign body, trauma, pelvic inflammation and radiation. In addition, recto-vaginal fistulae often result as a complication of obstetric injury or surgery. The majority of the fistulae, though, are cryptoglandular in origin, i.e. occurrence of perianal fistula without the presence of an underlying disease [1]. According to this concept the fistulae result from infection of the anal glands and transmural spread of infection. Parks has divided the cryptoglandular fistulae into intersphincteric, transsphincteric, suprasphincteric and extrasphincteric fistulae [19]. Park's classification in fact describes the relationship of the fistula to the anatomical structures of the anorectum. Importance of imaging in patients with perianal fistulae lies in displaying this relationship in all its complexity. Incorrect classification of a perianal fistula could either result in recurrence or lead to unnecessary faecal incontinence.

Colorectal cancer ranks second to lung cancer in males and second to breast cancer in females [53]. Approximately one half of these cancers are located in the recto-sigmoid. Most rectal carcinomas start as benign adenomas that undergo malignant transformation into adenocarcinoma [1]. Primary tumours of the anal canal are rare [1]. The anal canal is lined with different kinds of epithelium. The anorectal junction is a transitional area with columnar, cuboidal, transitional or squamous epithelium, which gives rise to a variety of neoplasms.

For staging of the ano-rectal tumours TNM-classification [39] can be used. For rectal tumours also Dukes' classification [33] is available. For the surgical management, the staging is essential. To decide whether a sphincter saving procedure or an abdominoperineal resection should be performed, the relationship of the tumour to the anal sphincter complex is, in our opinion, important.

1.4 Recent developments in imaging techniques

Imaging of anorectal diseases has improved drastically during the last decade. For years conventional contrast studies have been used to examine bowel diseases. With this method only the lumen of the bowel is seen and the deep extension of the disease remains obscure. For functional examination of the ano-rectum, however, a dynamic contrast study such as proctography is an excellent method. Computed Tomography (CT) has been of paramount importance to evaluate the extension of bowel diseases. CT, though, cannot differentiate between the different layers of bowel wall [2], which is necessary for the staging a malignant tumour. Transrectal ultrasound (TRUS), which was originally applied in the assessment of the abnormalities of the prostate, is currently being used for rectal tumour staging [34,44]. With a few technical modifications, TRUS was converted into endoanal sonography [52], which can be used for the identification of patients with faecal incontinence due to anal sphincter defects and for the classification of anal fistulae.

From our experience, a number of findings with endoanal sonography were remarkable. The internal anal sphincter is demonstrated as a hypoechoic concentric structure. Imaging of the remaining components of the anal sphincter complex appeared to be unsatisfactory. For instance, the external anal sphincter has a variable echogenicity, the perianal anatomical spaces are not well visualized and sonography is mainly restricted to the axial plane. Moreover endoanal sonography is operator-dependent. These limitations cause diagnostic flaws.

To overcome the limitations of the endoanal sonography, Magnetic Resonance Imaging (MRI) was used to examine the abnormalities of the anal sphincter complex. MRI surface coils resulted, initially, in poor imaging of anal sphincters because of the low signal-to-noise ratio and a low spatial resolution. A recently developed endoanal MRI coil was applied to improve the imaging of the anal sphincter complex [54-55]. This resulted in high resolution images of the anal sphincters. Particularly, due to its multiplanar capacity and high inherent soft tissue contrast, the initial results indicated that endoanal MRI may be superior to endoanal sonography.

1.5 Aims of the study

The controversies existing in the surgical and anatomic literature can, in our experience, cause diagnostic problems. For instance, for interpretation of the endosonographic images, different anatomic concepts have been used by different workers [6,7,11,12] to explain the normal structures and abnormalities. Currently, there is no description of the normal MR imaging anatomy of the anal sphincter complex, which could be used as a reference to understand pathology.

Ideally, the questions to be answered by the evaluation in the current study are:
- Can the normal anatomy of the anal sphincter be described with the recently developed endoanal coil?
- Is one of the imaging techniques better than the other?
- Is it possible to explain the controversies about the anal sphincter anatomy in the surgico-anatomical and sonographic literature?
- Do the new imaging findings correlate to the cross-sectional anatomy and histology?
- Can the new anatomical insights be applied in patient population to improve the imaging and interpretation of diseases related to the anal sphincter complex?

1.6 Outline of the study

After the introductory remarks in chapter 1, the imaging techniques are described in chapter 2.

Normal anatomy has been described in chapters 3-6:
- Chapter 3 describes the normal anal sphincter complex with high-resolution endoanal MRI.
- Chapter 4 compares the anal sphincters with endoanal sonography and endoanal MRI.
- Chapter 5 describes the differences and the similarities of female and male

anal sphincters and related structures.

- Chapter 6 correlates endoanal MRI findings of the anal sphincters to the cross-sectional cadaveric anatomy and histology.

Pathology has been described in chapters 7-9:

- Chapter 7 compares endoanal sonography to endoanal MRI in patients with perianal fistulae.
- Chapter 8 compares endoanal sonography to endoanal MRI in patients with faecal incontinence.
- Chapter 9 evaluates tumour invasion of the anal sphincter complex in patients with anorectal tumours.

The results are discussed and conclusions, concerning the concept of the normal anal sphincter anatomy and the imaging modality of choice in each of the three groups of patients with fistulae, incontinence and tumours, are drawn in chapter 10.

1.7 REFERENCES

1. Gordon PH, Nivatvongs S. Principles and practice of surgery for the colon, rectum, and anus. St. Louis: Quality Medical Publishing Inc., 1992

2. Grabbe E, Lierse W, Winler R. The perirectal fascia: morphology and use in staging of rectal carcinoma. Radiology 1983;149:241-246

3. Khubchandani IT, Reed JR. Sequelae of internal sphincterotomy for chronic fissure in ano. Br J Surg 1989;76:431-434

4. Setti Carraro P, Kamm MA, Nicholls RJ. Long term results of post anal repair for neurogenic faecal incontinence. Br J Surg 1994;81:140-144

5. Snooks SJ, Swash M, Henry MM, Setchell M. Risk factors in childbirth causing damage to the pelvic floor inervation. Int J Colorect Dis 1986;1:20-24

6. Sultan AH, Kamm MA, Hudson CN, Bartram CI. Anal sphincter disruption during vaginal delivery. New Eng J Med 1993;329:1905-1911

7. Christiansen J, Pedersen IK. Traumatic anal incontinence. Results of surgical repair. Dis Colon Rectum 1987;30:189-191

8. Womack NR, Morrison JFB, Williams NS. The role of pelvic floor denervation in the aetiology of idiopathic faecal incontinence. Br J Surg 1986;73:404-407

9. Kiff ES, Swash M. Slowed conduction in the pudendal nerves in idiopathic (neurogenic) faecal incontinence. Br J Surg 1984;71:614-616

10. Cuesta MA, Meijer S, Derksen EJ, Boutkan, Meuwissen SGM. Anal sphincter imaging in fecal incontinence using endosonography. Dis Colon Rectum 1992;35:59-63

11. Law PJ, Kamm MA, Bartram CI. Anal endosonography in the investigation of faecal incontinence. Br J Surg 1991;78:312-314

12. Nielsen MB, Hauge C, Pedersen JF, Christiansen J. Endosonographic evaluation of patients with anal incontinence: findings and influence on surgical management. AJR 1993;160: 771-775

13. Sultan AH, Kamm MA, Talbot IC, Nicholls RJ, Bartram CI. Anal endosonography for identifying external defects confirmed histologically. Br J Surg 1994;81:463-465

14. Browning GGP, Motson RW. Anal sphincter injury. Management and results of Parks sphincter repair. Ann Surg 1984;199:351-357

15. Keighley MRR, Fielding JWL. Management of faecal incontinence and results of surgical treatment. Br J Surg 1983;70:463-468

16. Wexner SD, Marchetti F, Jagelman DG. The role of sphincteroplasty for fecal incontinence reevaluated: a propective physiologic and functional review. Dis Colon Rectum 1991;34: 22-30

17. Parks AG. Anorectal incontinence. Proc R Soc Med 1975;68:681-690

18. Sainio P. Fistula-in-ano in defined population. Incidence and epidemiological aspects. Acta Chir Gynaecol 1984;73:219-224

19. Parks AG, Gordon PH, Hardcastle JD. A classification of fistula-in-ano. Br J Surg 1976;63:1-12

20. Weisman RI, Orsay CP, Pearl RK, Abcarian H. The role of fistulography in fistula-in-ano. Dis Colon Rectum 1991;34:181-184

21. Kuijpers HC, Schulpen T. Fistulography for fistula-in-ano. Dis Colon Rectum 1985;28: 103-104

22. Guillaumin E, Jeffrey RB Jr, Shea WJ, Asling CW, Goldberg HI. Perirectal inflammatory disease: CT findings. Radiology 1986;161:153-157

23. Lunniss PJ, Armstrong P, Barker PG, Reznek RH, Phillips RK. Magnetic resonance imaging of anal fistulae. Lancet 1992;340:394-396

24. Myhr GE, Myrvold HE, Nilsen G, Thoresen JE, Rinck PA. Perianal fistulae: use of MR imaging for diagnosis. Radiology 1994;191:545-549

25. Barker PG, Lunniss PJ, Armstrong P, Reznek RH, Cottam K, Phillips RK. Magnetic resonance imaging of fistula-in-ano: technique, interpretation and accuracy. Clin Radiol 1994;49:7-13

26. Law PJ, Talbot RW, Bartram CI, Northover JMA. Anal endosonography in the evaluation of perianal sepsis and fistula in ano. Br J Surg 1989;76:752-755

27. Tio TL, Mulder CJJ, Wijers OB, Sars PRA, Tytgat GNJ. Endosonography of peri-anal and peri-colorectal fistula and/or abscess in Crohn's disease. Gastroint Endoscopy 1990;36: 331-336

28. Choen S, Burnett S, Bartram CI, Nicholls RJ. Comparison between anal endosonography and digital examination in the evaluation of anal fistulae. Br J Surg 1991;78:445-447

29. Altman DG. Practical statistics for medical research. London: Chapman & Hall, 1991.

30. Lilius HG. Investigation of human foetal anal ducts and intermuscular glands and a clinical study of 150 patients. Acta Chir Scand 1968;S383

31. Choen S, Phillips RKS. Insights gained from the management of problematical anal fistulae at St. Mark's Hospital, 1984-88. Br J Surg 1991;78:539-541

32. Held D, Khubchandani I, Sheets J, Stasik J, Rosen L, Riether R. Management of anorectal horseshoe abscess and fistula. Dis Colon Rectum 1986;29:793-797

33. Dukes CE, Bussy HJR. The spread of rectal cancer and its effect on prognosis. Br J Cancer 1958;12:309-320

34. Tio TL, Coene PPLO, Van Delden OM, Tytgat GNJ. Colorectal carcinoma: preoperative TNM classification with endosonography. Radiology 1991; 179:165-170

35. Nivatvongs S.: in Gordon PH, Nivatvongs S. Principles and practice of surgery for colon, rectum, and anus. St. Louis, Missouri: Quality Medical Publishing Inc.,1992

36. Mirowitz SA, Brown JJ, Heiken JP. Evaluation of the prostate and prostate carcinoma with gadolinium-enhanced endorectal coil imaging. Radiology 1993;186:153-157

37. Imai Y, Kressel HY, Saul SH, Chan PW, Schnall MD, Lenkinski RE, Listerud JM, Daly JM. Colorectal tumors: an in vitro study of high-resolution MR imaging. Radiology 1990;177:695-701

38. Schnall MD, Furth EE, Rosato E, Kressel HY. Rectal tumor stage: correlation of endorectal MR imaging and pathologic findings. Radiology 1994;190:709-714

39. Spiessl B, Beahrs OH, Hermanek P, Hutter RVP, Scheibe O, Sobin LH, Wagner G. UICC TNM atlas, 3rd edition. Heidelberg: Springer-Verlag, 1992

40. Williams NS. The rationale for preservation of the anal sphincter in patients with low rectal cancer. Br J Surg 1984;71:575-581

41. Goligher JC, Hughes ESR. Sensibility of the rectum and colon: its role in the mechanism of anal continence. Lancet 1951;i:543-548

42. Scharli AF, Kieswater WB. Defaecation and continence: some new concepts. Dis Col Rectum 1970;13:81-107

43. Kirkegaard P, Hjartrup A, Sanders S. Bladder dysfunction after low anterior resection for mid rectal carcinoma. Am J Surg 1981;141:266-268

44. Beynon J, Mortensen NJM, Rigby HS. Rectal endosonography, a new technique for the preoperative staging of rectal carcinoma. Eur J Surg Oncol 1988;14:297-309

45. Hulsmans FJH, Tio TL, Fockens P, Bosma A, Tytgat GNJ. Assessment of tumor infiltration depth in rectal cancer with transrectal sonography: caution is necessary. Radiology 1994;190:715-720

46. Dalley II AF. The riddle of the sphincters. The morphophysiology of the anorectal mechanism reviewed. Am Surg 1987;53:298-306

47. Milligan ETC, Morgan CN. Surgical anatomy of the anal canal. The Lancet 1934;2: 150-156,1213-1217

48. Goligher JC, Leacock AG, Brossy JJ. The surgical anatomy of the anal canal. Br J Surg 1955;43:51-61

49. Oh C, Kark AE. Anatomy of the external anal sphincter. Br J Surg 1972;59:717-723

50. Shafik A. A new concept of the anatomy of the anal sphincter mechanism and the physiology of defecation. The external anal sphincter: a triple-loop system. Invest Urol 1975;12:412-419

51. Ayoub SF. Anatomy of the external anal sphincter in man. Acta Anat 1979;105:25-36

52. Bartram CI, Burnett SJD. Atlas of anal endosonography. Oxford: Butterworth-Heinemann Ltd., 1991

53. Gore RM, Levine MS, Laufer I. Textbook of gastrointestinal radiology. Philadelphia: WB Saunders Co., 1995

54. Hussain SM, Stoker J, Kuiper JW, Schouten WR, den Hollander JC, Laméris JS. MR imaging of anal sphincter complex with an endoanal coil: normal anatomy and pathology. Radiology 1994;193(P):445

55. Stoker J, Hussain SM, Van Kempen D, Elevelt AJ, Laméris JS. Endoanal coil in MR imaging of anal fistulas. AJR 1996;166:360-362

Chapter 2

IMAGING TECHNIQUES

2.1 Introduction

The relative inaccessibility of the pelvic region requires special modifications of the existing and the introduction of new imaging modalities in order to study the anatomy and pathology of this region. To do so, ultrasound (US)[1-6] and magnetic resonance imaging (MRI)[6-13], which are excellent for imaging the soft tissues in other areas, needed some modification for the pelvic region. For this purpose, the sonographic intraluminal probes and endorectal MRI coils have been introduced[1-11].

To understand the specialized applications of US and MRI in the anorectum, knowledge of the basic principles of these techniques is required. These principles will be explained in short. More interested readers are referred for sonography to "Cosgrove et al: Abdominal and general ultrasound"[14] and for MRI to "Stark et al: Magnetic resonance imaging"[12].

2.2 Sonography

To generate ultrasound images, the sound waves with frequencies of 2.5 - 15 MHz (MegaHertz), corresponding to wavelengths of 0.6 - 0.01 mm, are used. As a comparison, the frequencies of the audible sound lie between 16 - 20 000 Hz. The ultrasound waves are produced by the piezoelectric crystal(s) contained within the transducers. The transducer is also used as a receiver of the signals coming back from the tissues.

The ultrasound waves travelling through the living tissues, with a speed of about 1540 m/s, can undergo either reflection, attenuation or almost total transmition. The signals received back by the transducer are converted into grey scale, real time images.

The hypoechoic or echopoor structures appear black, relative to another structure, on the image. The hyperechoic or echogenic structures appear relatively white.

2.2.1 Transrectal and endoanal sonography

In the current study, for sonography, a Brüel & Kjaer (Naerum, Denmark) scanner was used with a rotating probe providing a 360° image. A 5-7 MHz transducer with minimum beam width of 1.1 mm and a focal length of about 3 cm, was used.

For transrectal ultrasound (TRUS), a water-filled balloon, which covered the rotating ultrasound probe, was used for the imaging of rectal tumours. The probe was slowly retracted to allow the visualization of any alterations of the rectal wall and perirectal structures.

For endoanal sonography the balloon was replaced by a hard, sonolucent plastic cone, with a diameter of 17 mm, which covered the transducer. This cone was filled with degassed water for acoustic coupling.

Axial images were obtained through the anorectum during the retraction of the probe. The transrectal and the endoanal probes were retracted with a constant speed during examination and the images were taken at every half centimetre.

2.3 Magnetic Resonance Imaging (MRI)

To generate MR images, mainly the spinning hydrogen nuclei are used. To obtain an image an object containing protons, e.g. human body, is placed within a strong magnetic field, B_0. In clinical practice, the strength of this main magnetic field, B_0, can range from 0.3-2.0 Tesla (T). Typically, for imaging purposes, the MR scanners with a strength of 0.5T, 1.0T or 1.5T are used.

After placing the patient in the MR scanner, the protons within the body tend to align in the direction of the main magnetic field and establish a net magnetization, M_0. This is also called the "longitudinal magnetization". M_0 can not be measured directly, therefore a short RF (radiofrequency) pulse is applied to convert the "longitudinal magnetization" into the "transverse magnetization" which is perpendicular to the main magnetic field, B_0. Immediately after this pulse, with the nuclei spinning in phase, the transverse magnetization precesses about the main magnetic field with a frequency which is proportional to the strength of this field. According to Faraday's law, a changing magnetic field will produce an electric current in a loop of wire surrounding it. Since the transverse magnetization is precessing, it can generate a signal, which can be measured by an antenna (the receive coil).

When the RF pulse is turned off, the protons undergo two important events. First, the spins try to realign with the main external field which results in a gradual reappearance of the longitudinal magnetization, M_0. This process is known as T1 relaxation. T1 relaxation time is defined as the time in which 63% of the net longitudinal magnetization has recovered. The second event results in a decrease in the net transverse magnetization. Due to small fluctuations in the local magnetic field, each spin will precess at a slightly different frequency and will gradually become out of phase (dephasing). This process is called T2 relaxation. T2 relaxation time is defined as the time in which 63% of the net transverse magnetization has decayed. The term relaxation means that, after having been excited by the RF pulse, the protons return to the equilibrium position.

The MR signal that can be measured after a 90 degree pulse is called Free Induction Decay (FID). FID is a signal with an amplitude which changes in time and can be complex. FID can be analysed into sets of single-frequency components by using Fourier transformation.

The measurement of MR signal, with its application in spectroscopy, has been possible since the discovery of the MR phenomenon by Purcell and Bloch in 1946. The MR imaging became into being when Lauterbur described the possibility of spatially encoding the MR signals in 1970.

2.3.1 Spin-echo sequence

In a spin-echo sequence, a 90 degree RF pulse is followed by a 180 degree pulse. The longitudinal magnetization, after been put into the transverse plane by the 90 degree pulse, decays very fast due to the dephasing of the spinning protons. The 180 degree pulse promotes re-phasing of the nuclei and regenerates the signal as an echo. The interval between the 90 degree pulse and the peak of the first echo is called the echo time (TE). The interval between two 90 degree pulses is called the repetition time (TR).

Each set of 90 and 180 degree pulses allows one measurement of the frequency and phase of a group of spins at a certain place in space. To acquire one MR slice, a number of phase-encoding steps, which depends on the matrix, has to be taken. For instance in an image matrix of 256x128, respectively 256 frequency-encoding and 128 phase-encoding steps are necessary to determine spatial encoding of the signals.

The contrast in spin-echo images depends on T1 and T2 weighting, which can be determined by choosing certain values of TE and TR. T1 weighted spin-echo images have a relatively short TR and a short TE. Such a value of TE and TR allow maximal differences among the T1 relaxation times of the tissues involved and minimizes the influence of T2 relaxation on image contrast. T2 weighted spin-echo images have a long TR and a long TE. Such values of TR and TE practically rule out the influence of T1 relaxation and maximize the differences among T2 relaxation times of the tissues.

The signal intensities with T1 and T2 weighting in a few substances and tissues have been presented in Table 2.1.

Table 2.1 Signal intensities with T1 and T2 weighting in a spin echo sequence. (interm. = intermediate)

Substance or tissue	T1w	T2w
Water	dark	bright
Fat	bright	dark
Skeletal muskle	dark	dark
Smooth muscle	interm	interm
Connective tissue	interm	bright
Scar tissue	dark	dark

2.3.2 Turbo spin-echo imaging

This sequence is a modification of the conventional spin-echo sequence. With a turbo spin-echo (TSE) sequence, mainly T2 weighted images can be acquired in a relatively short period of time. The imaging time can be reduced by acquiring multiple phase-encoding steps during each TR. The number of steps that are simultaneously acquired is called the "turbo factor" or the "echo train". If all other parameters are held constant, a turbo factor of ten will reduce the imaging time by a factor of ten.

2.3.3 Gradient echo imaging

This technique reduces the imaging time by eliminating the 180 degree pulse required in spin-echo imaging. The re-phasing of the spins after the 90 degree pulse is accomplished by changing the magnetic field in a certain direction (gradient) for a short period of time. Very short TE (2-4 msec) and TR (8-10 msec) are possible, which substantially reduces the imaging time.

The contrast in a gradient echo image is determined by three parameters: TE, TR and the flip angle. In contrast to spin-echo sequences, in gradient echo images, smaller flip angles than 90 degree are possible. Contrast-enhanced fast field echo (CEFFE) is the name of the gradient echo sequence used in our Hospital (Philips Medical Systems). In this sequence a flip angle of 60 degree is used.

2.3.4 Transrectal and endoanal MRI

In the current study, MR imaging was performed at 0.5T (Gyroscan T5-II, Philips Medical Systems, Best, The Netherlands). To reduce the bowel motion, one ml of butylscopolaminebromide (Buscopan 20 mg/ml, Boehringer Ingelheim KG, Ingelheim, Germany) was injected intramuscularly before scanning.

For performing surveys and for imaging a large area of the pelvis, a 25x100 cm body wrap around surface coil was used. A multi-slice survey was obtained for planning the scans. Incidentally, imaging of a large area of the pelvis was necessary when a lesion, for instance a pelvic abscess or a tumour, extended outside the range of an intraluminal coil. For staging a rectal tumour, a body wrap around coil, in combination with an intraluminal coil, was routinely used.

A recently developed endoanal coil (Philips Medical Systems, Best, The Netherlands) was used. This coil consists of a fixed tuned, rectangular, 60mm long rigid receive coil with a width of 16mm; this was contained within an 80mm long cylindrical coil holder with a diameter of 19mm. Before introduction, a condom was placed over the coil and ultrasound gel was used as a lubricant. The coil was introduced while the patient was lying in the right lateral position. After introduction, the patient carefully turned on the back and the position of the coil was rechecked.

A multi-slice survey was obtained by using a 25x100 cm body wrap around coil placed around the pelvis. The coronal slices of the survey were angulated parallel to the long axis of the anal canal. After confirming the optimal position of the endoanal coil, an axial T2-weighted 3D gradient-echo sequence [T2w contrast enhanced fast field echo (CE-FFE), acquisition time 6.5 minutes, imaging matrix 205x256, number of signal averages (NSA) 2, repetition time (TR) 30 ms, echo time (TE) 13 ms, flip angle 60°, field of view (FOV) 140 mm, slice thickness 2 mm], was placed perpendicular to the long axis of the endoanal coil. Thirty-two contiguous slices were obtained. For the sagittal and the coronal scans, a T2-weighted turbo spin-echo was performed [turbo spin-echo (TSE), acquisition time 5.0 minutes, imaging matrix 186x256, NSA 8, TR 2800, TE 120, turbo factor 10, FOV 120 mm, slice thickness 4.0 mm with an interslice gap of 0.4 mm]. The coronal slices were parallel to the long axis of the endoanal coil.

2.4 REFERENCES

1. Bartram CI, Burnett SJD. Atlas of anal endosonography. Oxford: Butterworth-Heinemann Ltd., 1991

2. Law PJ, Kamm MA, Bartram CI. Anal endosonography in the investigation of faecal incontinence. Br J Surg 1991;78:312-314

3. Nielsen MB, Hauge C, Pedersen JF, Christiansen J. Endosonographic evaluation of patients with anal incontinence: findings and influence on surgical management. AJR 1993;160:771-775

4. Sultan AH, Kamm MA, Talbot IC, Nicholls RJ, Bartram CI. Anal endosonography for identifying external defects confirmed histologically. Br J Surg 1994;81:463-465.

5. Beynon J, Mortensen NJM, Rigby HS. Rectal endosonography, a new technique for the preoperative staging of rectal carcinoma. Eur J Surg Oncol 1988;14:297-309

6. Hulsmans FJH, Tio TL, Fockens P, Bosma A, Tytgat GNJ. Assessment of tumor infiltration depth in rectal cancer with transrectal sonography: caution is necessary. Radiology 1994;190:715-720

7. Mirowitz SA, Brown JJ, Heiken JP. Evaluation of the prostate and prostate carcinoma with gadolinium-enhanced endorectal coil imaging. Radiology 1993;186:153-157

8. Imai Y, Kressel HY, Saul SH, Chan PW, Schnall MD, Lenkinski RE, Listerud JM, Daly JM. Colorectal tumors: an in vitro study of high-resolution MR imaging. Radiology 1990;177:695-701

9. Schnall MD, Furth EE, Rosato E, Kressel HY. Rectal tumor stage: correlation of endorectal MR imaging and pathologic findings. Radiology 1994;190:709-714

10. Hussain SM, Stoker J, Kuiper JW, Schouten WR, den Hollander JC, Laméris JS. MR imaging of anal sphincter complex with an endoanal coil: normal anatomy and pathology. Radiology 1994;193(P):445

11. Stoker J, Hussain SM, Van Kempen D, Elevelt AJ, Laméris JS. Endoanal coil in MR imaging of anal fistulas. AJR 1996;166:360-362

12. Stark DD, Bradley WG Jr. Magnetic resonance imaging. St. Louis: The C.V. Mosby Company, 1988

13. Cardoza JD, Herfkens RJ. MRI survival guide. New York: Raven Press, 1994

14. Cosgrove D, Meire H, Dewbury K. Abdominal and general ultrasound. Edinburgh: Churchill Livingstone, 1993

Chapter 3

ANAL SPHINCTER COMPLEX: ENDOANAL MR IMAGING OF NORMAL ANATOMY

3.1 INTRODUCTION

Currently endoanal sonography is the only imaging modality to examine the anatomy of the anal sphincter complex [1]. From our experience of more than two years with endoanal sonography, a number of findings are obvious. The internal anal sphincter is the only structure that is consistently visible as a hypoechoic concentric ring; other structures are either variable in appearance or they are not visible at all. The external anal sphincter for instance, is said to be of high echogenicity [1]. In our experience, however, it has a variable echogenicity. Because of the similar echogenicity, the external sphincter is often indistinct from the surrounding ischioanal space. The perianal anatomical spaces, such as intersphincteric and supralevator space, are not well recognizable. Moreover endoanal sonography is operator-dependent and mainly restricted to the axial plane which prevents the sonographer to understand the complex anatomical nature of the sphincter apparatus.

The limitations of endoanal sonography cause diagnostic problems. This modality is currently applied for detection of sphincter defects in patients with fecal incontinence and for anal fistulae. Surgical anal repair is considered in cases with an external anal sphincter defect. Defects of the external sphincter can be difficult to recognize sonographically. For surgical treatment of anal fistulae, preoperative Parks' classification [2] is preferred. On ultrasound, non-visualization and complex nature of fistulous tracks, can hamper the exact classification. A newly developed endoanal MRI coil was applied to overcome these problems. Knowledge of the normal endoanal MR anatomy of the anal sphincter complex is essential to detect pathology in this area. In this chapter, the normal findings of endoanal MRI of the anal sphincter complex in healthy volunteers will be described.

3.2 PATIENTS AND METHODS

Ten volunteers (six women and four men aged 21-26 years [mean, 22.7 years]) with no history of anorectal disease or surgery entered the study after informed consent was obtained. MR imaging was performed at 0.5T (Gyroscan T5-II, Philips Medical Systems, Best, The Netherlands), without bowel preparation. To reduce the bowel motion, one ml of butylscopolaminebromide (Buscopan 20 mg/ml, Boehringer Ingelheim KG, Ingelheim, Germany) was injected intramuscularly before scanning. No sedation was given. A newly developed endoanal coil (Philips Medical Systems, Best, The Netherlands) was used. This consisted of a fixed tuned, rectangular, 60mm long rigid receive coil with a width of

---

This chapter was published as: SM Hussain, J Stoker, JS Laméris. Anal sphincter complex: endoanal MR imaging of normal anatomy. Radiology 1995; 197: 671-677

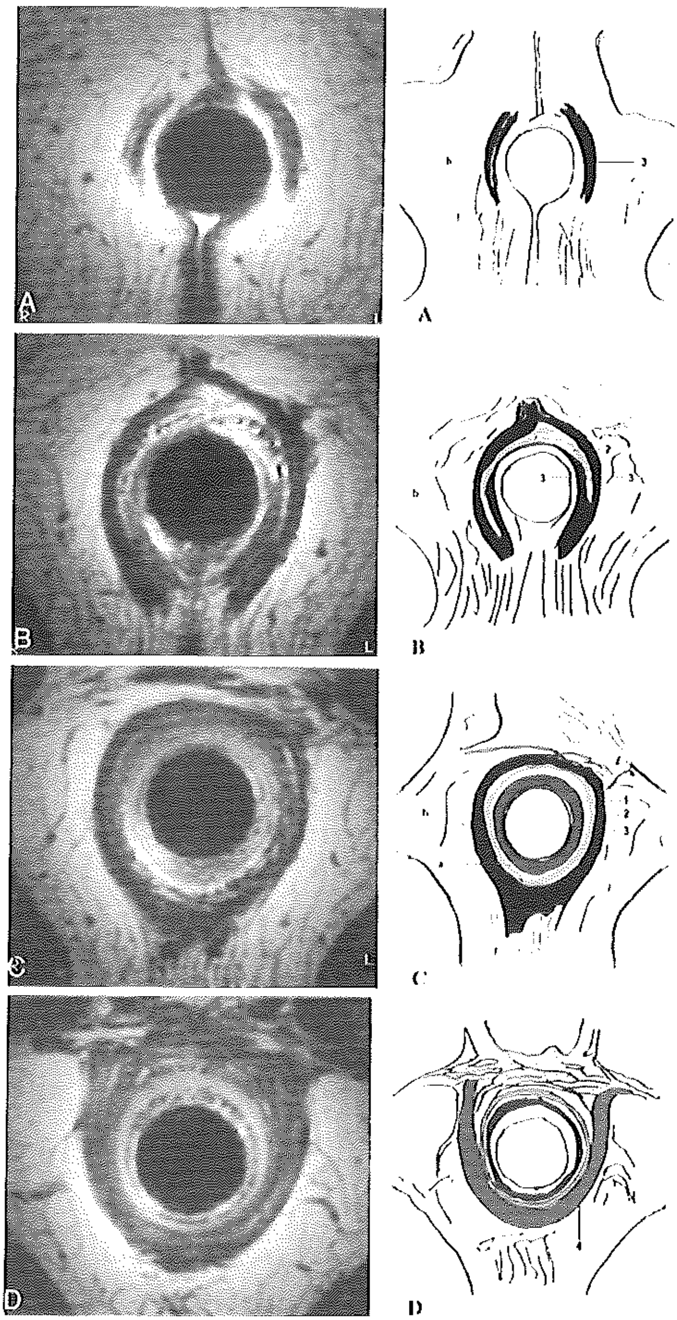

Fig. 3.1 Axial T2w contrast enhanced fast field echo (T2w CEFFE).
A. A slice through the lowest part of the external sphincter. Two halves of the external sphincter (3) are embedded within the ischioanal space (b); note the multiple septae within this space.
B. (Slightly cranial to A). Between the two folds of the external sphincter (3), small bundles of the fan-shaped longitudinal muscle layer (2) are visible. Anteriorly the two halves of the external sphincter are connected to each other. Ischioanal space (b).
C. (Slightly cranial to B). Compare the signal intensity of the internal sphincter (1) to the other structures. The external sphincter (3) is circular anteriorly while it shows an thickened extension posteriorly. Left antero-laterlly the external sphincter is in contact with the lower fibres of the superficial perineal muscle of the urogenital diaphragm(arrows). The intersphincteric space (a) and the longitudinal layer (2) are well displayed. Ischioanal space (b).
D. (Slightly cranial to C). The puborectalis muscle (4), visible as a sling, sends also fibres to the urogenital diaphragm anteriorly.

16mm; this was contained within an 80mm long cylindrical coil holder with a diameter of 19mm. Before introduction, a condom was placed over the coil and ultrasound gel was used as a lubricant. The coil was introduced while the patient was lying in the right lateral position. After introduction, the patient carefully turned on the back and the position of the coil was rechecked. A multi-slice survey was obtained by using a 25x100cm body wrap around coil placed around the pelvis. The coronal slices of the survey were angulated parallel to the long axis of the anal canal. After confirming the optimal position of the endoanal coil, an axial T2-weighted 3D gradient-echo sequence [T2w contrast enhanced fast field echo (CE-FFE), acquisition time 6.5 minutes, imaging matrix 205x256, number of signal averages (NSA) 2, repetition time (TR) 30ms, echo time (TE) 13ms, flip angle 60°, field of view (FOV) 140mm^2, slice thickness 2mm], was placed perpendicular to the long axis of the endoanal coil. Thirty-two contiguous slices were obtained. For the sagittal and the coronal scans, a T2-weighted turbo spin-echo was performed [turbo spin-echo (TSE), acquisition time 5.0 minutes, imaging matrix 186x256, NSA 8, TR 2800, TE 120, turbo factor 10, FOV 120mm^2, slice thickness 4.0mm with an interslice gap of 0.4mm]. The coronal slices were parallel to the long axis of the endoanal coil. The total exam length was 45-60 minutes. All examinations were reviewed systematically to identify the different anatomic structures and anatomical spaces in order to understand the normal appearance of the anal sphincter complex.

3.3 RESULTS

The endoanal coil was well tolerated by all volunteers. In four cases there were slight motion artefacts. Endoanal MRI revealed a complex anal sphincter apparatus (Fig. 3.1-3.4). The anal canal appeared as a cylindrical structure, extending from the attachment of the levator ani muscle to the rectum - to the lower edge of the external anal sphincter. The average length of the anal canal, in mid-coronal plane, was 57mm (range:48-63); in mid-sagittal plane, the mean length alongside the posterior wall, was 42mm (30-48) and anteriorly 36mm (28-50). The muscle layers of the lower and upper part of the anal canal were different (Fig. 3.2C). The lower part was surrounded by the internal anal sphincter, the longitudinal muscle layer and the external anal sphincter; the upper part was comprised of the internal anal sphincter, the longitudinal muscle layer and the puborectalis muscle, which slinged the anal canal instead of completely surrounding it. Between the internal anal sphincter, and the external sphincter and puborectalis, there was a slit-like space, *i.e.* the intersphincteric space; this space contained the longitudinal layer. The whole sphincter apparatus was embedded within the ischioanal space or fossa. At its upper end the puborectalis was attached to the funnel-shaped levator ani muscle, which anchored the sphincter complex to the inner side of the pelvis. The levator ani muscle also separated the ischioanal space below, from the supralevator space above it. The urogenital diaphragm was connected to the puborectalis and the external sphincter anteriorly (Fig. 3.1CD). Posteriorly the external sphincter and the puborectalis muscle were attached to the coccyx by the ano-coccygeal ligament (Fig. 3.3CD). Anterior morphology of the external sphincter and its relation to the longitudinal layer, the

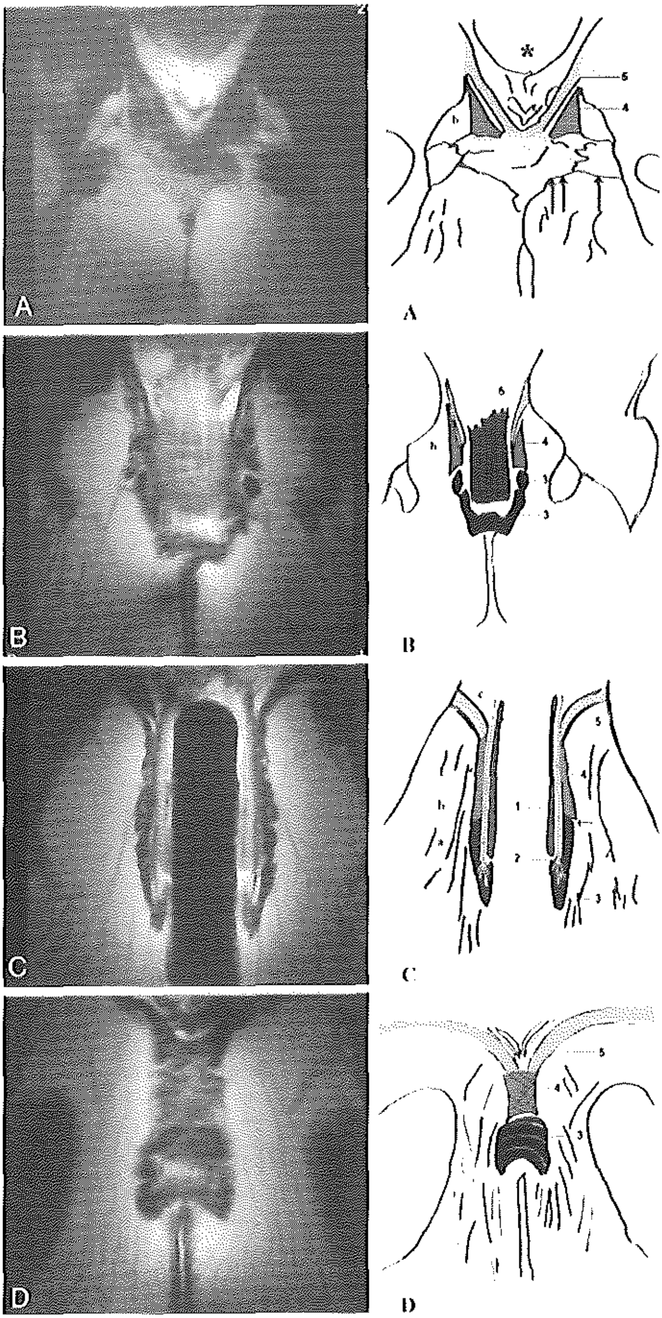

Fig. 3.2 Coronal T2w turbo spin-echo (T2w TSE).
A. A slice anterior to the anal canal. Puborectalis (4) is infero-lateral to the levator ani (5). Both muscles, being hardly distinguishable from each other, are perpendicular to the urogenital diaphragm (6), which consists mainly of the superficial and the deep perineal muscles. Note the anterior extension of the ischioanal space (b). Ischiocavernosus muscle (7).
B. (Slightly posterior to A; through the anterior anal canal wall). The upper part of the external sphincter is visible as a separate bundle (3). Note the funnel-shaped levator ani and septae extending from the triangular puborectalis muscle (4) into the ischioanal space (b).
C. The mid-coronal slice, i.e. the coronal slice through the mid-part of the anal canal. Note the muscles of the lower part of the anal canal: the internal anal sphincter (1), the longitudinal muscle layer (2) and the external anal sphincter (3). The longitudinal layer terminates between the folded ends of the external sphincter. A cleft (arrowhead) can seen between the external sphincter (3) and puborectalis (4). Levator ani muscle (5). Intersphincteric space (a); ischioanal space (b): supralevator space (c). The endoanal coil (*).
D. (Slightly posterior to C). The direction of the fibres and their signal intensity differ within the external sphincter (3) and the puborectalis muscle (4). The levator ani (5) is more horizontal in shape.

urogenital diaphragm and the bulbocavernosus muscle in both sexes, were quite different (Fig. 3.3CD). Compared to the high signal intensity of the fat-containing anatomical spaces, all muscles, except the internal anal sphincter, were hypointense. The internal sphincter had an intermediate signal intensity (Fig. 3.1C). The anatomical structures will be described separately.

The internal anal sphincter was the innermost muscle layer. It was visible as a direct continuation of the circular smooth muscle of the rectum (Fig. 3.2C). The average maximum thickness was 2.5mm (range:2-4).

The longitudinal muscle layer, the second muscle layer, visible as a continuation of the outer longitudinal smooth muscle of the rectum, was often joined by the fibres originating from the puborectalis muscle (Fig. 3.2B, 3.3CD). In all cases this layer was recognizable as a thin structure with an average thickness of 1mm (range:1-1.5). Distally, the layer divided into discrete bundles, which anchored into the external sphincter.

The external anal sphincter, the outer muscle layer, surrounded only the lower part of the anal canal. In the *axial* plane through the lowermost part of the external sphincter, two separate halves of the sphincter were visible (Fig. 3.1A). More cranially, the two halves gradually met to become circular anteriorly (Fig. 3.1BC). While posteriorly and further cranially the external sphincter became thickened to form the most prominent part of the sphincter (Fig. 3.1C). In the upper part, the innermost fibres of the external sphincter were completely circular, while the outer fibres gained attachments to the surrounding muscles and the septae of the ischioanal fossa. In the *coronal* plane, a cleft was seen between the external sphincter and the puborectalis (Fig. 3.2C). On the anterior coronal slices, the uppermost fibres of the external sphincter formed a separate bundle, which traveled towards the urogenital diaphragm instead of the anterior part of the external sphincter (Fig. 3.2B). Just below the uppermost fibres, the external sphincter showed varying degree of septation in many subjects. Posteriorly, the external sphincter consisted of one muscle layer (Fig. 3.2D). One of the remarkable findings in the coronal plane was that the lower ends of the external sphincter were folded inwards and upwards, forming a double-layered external muscle at lower ends (Fig. 3.2C). In the *sagittal* plane the prominent posterior external sphincter, attached to the coccyx with the ano-coccygeal ligament, was well delineated (Fig. 3.3CD). The average thickness of the external sphincter was anteriorly 2.5mm (range:1-4), laterally 3.0mm (range:2-5), and posteriorly 16mm (range:10-20). The average cranio-caudal length of the external sphincter in the mid-coronal plane was 27mm (range:24-33mm); in the mid-sagittal plane, the length of the external sphincter posteriorly, was 19mm (15-26) and anteriorly 18mm (14-26).

The Puborectalis muscle slinged the upper part of the anal canal as a ribbon-like layer (Fig. 3.1D). Anteriorly, the puborectalis muscle was located infero-laterally to the levator ani muscle. Slightly posteriorly, the puborectalis was still more or less triangular in shape and gained attachments to the urogenital diaphragm (Fig. 3.2A). At the level of the anal canal, the puborectalis was oblong in shape (Fig. 3.2C). At this level, the average thickness was 4mm (range:2-6) and the cranio-caudal length was 23mm (15-34).

The levator ani muscle was funnel-shaped anteriorly, while posteriorly it gradually became horizontal in shape (Fig. 3.2). The average thickness was 2mm (range:2-3).

The urogenital diaphragm comprised mainly the transversus perineii superficialis and

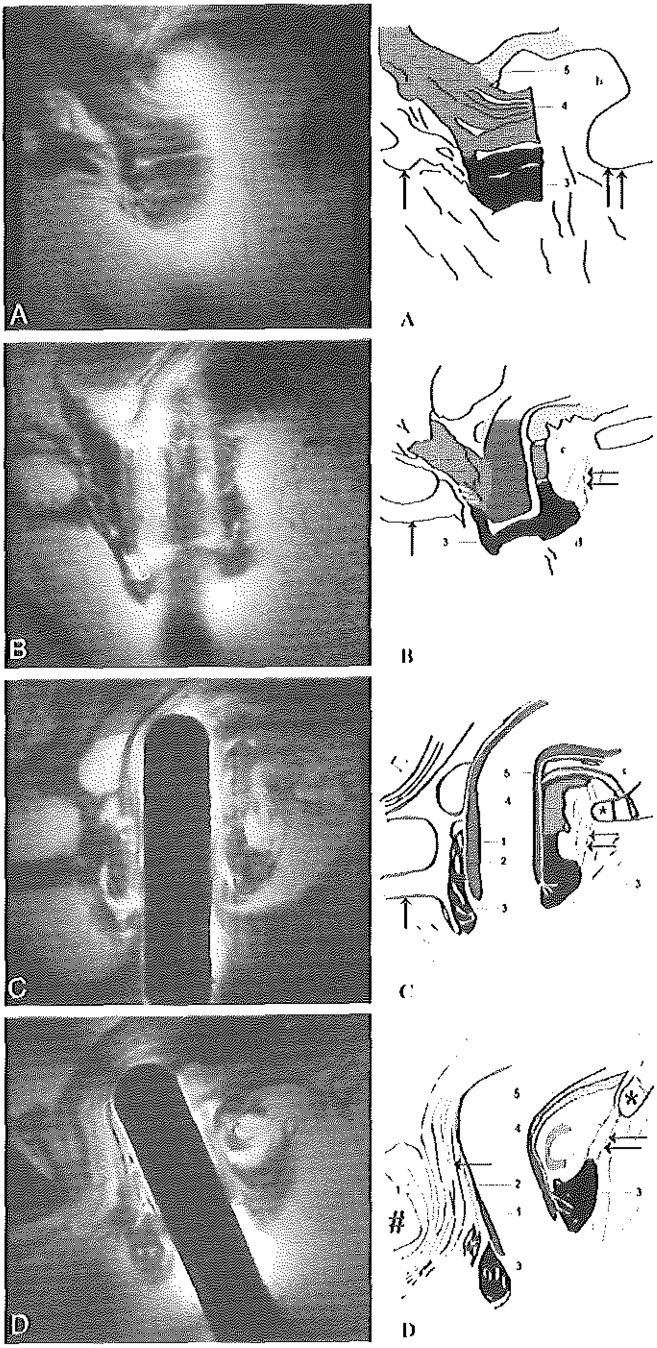

Fig. 3.3 Sagittal T2w turbo spin-echo (T2w TSE).
A. A slice through the left lateral wall of the anal canal. Note the puborectalis (4) traveling towards the pubic bone. External sphincter (3). Levator ani muscle (5). Bulbocavernosus muscle (arrow). Gluteus maximus (dubble arrows).
B. (Slightly medial to A). Note the parts of the puborectalis muscle forming the urogenital diaphrgm (6). The fibres of the ano-coccygeal ligament (double arrows) separate the superficial (d) from the deep (e) postanal space. There is a close relation between the external sphincter (3) and the bulbocavernosus muscle (arrow).
C. Mid-sagittal slice (*male anatomy*). The internal sphincter (1) is clearly seen. Note the subtle difference in signal intensity of the thickened posterior external sphincter (3) and the puborectalis muscle (4). Ano-coccygeal ligament (dubble arrows) connects the external sphincter (3) to the os coccyx (*). Levator ani muscle (5) and the supralevator space (c) are difficult to recognize in this slice. The external sphincter (3) is supported by the bulbocavernosus muscle (arrow) anteriorly.
D. Mid-sagittal slice (*female anatomy*). Most of the posterior structures are identical in both sexes. The puborectalis muscle (4) is though more curved. Note the oval-shaped anterior external sphincter (3), with the longitudinal muscle layer (2) terminating just cranial to it. Anterior to the external sphincter (3), unlike in the male, the bulbocavernosus muscle, is lacking. The external sphincter remains unsupported anteriorly. Vagina (arrowheads). Urethra (arrow). Levator ani muscle (5). Ano-coccygeal ligament (double arrows). Os coccyx (*).

profunda muscles (Fig. 3.2A), though it also received fibres from the external sphincter (Fig. 3.1C) and the puborectalis muscles (Fig. 3.1D). In the mid-line anteriorly, the urogenital diaphragm divides to form the *hiatus diaphragm urogenitales*. In males the urethra, and in females, the urethra and the vagina pass the hiatus (Fig. 3.3CD).

Male versus female anatomy of the anal sphincter complex: The morphology of the anterior part of the external anal sphincter was quite different in both sexes (Fig. 3.3CD). In the *male*, the anterior part of the external sphincter was thin and oblong. It was, however, supported by the bulbocavernosus muscle anteriorly (Fig. 3.3C). The external sphincter and the bulbocavernosus showed muscular connections; in some cases it was even difficult to distinghuish between the fibres of these two muscles. In the *female*, the anterior external sphincter was thickened and oval in shape. The longitudinal layer was seen to terminate just cranial to the external sphincter. Since the bulbocavernosus muscle was divided by the vagina into two halves, there was no muscular support for the external sphincter in the anterior mid-line. Just lateral to the mid-line on both sides, however, this support was probably provided by a downward muscular extension of the urogenital diaphragm, visible as a shield-like muscle layer just anterior to the external sphincter. Since the bulbus of the penis, which lies just caudal to the urogenital diaphragm, is lacking, the female urogenital diaphragm was situated at a lower level than its male counterpart. In both sexes, there was little difference in the cranio-caudal length of the anterior and the posterior part of the external anal sphincter (Fig. 3.3CD).

The perianal anatomical spaces. There was direct visualization of the anatomical spaces because of great contrast difference among the fat-containing anatomical spaces and the muscle layers (Fig. 3.1-3.3). Within the fatty tissue of the spaces, there were multiple fibrous septae. The intersphincteric space, located between the internal and the external sphincters containing the longitudinal layer, was visible in all cases (Fig. 3.1C and 3.2C). The ischioanal space, which surrounded the anal canal, was pyramid-shaped. On coronal planes, its apex was visible at the origin of the levator ani from the obturator fascia. Inferiorly, it extended to the level of the perineal skin. The medial wall was formed by the levator ani, the puborectalis and the external sphincter. Anteriorly, the ischioanal space had important extensions forward, above the urogenital diaphragm (Fig. 3.2A). Posteriorly, this space was seen to have important communications: one, below the anococcygeal ligament (superficial postanal space) and a second, above it (deep postanal space, i.e. the retrosphincteric space of Courtney) (Fig. 3.3CD). The supralevator space was visible above the levator ani.

3.4 DISCUSSION

The anatomical concept emerging from the endoanal MRI data of the ten volunteers in the current study, is in many aspects different than the present-day anatomical view of the anal sphincter complex. Within this relatively small number of subjects in our study, a basic anatomical pattern could be recognized. The anal sphincter complex is responsible for the mechanism of fecal continence. This mechanism is however still obscure [3]. Unfamiliarity with the exact anatomy, accompanied by the many controversies could be

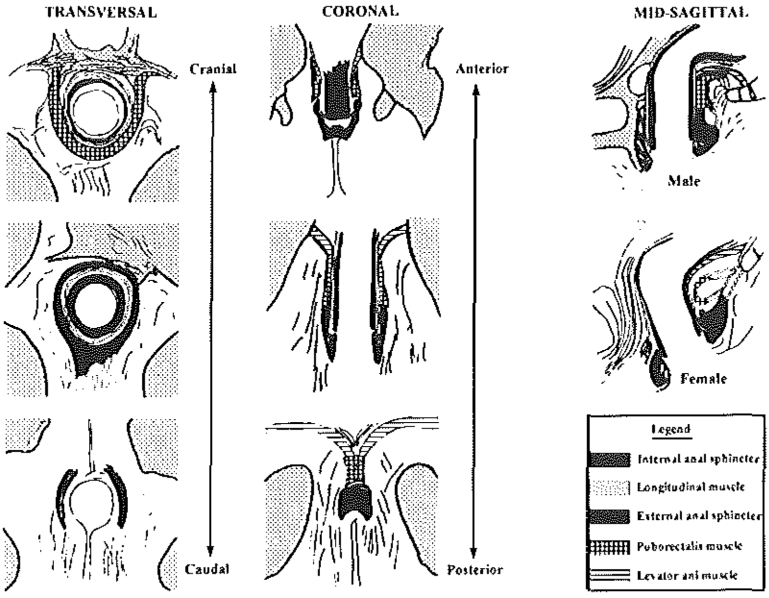

Fig. 3.4 The schematic representation of the normal anal sphincter complex. Note the changing pattern of the anal sphincter complex at various levels in the three planes. Compare particularly the configuration of the external sphincter, the puborectalis muscle and the levator ani muscle. Note the two-part external sphincter with the vertical configuration of the puborectalis and the levator ani in the coronal plane anteriorly. Note also the differences in male and female external sphincter.

responsible for this obscurity. The external anal sphincter has been described consisting of one, two or three parts [3]. According to Milligan and Morgan [4] the external sphincter consists of subcutaneus, superficial and deep part. Goligher et al [5] found no suggestion of division of the external sphincter into three separate parts. The muscle was one continous sheet. Oh and Kark [6] found either a bilaminar or a trilaminar arrangement and proposed a two compartment view, which seems to be a merger of the previous ideas. The earlier concepts are compared to the current findings in Fig. 3.5.

Current data confirm the previous findings of the internal sphincter [4-5]. The longitudinal muscle is, however, not thicker than the internal sphincter, as mentioned before [7] and it was seen to traverse only the lower part of the external sphincter distally. The longitudinal layer, as mainly consisting of smooth muscle, shows connections to the external sphincter (skeletal muscle). So the smooth and the skeletal muscles seem to be integrated into one firm sphincter apparatus. The configuration of the external sphincter

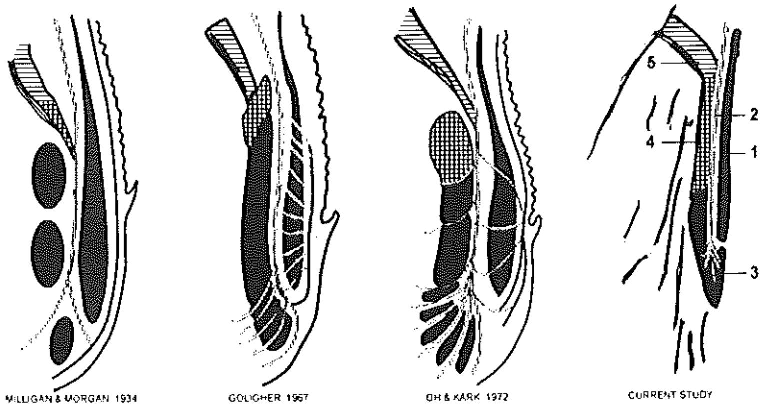

Fig. 3.5 Findings of the anatomy of the right side of the anal canal viewed in the coronal plane in this study are compared with those in previous studies. The anatomy of the internal sphincter (1) does not differ between studies. The anatomy of the longitudinal muscle (2) in this study is similar to that of Milligan and Morgan [4]; in the other two studies [5,6], the longitudinal muscle runs through both the "external" and the internal sphincter. In this study, the external sphincter (3) appeared to surround only the lower part of the anal canal; in previous studies, the major part of the anal canal was surrounded by the external sphincter. The puborectal muscle (4) is, according to Milligan and Morgan [4], a part of the levator ani muscle (5). In the Goligher model [5], it lies between the external sphincter and the levator ani muscle; according to Oh and Kark [6], it is a part of the external sphincter.

did not only differ laterally as explained in Fig. 3.5, also the thickened posterior part and the folded lower ends have not been described before. The most striking finding, however, was that the external sphincter surrounded only the lower part of the anal canal while the upper part was slinged by the puborectalis. This finding, in our opinion, will have implications for the clinical and surgical approach of disease in this area. For instance for sphincter repair in patients with fecal incontinence, the extent of the sphincter damage, with or without accessory damage of puborectalis, can be evaluated more accurately. To reduce the risk of incontinence in patients with a perianal fistula, the fistulous track can be exactly described in relation to the external sphincter and the puborectalis. In the latter group of patients also the direct visualization of the perianal anatomical spaces is essential for diagnosis and treatment.

As inherent to all anatomical structures, the occurrence of the anatomical variation of anal sphincter complex should be kept in mind. Even among this small group of subject studied currently, the external sphincter and the puborectalis were variable in appearance. Also within one individual, the appearance of muscles differed at various levels in one plane. In coronal plane, the puborectalis appears as a part of the levator ani anteriorly (Fig. 3.2B), while at the level of the anal canal it is, as an oblong layer, closely related to the external sphincter (Fig. 3.2C) and further posterioly, the external sphincter and the puborectalis seem one continous muscle sheet (Fig. 3.2D). With the multiplanar capacity of MRI, one can go back and forth in a certain plane to understand the 3D anatomical concept. Previously [4-7], different (dissection) techniques with low reproducibility, were used to study the anal sphincter complex. Probably the puborectalis at the level of the anal canal was often misinterpreted as the deep external sphincter, and together with the variable appearance of the upper part of the external sphincter, may have led to the laminar concept of the anal sphincter.

Oh and Kark [6] are the only authors who have paid attention to the marked dissimilarity of the anterior part of the external anal sphincter in both sexes. The current findings confirm the observations of the anterior external sphincter. Though the posterior part of the external sphincter was not twice as long as the anterior part [6]. The cranio-caudal length of the posterior and the anterior parts of the external sphincter did not differ significantly from each other in both sexes. The puborectalis has probably once again been misconceived as a part of the external sphincter posteriorly.

An endoanal coil has the advantage of an increased signal-to-noise ratio at the anal sphincters. Voxel size can therefore be decreased to increase spatial resolution. The higher spatial resolution is required to fully appreciate the complex anatomy of this region. Aronson et al [8] studied anatomy of anal sphincter with MRI in five continent women with a surface coil. The proximal, middle and distal external sphincter as well as the internal sphincter could be distinguished. The sphincters were measured: the thickness of internal sphincter was about 9mm anteriorly and 12mm posteriorly and the external sphincter 8mm and 12mm respectively. In our study (including six continent women), the internal sphincter was at least three times thinner, which could be explained due to the thinning-effect of the endoanal coil in situ. The external sphincter was about three times thinner anteriorly, however posteriorly it was (despite the thinning-effect of the coil) on average even thicker. Apart from the differences in the measurements, the observation of a three part configuration [8] is at least doubtful. In our opinion, the muscle layers of the anal canal are not well recognizable on images obtained by the surface coil.

Endoanal MRI is excellent in imaging the anal sphincter complex. Contrary to the previous studies, high quality multiplanar images with superb soft tissue contrast can be obtained in vivo. Small anatomic variations can be readily appreciated and the images can be used as a road-map for planning surgical treatment. The current findings may change the present-day anatomical concept of the anal sphincters.

3.5 ACKNOWLEDGEMENTS

Thanks are due to Dr J.W. Kuiper, for helping to coordinate the study, and to T. Rijsdijk and A.W. Zwamborn for preparing the high quality photographs and excellent drawings.

3.6 REFERENCES

1. Nielsen MB, Pedersen JF, Hauge C, Rasmussen OO, Christiansen J. Endosonography of the anal sphincter: findings in healthy volunteers. AJR 1991;157:1199-1202

2. Parks AG, Gordon PH, Hardcastle JD. A classification of fistula-in-ano. Br J Surg 1976;63:1-12

3. Dalley AF. The riddle of the sphincters. The morphophysiology of the anorectal mechanism reviewed. Am Surg 1987;53:298-306

4. Milligan ETC, Morgan CN. Surgical anatomy of the anal canal. The Lancet 1934;2:1150-1156

5. Goligher JC. Surgery of the anus, rectum and colon. 2nd ed. London, England: Bailliere Tindall, 1967

6. Oh C, Kark AE. Anatomy of the external anal sphincter. Br J Surg 1972;59:717-723

7. Shafik A. A new concept of the anatomy of the anal sphincter mechanism and the physiology of defecation. III. The longitudinal anal muscle: anatomy and role in anal sphincter mechanism. Investigative Urology 1976;13:271-277

8. Aronson MP, Lee RA, Berquist TH. Anatomy of anal sphincters and related structures in continent women studied with magnetic resonance imaging. Obstet Gynecol 1990;76:846-851

Chapter 4

ANAL SPHINCTER COMPLEX: ENDOANAL SONOGRAPHY vs ENDOANAL MRI

4.1 INTRODUCTION

After the first description of the technique and normal anatomy with anal endosonography [1], several workers have described the normal anal sphincters [2,3]. In the anatomical and surgical literature, though, there has never been a consensus about the normal anatomy of the anal sphincter complex [4]. For instance, the external anal sphincter has been described as an one [5], two [6] or three-part [7] structure. To describe the sonographic findings, some authors [2] have accepted the one-part view while others [3] adopted the three-part concept as the true representation of the anatomy.

With endoanal sonography, the internal anal sphincter has been described as a hypoechoic concentric structure by all authors [2,3]. The appearance of the longitudinal muscle layer and the external sphincter is controversial [2,3]. By assuming the one-part view, the external sphincter was described as a continuous echogenic structure [2]. With the three-part concept as starting-point, its configuration was said to be different at each level [3]. Moreover there were sex-dependent differences in echogenicity [3,8]. In our experience, the internal anal sphincter is the only structure well depicted sonographically while all other structures are either variable in echogenicity or not visible at all. Recently, we have described the normal anatomy of the sphincter complex with endoanal MRI [9].

In this chapter, the findings of endoanal sonography and endoanal MRI will be compared in order to clarify the controversies concerning the sonographic appearance of the sphincter.

4.2 PATIENTS AND METHODS

Twelve patients (six women and six men aged 21-35 years (mean, 25.8 years)) entered the study after informed consent was obtained. Their complaints were unrelated to the gastrointestinal tract and they had no history of anorectal disease or surgery. In each patient, both endoanal sonography and endoanal MRI were performed at the same day.

Endoanal sonography

For endoanal sonography, a Brüel & Kjaer (Naerum, Denmark) ultrasound scanner (type 3535) was used with a rotating probe (type 1850) providing a 360° image. A 7 MHz transducer with minimum beam width of 1.1 mm was used. A hard, sonolucent plastic cone with an external diameter of 17 mm covered the transducer and was filled with degassed water for acoustic coupling. The cone was covered with a condom with

---

Submitted for publication as: SM Hussain, J Stoker, JS Laméris. Anal sphincter complex: endoanal sonography vs endoanal MRI. Presented at the Röntgen Centenary Congress, Birmingham, UK, 1995.

ultrasound gel applied to both surfaces. All sonographic images were orientated such that anterior was to the top. Axial images were performed through the anal canal.

Endoanal MRI

MR imaging was performed at 0.5T (Gyroscan T5-II, Philips Medical Systems, Best, The Netherlands), without bowel preparation. To reduce bowel motion, one ml of butylscopolaminebromide (Buscopan 20 mg/ml, Boehringer Ingelheim KG, Ingelheim, Germany) was injected intramuscularly before scanning. A newly developed endoanal coil with a diameter of 19 mm (Philips Medical Systems, Best, The Netherlands) was used. The coilholder was covered with a condom and ultrasound gel was applied to the surface. A multi-slice survey was obtained by using a 25x100cm body wrap around coil placed around the pelvis. An axial T2-weighted 3D gradient-echo sequence [T2w contrast enhanced fast field echo, acquisition time 6.5 minutes, imaging matrix 205x256, number of signal averages (NSA) 2, repetition time (TR) 30ms, echo time (TE) 13ms, flip angle 60°, field of view (FOV) 140mm, slice thickness 2mm], was placed perpendicular to the long axis of the endoanal coil. Thirty-two contiguous slices were obtained. For the sagittal and the coronal scans, a T2-weighted turbo spin-echo was performed [acquisition time 5.0 minutes, imaging matrix 186x256, NSA 8, TR 2800, TE 120, turbo factor 10, FOV 120mm, slice thickness 4.0mm with an interslice gap of 0.4mm]. The coronal slices were parallel to the long axis of the endoanal coil.

The examination time for endoanal sonography was about 10-15 minutes and for endoanal MRI 45-60 minutes. The endosonographic probe and the endoanal MR coil had a comparable diameter (Fig. 4.1). All examinations were reviewed and compared systematically to evaluate the appearance of the anatomic structures with both imaging techniques.

4.3 RESULTS

The comparative axial images with endoanal sonography and endoanal MRI at four different levels have been displayed in a female (Fig. 4.2-4.4) and at one level in a male (Fig. 4.5). To facilitate comparison, the same magnification factor was used for axial images.

With endoanal MRI, all muscle layers of the anal canal wall were consistently visible. With endoanal sonography, the internal sphincter was well recognizable as a hypoechoic layer (Fig. 4.3). Just outside the internal sphincter, another thin hypoechoic layer was visible in one male and four females. This structure corresponded to the longitudinal layer visible in all cases with endoanal MRI (Fig. 4.3). The external sphincter showed two sonographic patterns: a hyperechoic band containing hypoechoic fibres (two male and four females; Fig. 4.3-4.4) or a hypoechoic structure (four males and two females; Fig. 4.5). Within one individual, the external sphincter and the puborectalis had the same sonographic appearance. In subjects with a hyperechoic band at the level of the puborectalis there was a reasonable correlation with the well-delineated sling of the puborectalis on the endoanal MR images (Fig. 4.2). The hyperechoic band, at the level of

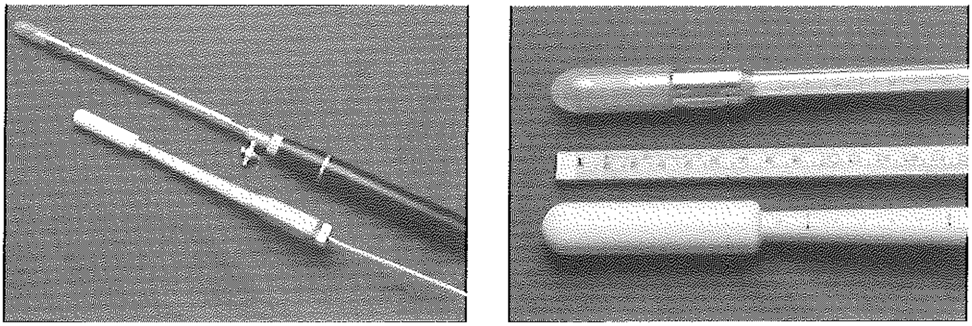

Fig. 4.1 The endosonographic probe and the endoanal coil have a comparable diameter.

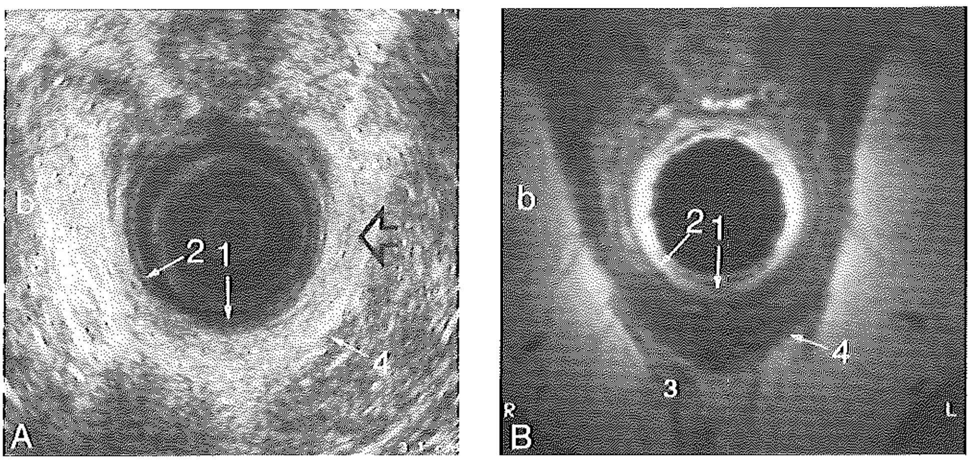

Fig. 4.2 *Axial images through the upper part of the puborectalis in a female (level indicated in Fig. 4.6).* Endoanal sonography (A); endoanal MRI (B). With sonography, the hyperechoic puborectalis muscle (4) contains subtle hypoechoic fibres (open arrow). Sonographic configuration of the sling correlates well with the hypointense, well-demarcated puborectalis on MR image. Internal sphincter (1). Longitudinal layer (2). Ischioanal space (b).

the external sphincter, did not show any correlation with the external sphincter on MR images (Fig. 4.3-4.4). Endoanal MRI revealed a totally different configuration of the external sphincter as compared to the sonographically visible hyperechoic band. In subjects with a hypoechoic external sphincter, there was an excellent correlation between the ultrasound and the MR findings (Fig. 4.5). The coronal image facilitated the understanding of the complex nature of the sphincters. As compared to the axial MR images, the coronal view provided better understanding of the relationship among the

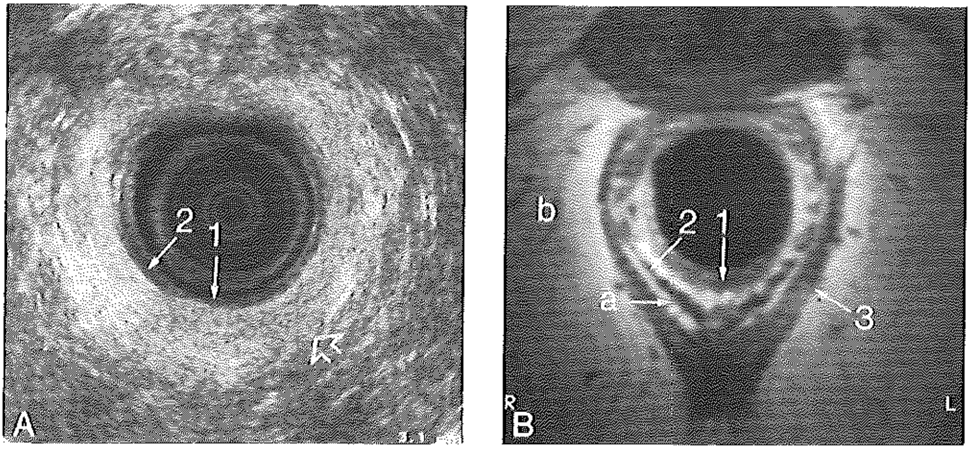

Fig. 4.3 *Axial images through the upper part of the external sphincter in a female (level indicated in Fig. 4.6).* At this level the internal anal sphincter (1) is well recognizable with both modalities. Just outside the internal sphincter, another thin hypoechoic layer is visible sonographically which corresponds well with the longitudinal layer (2) on the MR image (B). The hyperechoic band containing hypoechoic fibres (open arrow) (A) shows no correlation with the external sphincter (3) apparent with MRI (B). Intersphincteric space (a); Ischioanal fossa (b).

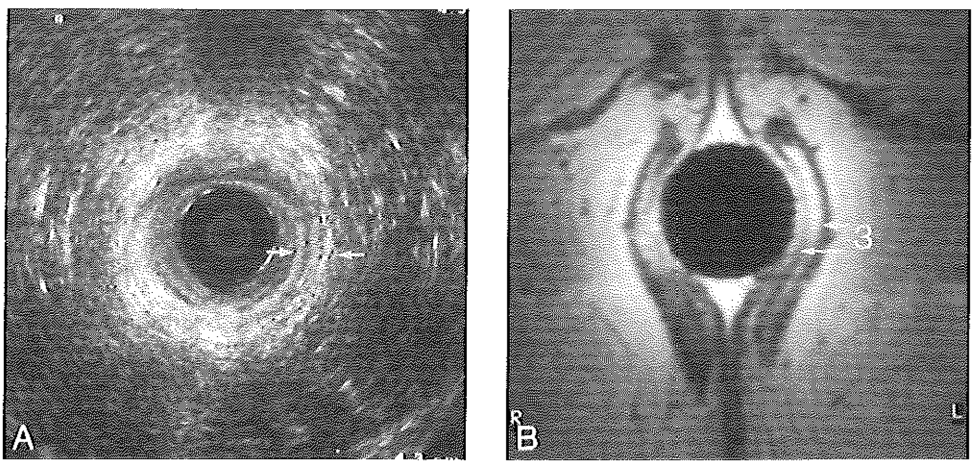

Fig. 4.4 *Axial image through the lower part of the external sphincter in a female (level indicated in Fig. 4.6).* At this level no internal sphincter is present. The hyperechoic band (between the arrows) is much thicker (A) than the double-layered external sphincter (3), well-delineated with MRI (B).

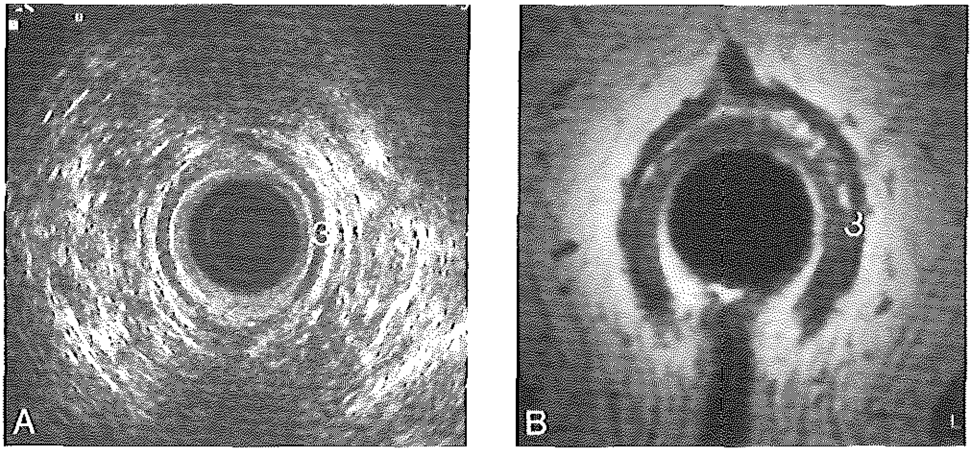

Fig. 4.5 *Axial images through the lower part of the external sphincter in a male (level corresponds to Fig. 4.4).* The hypoechoic external sphincter (3) shows practically the same thickness and configuration with both modalities (A and B).

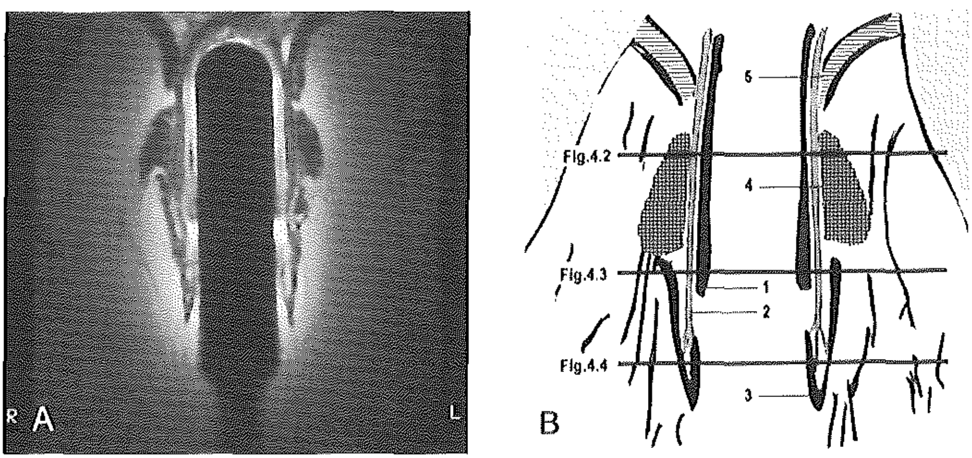

Fig. 4.6 *Coronal MR image through the mid-part of the anal canal (A), with the line drawing (B) (the levels of the Fig. 4.2-4.4 are indicated).* The muscle layers of the lower part differ from the upper part. Note the folded distal ends of the external sphincter (3). Internal sphincter (1); longitudinal layer (2); puborectalis muscle (4); levator ani muscle (5).

external sphincter, the puborectalis and the levator ani (Fig. 4.6). Sonographically, none of the perianal anatomical spaces was visible. Around the anal canal multiple artefact were present without a clear demarcation between the anatomical spaces and the muscle layers. With endoanal MRI there was a direct visualisation of all perianal anatomical spaces. The anatomical structure and the spaces were clearly delineated.

4.4 DISCUSSION

Due to the high inherent soft tissue contrast and multiplanar capability, current findings show that endoanal MRI, as compared to endoanal sonography, is superior in imaging the anal sphincter complex. Particularly the direct visualization of the external anal sphincter and the perianal anatomical spaces can be of great clinical importance. Moreover endoanal MRI facilitates the understanding of the complex nature of the anal sphincter apparatus. Subtle anatomic variations can readily be appreciated which can be important for detection of pathology.

Sonographically there is no disagreement about the appearance of the internal anal sphincter [2,3]. The longitudinal muscle layer, though, has been described by one group as a thin hypoechoic layer [2] and by others as a thick hyperechoic structure [3]. Currently, the comparative images showed that the hypoechoic thin layer just outside the internal sphincter corresponds best to the longitudinal layer on the MR images.

The sonographic appearance of the external sphincter is also controversial [2,3,8]. Nielsen et al studied fourteen healthy women and described the external sphincter as a circular hyperechoic band just outside the internal anal sphincter [2]. Sultan et al described the normal anatomy in 93 females and in 21 males and stated that endosonography did not reveal any plane of cleavage between the components of the external sphincter, though a changing pattern at different levels confirming to a trilaminar arrangement was apparent [3]. The configuration of the three parts of the sphincter was respectively annular, elliptical and conical [3]. This view seems very much inspired by the original three-part description by Milligan and Morgan, who characterized the sphincters as annular, elliptical and annular [7]. Current study confirms the changing shape of the external sphincter, though, this finding is, in our opinion, not related to a laminar concept [9].

In analogy with the shape, the echogenicity of the external sphincter could change at various levels in the same subject [3]. Moreover the external sphincter was hyperechoic in the females and hypoechoic in the majority of the males [8]. The current study confirms the two sonographic patterns of the external sphincter described previously [3,8]. Though, a majority of females currently showed a hyperechoic external sphincter, the hypoechoic pattern was present in both sexes. The puborectalis is not always hyperechoic as mentioned before [2,3,8].

The change in the direction of the muscle fibres as an explanation for two sonographic patterns of the external sphincter [3,8], seems not quite plausible because a change of muscle fibres was often present without a significant change in the echogenicity. For instance, the external sphincter in Fig. 4.6 changes its shape considerably in cranio-caudal direction while in this subject, the same sonographic pattern is present at two different levels (Fig.

4.3-4.4). A variation in the histological composition of the muscle fibres may be an important factor. Whatever the exact explanation for the sonographic appearances of the external sphincter, the most striking finding was that only the hypoechoic external sphincter correlated with the MRI findings while the hyperechoic band appeared not to be the external sphincter as originally described [1,2]. This finding will have important implications for endoanal sonography as it is the imaging modality currently used in assessment of sphincter defects particularly in female patients with faecal incontinence.

Both techniques have advantages and disadvantages. In our hospital, endoanal sonography has a 3-4x shorter exam time. It is 4-5x cheaper and readily available. The main advantage, in our opinion, is the real-time capability. The disadvantages are the poor soft tissue contrast, mainly restriction to the axial plane and operator-dependency. The main advantages of endoanal MRI are a better tissue characterization and the multiplanar capability. Its disadvantages are a lengthy exam time, high cost with a lower availability in some areas.

This, however, does not counterbalance the diagnostic yield of this modality, particularly, in patients with recurrent or complex nature of pathology. The anal sphincter complex is responsible for the extremely important mechanism of continence. During the treatment of a certain disease in this area, for instance a fistula, one is keen to keep this mechanism as intact as possible. The current finding that a number of anatomical structures of anal sphincters is either variable in appearance or not visible at all with endoanal sonography, should have consequences for the imaging modality to be used for the management of patients.

4.5 REFERENCES

1. Law PJ, Bartram CI. Anal endosonography: technique and normal anatomy. Gastrointestinal Radiology 1989;14:349-353

2. Nielsen MB, Pedersen JF, Hauge C, Rasmussen OO, Christiansen J. Endosonography of the anal sphincter: findings in healthy volunteers. AJR 1991;157:1199-1202

3. Sultan AH, Kamm MA, Hudson CN, Nicholls RJ, Bartram CI. Endosonography of the anal sphincters: normal anatomy and comparison with manometry. Clinical Radiology 1994;49:368-374

4. Dalley AF II. The riddle of the sphincters. The morphophysiology of the anorectal mechanism reviewed. The American Surgeon 1987;53:298-306

5. Goligher JC, Leacock AG, Brossy JJ. The surgical anatomy of the anal canal. British Journal of Surgery 1955;43:51-61

6. Oh C, Kark AE. Anatomy of the external anal sphincter. British Journal of Surgery 1972;59:717-723

7. Milligan ETC, Morgan CN. Surgical anatomy of the anal canal. The Lancet 1934;2:1150-1156

8. Sultan AH, Nicholls RJ, Kamm MA, Hudson CN, Beynon J, Bartram CI. Anal endosonography and correlation with in vitro and in vivo anatomy. British Journal of Surgery 1993;80:508-511

9. Hussain SM, Stoker J, Laméris JS. Anal sphincter complex: endoanal MR imaging of normal anatomy. Radiology 1995;197:671-677

Chapter 5

MAGNETIC RESONANCE IMAGING OF THE ANAL SPHINCTERS AND RELATED STRUCTURES: FEMALE versus MALE ANATOMY

5.1 INTRODUCTION

In the current anatomical and surgical literature there is no consensus on the exact anatomy of the normal anal sphincter complex and its relationship to the surrounding structures [1]. Particularly the configuration of the external anal sphincter and the puborectalis muscle has been controversial [2,3]. From the anatomical dissection studies, it was apparent that the configuration of the external anal sphincter showed distinct differences in arrangement in the anterior aspect as compared to the lateral and posterior appearance [4]. Moreover there was a marked dissimilarity of the anterior part of the external sphincter in men and women [4]. According to Oh and Kark in the male the external sphincter was approximately the same length anteriorly and posteriorly, whereas in the female the anterior portion condensed to a narrow bundle of muscle less than half of the posterior length. This model was contradicted by using magnetic resonance imaging (MRI) to study the anal sphincter in continent women, using an external surface coil [5]. The spatial resolution of such a coil is, in our opinion, too low to assess the complex anatomy of the sphincters.

A recently developed endoanal coil was used to study the sphincter complex. The normal endoanal MRI findings were described with acknowledging a few sex-dependent differences [6]. In this chapter, the anterior part of the female and male anal sphincter complex and related structures will be compared in detail.

5.2 MATERIALS AND METHODS

Fourteen continent, nulliparous females and six male patients (mean age 26.7 years; range, 22-32 years) were examined after an informed consent was obtained. Their complaints were unrelated to the anorectum and they had no history of perianal disease. MR imaging was performed at 0.5 Tesla (Gyroscan T5-II, Philips Medical Systems, Best, The Netherlands), without bowel preparation. To reduce bowel motion, one ml of butylscopolaminebromide (Buscopan 20 mg/ml, Boehringer Ingelheim KG, Ingelheim, Germany) was injected intramuscularly before scanning. A newly developed endoanal coil with a diameter of 19 mm (Philips Medical Systems, Best, The Netherlands) was used. The coilholder was covered with a condom and ultrasound gel was applied to the surface. A multi-slice survey was obtained by using a 25x100cm body wrap around coil placed

---

Submitted for publication as: SM Hussain, J Stoker, AC Drogendijk, IL Tan, AW Zwamborn, JS Laméris. Magnetic resonance imaging of the anal sphincters and related structures: female versus male anatomy.

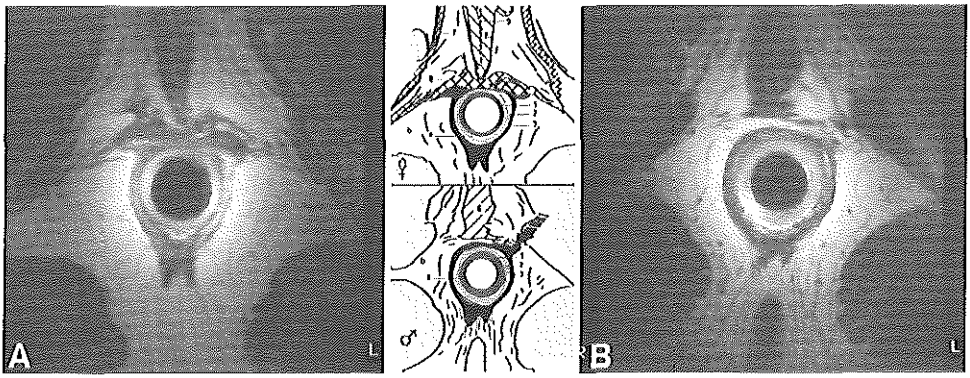

Fig. 5.1 Axial images (female: (A), upper drawing; male: (B), lower drawing) through the upper part of the external sphincter. The shield-like muscle (8) is visible just anterior to the anal canal. Note the similar orientation of the vagina (9) in the female and the bulbocavernosus muscle (6) in the male. In the male, the external sphincter and the bulbocavernosus are connected (arrow). 1=internal sphincter; 2=longitudinal layer; 3=external sphincter; 7=ischiocavernosus muscle; a=intersphincteric space; b=ischioanal space

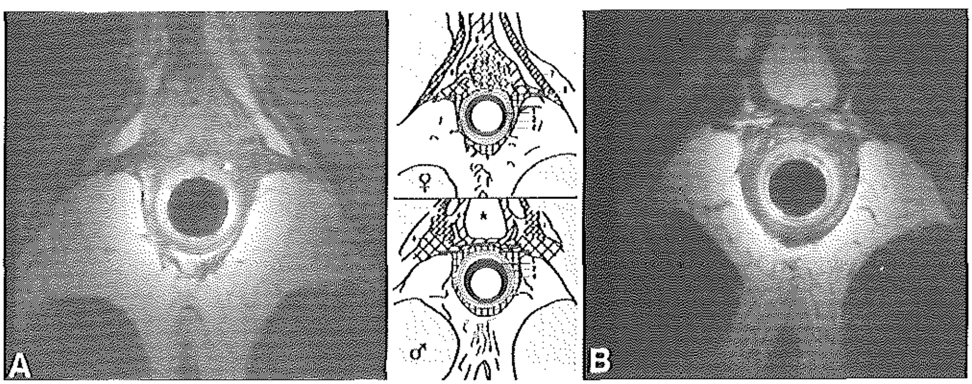

Fig. 5.2 Axial images through the level of the puborectalis sling. The urogenital diaphragm is clearly visible in the female (A) while in the male (B), at this level, the corpus spongiosum of the penis (*) is present with its attachment to the anal canal. Bulbocavernosus muscle (6). Ischiocavernosus muscle (7). Perineal muscle (8). Vagina (9).

around the pelvis. An axial T2-weighted 3D gradient-echo sequence [T2w contrast enhanced fast field echo, acquisition time 6.5 minutes, imaging matrix 205x256, number of signal averages (NSA) 2, repetition time (TR) 30ms, echo time (TE) 13ms, flip angle 60°, field of view (FOV) 140mm, slice thickness 2mm], was placed perpendicular to the

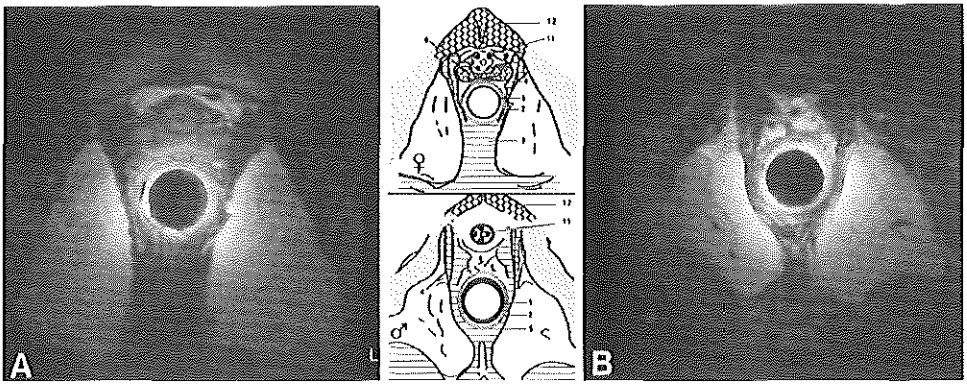

Fig. 5.3 Axial images cranial to the puborectalis muscle. Note the vagina (9) and the urethra (11) in the female (A), and only the urethra (11) in the male (B) anterior to the anal canal. Os pubis (12). Space of Retzius (✱).

long axis of the endoanal coil. Thirty-two contiguous slices were obtained. For the sagittal and the coronal scans, a T2-weighted turbo spin-echo was performed [acquisition time 5.0 minutes, imaging matrix 186x256, NSA 8, TR 2800, TE 120, turbo factor 10, FOV 120mm, slice thickness 4.0mm with an interslice gap of 0.4mm]. All exams were reviewed and systematically compared in order to understand the normal anatomy and the sex-dependent differences.

5.3 RESULTS

The muscle layers of the anal canal wall comprised of the internal sphincter, the longitudinal layer, the external sphincter and the puborectalis muscle, as well as the surrounding structures were well displayed in both sexes. The sex-dependent differences were visible in all three dimensions. Therefore, the findings have been presented in the axial (Fig. 5.1-5.3), the coronal (Fig. 5.4-5.5) and the sagittal planes (Fig. 5.6).

In the axial plane, anterior to the lower part of the external sphincter, a shield-like, downward extension of the superficial transverse perinei muscle was seen in all females while in the male, except in one case, such a structure was absent (Fig. 5.1). At a slightly upper level, the shield-like muscle became thickened. At this level, the vagina was visible in a vertical orientation anteriorly while in the male, the bulbocavernosus muscle, having the same orientation as the vagina, showed muscular connections to the anterior part of the external sphincter. More cranially, in the female, the urogenital diaphragm was clearly visible while in the male, at this level, the corpus spongiosum was present. At this level in the male, a striking feature was the decussation between the bulbocavernosus

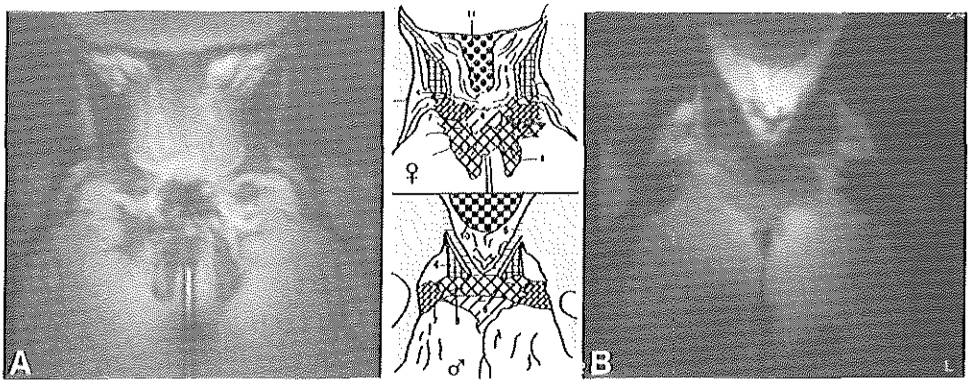

Fig. 5.4 Coronal images at the level of the urogenital diaphragm. The downward muscular extension of the perineal muscles is just visible in the female (A) while in the male (B) only the posterior part of the bulbocavernosus muscle (6) is present. Urethra (11). Prostate (10).

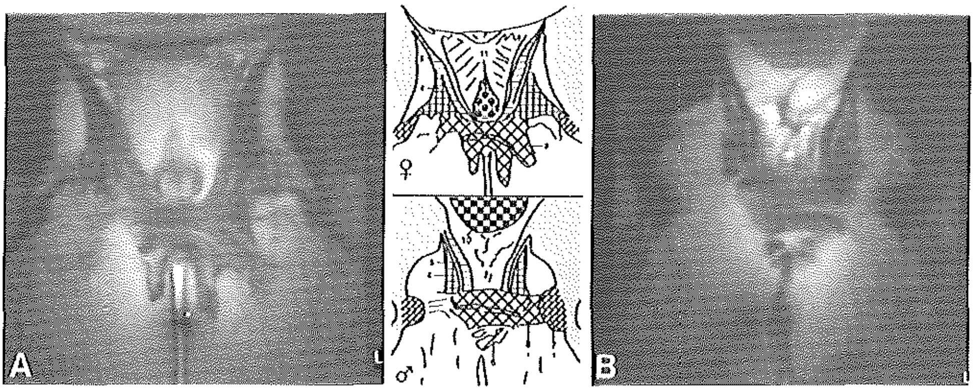

Fig. 5.5 Coronal images at the level of the urogenital diaphragm, slightly posterior to Fig. 5.4. The shield-like muscular extension of the perineal muscle (8) is well visible at this level in the female (A) while in the male (B) the horizontally orientated perineal muscle fibres (8) can be recognised. Ischiocavernosus muscles (7). Urethra (11). Prostate (10).

muscle and the external sphincter fibres. Moreover, of the urogenital diaphragm, only the perineal muscles could be distinguished at this level in the male (Fig. 5.2). Above the level of the urogenital diaphragm, the vagina and the urethra were visible in the female while in the male only the urethra was present anteriorly (Fig. 5.3).

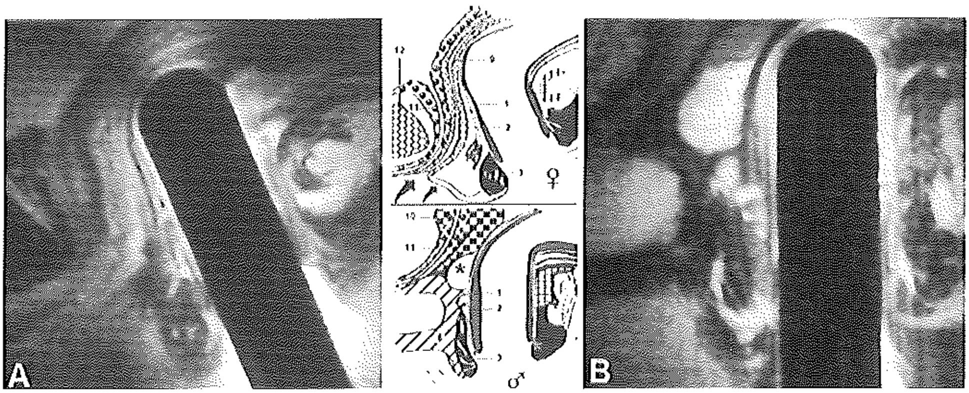

Fig. 5.6 Midsagittal images in a female (A) and a male (B) with the corresponding drawings. In the female, note the thickened and oval anterior part of the external sphincter (3) with longitudinal layer (2) terminating just cranial to it. In front of the external sphincter no other muscles or fibres are visible. In the male, the anterior part of the external sphincter (3) is supported by the bulbocavernosus muscle (6). Vagina (9). Urethra (11). Os pubis (12). Prostate (10). Introitus vaginae (curved arrows). Periprostatic space (*).

In the coronal plane, anteriorly, the funnel-shaped levator ani and the puborectalis muscles were present in both sexes. At this level, in the female, the perineal muscles with their downward extensions were clearly visible. In the male, at this level, only the bulbocavernosus muscle was present (Fig. 5.4). Slightly posteriorly, the perineal muscle in the female was more clearly visible in the female while in the male, the horizontally orientated perineal muscles without a downward extension could be seen (Fig. 5.5). More posteriorly, there was no difference in arrangement of the muscles in both sexes.

At the midsagittal level, the anterior part of the external sphincter had about the same cranio-caudal dimensions in both sexes. In females, though, this part of the external sphincter was often oval and thickened in shape. In the male, the external sphincter was supported by the bulbocavernosus muscle anteriorly while in the female, as the bulbocavernosus muscle is divided by the vagina, such a muscular support was absent. The longitudinal layer, in the male, ended into the distal part of the external sphincter while in the female, it terminated just cranial to the external sphincter. Anterior to the anal canal, the vagina and the urethra in the female and the prostate and the urethra in the male were well visible (Fig. 5.6).

5.4 DISCUSSION

Endoanal MRI is a new technique which produces high-resolution multiplanar images of both the female and the male anal sphincter complex and related structures. The sex-dependent differences are readily apparent. Initially, the newly developed endoanal MRI coil was intended to examine only the anal sphincters. Soon it was realised that this coil had sufficient range to provide also a good view of the related anatomical structures anterior to the anal sphincter complex.

Current study confirms Oh and Kark's [4] findings of the oval and thickened anterior part of the external anal sphincter in the female and the decussation of the anterior fibres of the external sphincter and the bulbocavernosus muscle in the male. A previous MRI study of the anatomy of anal sphincters and related structures in six continent women with a surface coil, did not appreciate the thickened and oval aspect of the anterior female external sphincter and stated that the entire anal canal was surrounded by the external sphincter with an anterior length almost equal to its posterior length [5]. Contrary to both studies [4,5], a recent description of the normal findings with endoanal MRI coil revealed that only the lower half of the anal canal was surrounded by the external anal sphincter in both sexes while the upper part was slinged by the puborectalis muscle [6]. The anterior and the posterior parts of the external sphincter had about the same length in both sexes [6]. The puborectalis has probably been mistaken for the deep part of the external sphincter previously [2-4]. Current study shows that the anal sphincter complex and related structures can change their shape and position even over a small distance. With endoanal MRI, one can easily identify an anatomic structure by following it on the consecutive images in a certain plane. With an anatomical dissection study, with a limited number of slices available and without knowing the exact position of the slices, it is almost impossible to identify the individual muscles accurately.

Currently, in all females, the longitudinal layer terminated just cranial to the external sphincter in the midline anteriorly. According to Oh and Kark, the whole anterior external sphincter appears as a single muscle bundle which is grossly encapsulated by a mixture of longitudinal fibres and anteriorly projecting fibres of the internal sphincter into the perineal body. Endoanal MRI in the midline did neither show any fibres encapsulating the external sphincter nor a perineal body was visible.

The perineal body is said to be the anatomic location in the central portion of the perineum where there is a meeting of the external sphincter, bulbocavernosus, and superficial and deep transverse perinei muscles [7]. According to Gordon et al [7], this combined muscular structure, separating the anus from the vagina, would give support to the perineum. With endoanal MRI, no evidence was found of such a structure. Perhaps parts of the shield-like extension of the perineal muscle or the longitudinal muscle have been mistaken for such an entity. The small space between the anterior external sphincter and the introitus vaginae is filled up with connective tissue. The amount and the location of this tissue is such that the term "perineal body" is not justifiable. Instead, the term *centrum tendinea perinei* (tendineal centre) is preferable. This phrase, also in use in classical anatomical literature, denotes an area with tendinous tissue. During anterior anal sphincter repair, restoration of this tissue is usually done by stitching together the more lateral and cranial structures, such as the perineal and the bulbocavernosus muscles.

Accurate knowledge of the anatomy of the anal sphincter complex and related structures is essential for diagnosis and treatment of patients, for instance, with faecal incontinence. In this respect, the endoanal MRI finding of the anterior part of the external sphincter in the female, being neither encapsulated nor protected in the midline anteriorly, is striking both from the clinical and surgical point of view. It explains the frequent involvement of the anterior part of the external sphincter in lacerations which can occur during a vaginal delivery. In such patients, when surgical repair is considered, endoanal MRI could be used in the preoperative assessment of the sphincter damage.

Endoanal sonography is currently the only imaging modality used to examine the anal sphincter damage [8]. A comparison of the normal anatomy with endoanal sonography and endoanal MRI revealed that, in a majority of females, with sonography the external sphincter is not visible at all [6]. Previously, with endoanal sonography, sphincter damage was detected in a relatively high number of primiparous women [8]. To assess the value of such findings and to decide which imaging modality should be used in the management of patients with a suspected obstetric injury, a comparative study will soon start in our hospital.

5.5 REFERENCES

1. Dalley AF II. The riddle of the sphincters. The morphophysiology of the anorectal mechanism reviewed. Am Surg 1987;53:298-306

2. Milligan ETC, Morgan CN. Surgical anatomy of the anal canal. The Lancet 1934;2:1150-1156

3. Goligher JC, Leacock AG, Brossy JJ. The surgical anatomy of the anal canal. Br J Surg 1955;43:51-61

4. Oh C, Kark AE. Anatomy of the external anal sphincter. Br J Surg 1972;59:717-723

5. Aronson MP, Lee RA, Berquist TH. Anatomy of anal sphincters and related structures in continent women studied with magnetic resonance imaging. Obstet Gynecol 1990;76:846-851

6. Hussain SM, Stoker J, Laméris JS. Anal sphincter complex: endoanal MR imaging of normal anatomy. Radiology 1995;197:671-677

7. Gordon PH, Nivatvongs S. Principles and practice of surgery for the colon, rectum and anus. St. Louis, Missouri: Quality Medical Publishing Inc. 1992

8. Sultan AH, Kamm MA, Hudson CN, Thomas JM, Bartram CI. Anal-sphincter disruption during vaginal delivery. New Eng J Med 1993;329:1905-1916

Chapter 6

ENDOANAL MRI OF THE ANAL SPHINCTER COMPLEX: CORRELATION WITH CROSS-SECTIONAL ANATOMY AND HISTOLOGY

6.1 INTRODUCTION

In the surgical literature, the external anal sphincter has been described consisting of one, two or three parts [1]. According to Milligan and Morgan [2] the external sphincter consists of subcutaneous, superficial and deep parts. Goligher et al [3] found no suggestion of division of the external sphincter into three separate parts. The muscle was one continuous sheet. Oh and Kark [4] proposed a two compartment view. Later on, a triple-loop system was proposed [5]. Recently, no plane of separation could be seen in any of the specimens dividing the sphincter into parts [6].

These concepts were based on dissection studies, often strengthened by the surgical experience [1]. After the introduction of endoanal sonography [7], it was possible to visualize the anal sphincters in vivo. With this modality, the internal anal sphincter is well visualized [7]. In our experience, other structures, including the external anal sphincter and the perianal anatomical spaces, were either variable in echogenicity or not visible at all. Moreover endoanal sonography is mainly restricted to the axial plane and is operator-dependent. Such limitations caused problems in identification of the external sphincter defects in patients with faecal incontinence and in preoperative classification of perianal fistulae.

To overcome these problems, magnetic resonance imaging (MRI) with an endoanal coil was applied [8]. The anatomical concept of the anal sphincter complex emerging from the endoanal MRI was in many aspects different than the present-day anatomical views [9]. In this chapter, MR-anatomic correlation of the anal sphincter complex will be obtained.

6.2 MATERIAL AND METHODS

Fourteen patients (eight men and six women with a mean age of 58.5 years, age range: 27-81 years) with rectal tumours were examined with a rigid endoanal MRI coil before undergoing abdominoperineal resection. An informed consent was obtained before examination. The resected rectal preparations were used to obtain anatomical and histological slices. In addition, twelve cadavers (six men and six women with a mean age of 64.3 years, age range: 56-71 years) were used to obtain anatomic sections. The cadavers belonged to the Department of Anatomy for research purposes.

Submitted for publication as: SM Hussain, J Stoker, AW Zwamborn, JC den Hollander, JW Kuiper, CAC Entius, JS Laméris. Endoanal MRI of the anal sphincter complex: correlation with cross-sectional anatomy and histology. Presented at the Röntgen Centenary Congress, Birmingham, 1995.

MRI study
In each patient MRI was performed at 0.5 Tesla (Gyroscan T5-II, Philips Medical Systems, Best, The Netherlands). To reduce bowel motion, one ml of butylscopolaminebromide (Buscopan 20 mg/ml, Boehringer Ingelheim KG, Ingelheim, Germany) was injected intramuscularly before scanning. A newly developed rigid endoanal coil with a diameter of 19 mm (Philips Medical Systems, Best, The Netherlands) was used. The imaging was performed in the axial, the coronal and the sagittal planes. The axial T2-weighted 3D gradient-echo sequence [T2w contrast enhanced fast field echo, acquisition time 6.5 minutes, imaging matrix 205x256, number of signal averages (NSA) 2, repetition time (TR) 30ms, echo time (TE) 13ms, flip angle 60°, field of view (FOV) 140mm, slice thickness 2mm], was placed perpendicular to the long axis of the endoanal coil. Thirty-two contiguous slices were obtained. For the sagittal and the coronal scans, a T2-weighted turbo spin-echo was performed [acquisition time 5.0 minutes, imaging matrix 186x256, NSA 8, TR 2800, TE 120, turbo factor 10, FOV 120mm, slice thickness 4.0mm with an interslice gap of 0.4mm].

Anatomic and histologic study
The rectal preparations were sliced in the axial, the coronal and the sagittal directions. For histology, anatomic slices of four different rectal preparations were fixed in 4% formalin for two days. After fixation, the slices were embedded in paraffin and sliced into the histological preparations with a thickness of 10 μm. These slices were stained with trichrome Masson for easy recognition of muscles, ligaments and collagenous fibrous tissue.

For cross-sectional anatomy, in each cadaver a rounded wooden stick used as a pseudocoil, was introduced in about the same angle as the endoanal coil in the subjects, and the cadavers were frozen immediately for at least three days. The pseudocoil had a diameter of 18 mm. The rationale for using a pseudocoil was to simulate all changes of the anal canal structures, as they would have been caused by the endoanal coil. In addition, the pseudocoil was used as a reference during sectioning of the cadavers. The plane for the axial slices was perpendicular to the pseudocoil. The plane for the coronal slices was parallel to the pseudocoil. The sagittal plane was determined by drawing a line between the processus spinosi and the pseudocoil.

The MRI scans and anatomico-histological sections of the rectal preparations and the cadavers were compared side-by-side in order to correlate MR findings to the anatomy and histology.

6.3 RESULTS

The endoanal MRI correlated well with the cross-sectional anatomy in the axial, the coronal and the sagittal planes (Fig. 6.1-6.2) as well as with histology (Fig. 6.3). In the axial plane, the layers of the anal canal wall correlated exactly to the anatomic section (Fig. 6.1A-D). In the coronal plane, the muscle layers of the lower and upper part of the anal canal were slightly different (Fig. 6.1B-E). The lower part of the anal canal was

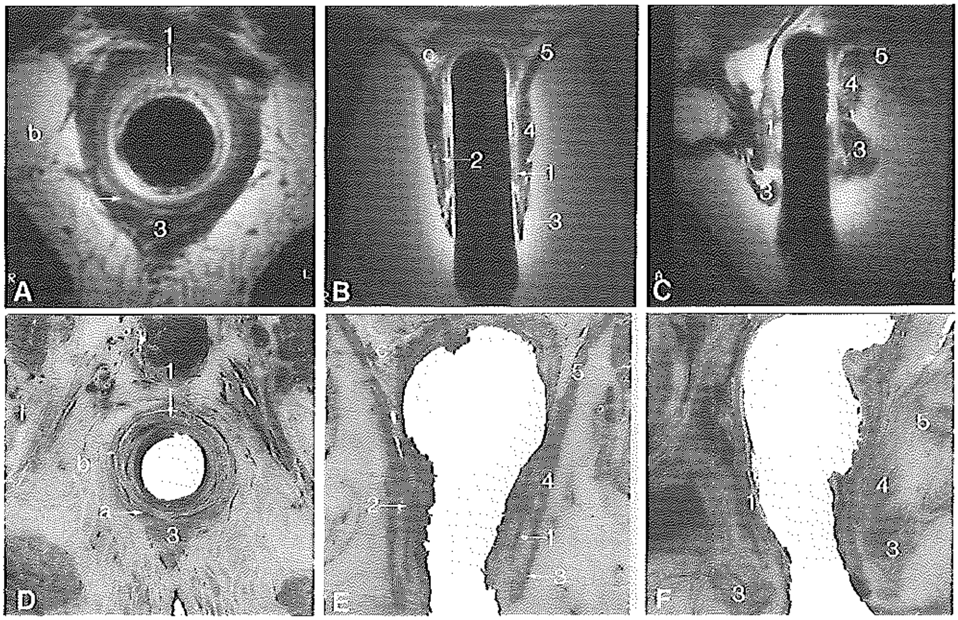

Fig. 6.1 *MR-anatomic correlation.* In the axial section A and D, the muscle layers, comprising the internal anal sphincter (1), the longitudinal layer (2) and the external anal sphincter (3), show an excellent correlation. Note the position of the external anal sphincter, the puborectal muscle and the levator ani muscle (5) in the coronal B and E and the sagittal C and F sections. Anococcygeal ligament (arrow). Supralevator space (C).

surrounded by the internal anal sphincter, the longitudinal muscle and the external anal sphincter. The upper part comprised of the internal anal sphincter, the longitudinal layer and the sling of the puborectal muscle. This arrangement of the muscles was confirmed in the consecutive sagittal sections (Fig. 6.2). The male and female differences were well illustrated with endoanal MRI and the cross-sectional anatomy (Fig. 6.1B-E and 6.2C).

Of the muscles, the *internal anal sphincter*, which is the inner-most muscle layer of the anal canal, showed an excellent MRI-anatomic correlation (Fig. 6.1B-E and 6.3). The *longitudinal layer*, the muscle layer next to the internal sphincter, traversed only the distal part of the external anal sphincter (Fig. 6.1B-E and 6.3). The *external anal sphincter* surrounded only the lower part of the anal canal. The double-layered distal ends, particularly on the mid-coronal planes, correlated well with anatomy (Fig. 6.3). The *puborectal muscle* formed a sling around the upper part of the anal canal (Fig. 6.2A-D). The *levator ani muscle* was well recognisable on MR images and anatomic sections (Fig. 6.1B and 6.2B).

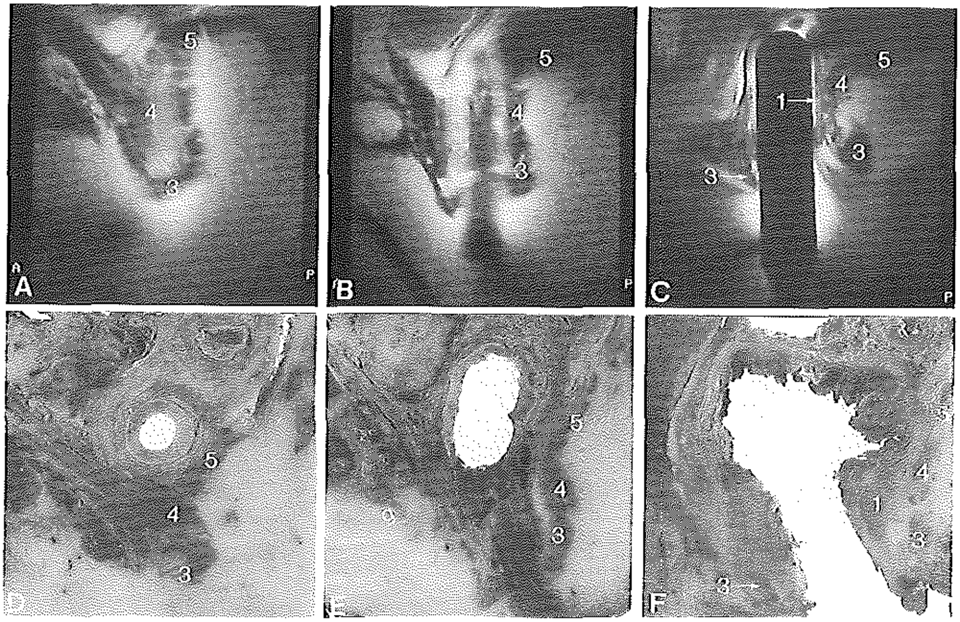

Fig. 6.2 *MR-anatomic correlation.* Consecutive sagittal images. (A-F). Note the MR-anatomic correlation in each section, with the changing appearances of the external sphincter (3), the puborectal muscle (4) and the levator ani muscle (5). Compare the female and male anatomy (Fig. 6.2C and 6.1C).

Of the perianal anatomical spaces, the *intersphincteric space*, i.e. the space between the internal anal sphincter and the external sphincter and puborectalis, was filled with connective tissue as well as fibres of the longitudinal layer (Fig. 6.3). The *ischioanal space*, i.e. the space around the anal canal, contained fatty tissue mixed with multiple fibrous septae (Fig. 6.1-6.3). Also the *deep postanal space of Courtney*, i.e. the space posterior to the anal canal and above the ano-coccygeal ligament, was clearly identifiable (Fig. 6.1c). The *supralevator space* was well identifiable above the levator ani muscle (Fig. 6.1b).

6.4 DISCUSSION

In the current study, MRI examinations of the patients were correlated with the resected rectal specimens of these patients as well as with the cross-sectional cadaveric anatomy. The cadaveric material was necessary because of often an incomplete resection of the anal sphincter complex during abdomino-perineal resections. A direct MR-anatomic correlation with the cadaveric material was not possible. MR examinations of the cadavers, performed before sectioning, had to be excluded. The muscles in the cadaveric MR

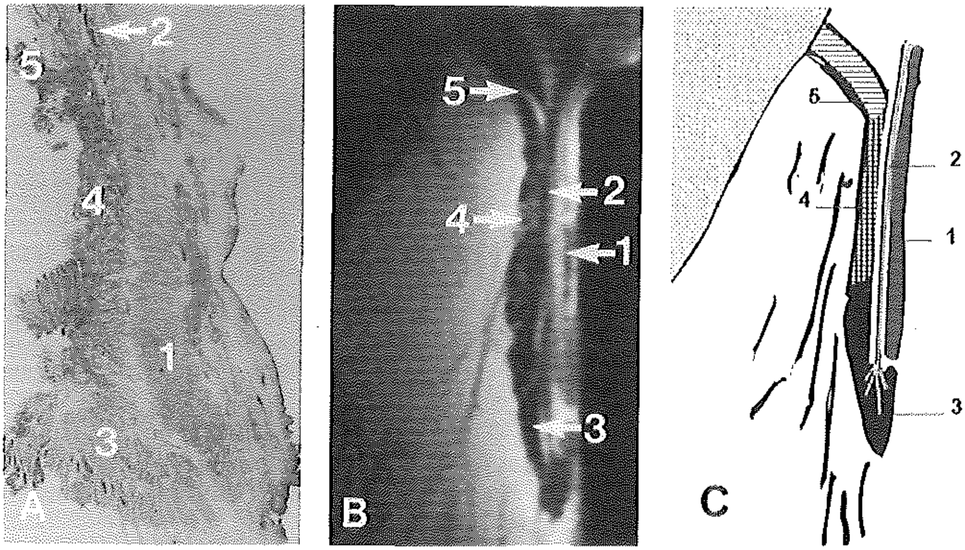

Fig. 6.3. *The right lateral half of the anal canal in coronal plane represented by the histological specimen (A), the endoanal MR image (B) and a drawing (C).* Endoanal MRI findings correlate with both the anatomy as well as the histology. Note that the muscles layers and the connective tissue are better delineated with histology due to the difference in staining of the these tissues. Internal anal sphincter (1). Longitudinal muscle layer (2). External anal sphincter (3). Puborectalis muscle (4). Levator ani muscle (5).

images were indistinct, probably due to tissue changes during fixation.

The basic anatomic concept of the anal sphincter complex has been controversial in the literature [1-6]. Endoanal MRI is a new technique which provides a different way of looking at the anatomy of the anal sphincter complex [8]. Endoanal MRI findings show an excellent correlation with the cross-sectional anatomy and histology.

The laminar concept of the external sphincter [3-5] has probably originated from using different dissection techniques and by studying slightly different parts of the sphincters. The differences between the previous concepts [2-4] and the endoanal MRI findings in the right lateral wall of the anal canal have been stressed in a previous paper [9]. There are also distinct differences between the endoanal MRI findings and the previous descriptions [4] of the anatomy in the midsagittal plane.

Soon after the introduction of endosonography [7], normal appearance of the sphincters was correlated with anatomy [10]. This study showed good correlation between endosonography and anatomy at certain levels of the anal canal in the axial plane [10]. Though, due to limitations of endosonography, the complex anatomic nature of this region was not fully understood.

An important observation during the current study was that the anal sphincter complex is contained within a volume not much larger than about 6 cm^3. Within this space, the muscles changed their configuration as well as their relationship to the adjacent structures over a small distance. For instance, in the coronal plane, at the level of the anal canal, the puborectalis muscle appears as a part of the external sphincter, while more anteriorly, in the same plane, it becomes a fraction of the levator ani muscle [9]. The puborectalis may, therefore, have been mistaken for the deep part of the external sphincter [2-5]. Currently the puborectalis muscle, apart its location in the upper part of the anal canal, was seen to contribute fibres to the longitudinal layer. This finding was important in distinguishing the puborectalis muscle from the external anal sphincter.

With a combination of multiplanar capability and high soft tissue contrast of endoanal MRI, it is easier to understand the complexity of the sphincters. The exact position of each MR slice is known. To identify a particular anatomical structure one can go back and forth within a series of slices. The previous workers [2-6] lack this facility during anatomical studies of the anal sphincter complex. This may also have played an important role in the development of many misconceptions about the sphincter anatomy existing in the literature [1]. Despite using an angle of reference in the current study, errors during sectioning were unavoidable in two cadavers.

The knowledge of the exact anatomy of the anal sphincter complex is essential for management of pathology in this area. In this respect, the findings of the current study can be of great clinical importance. For instance, in patients with fistula-in-ano, endoanal MRI could provide a road-map for surgical procedures. This could help in reducing the risk of the procedure-dependent complications. This could eventually lead to a reduction of the recurrence rate of fistulae and the occurrence of postoperative faecal incontinence. Due to the direct visualization of the external sphincter with endoanal MRI, this modality could also be valuable in patients with faecal incontinence. Currently, endoanal sonography is the modality of choice in patients with perianal fistulae and faecal incontinence [11,12]. To determine the value of endoanal MRI in both groups of patients, comparative studies with endoanal sonography and endoanal MRI are taking place in our hospital.

6.5 ACKNOWLEDGEMENT

Thanks are due to Mrs J.J.M. van Loon-van Luijt for preparation of the histological slices and to T. Rijsdijk for preparing excellent photographs.

6.6 REFERENCES

1. Dalley AF II. The riddle of the sphincters. The morphophysiology of the anorectal mechanism reviewed. Am Surg 1987;53:298-306

2. Milligan ETC, Morgan CN. Surgical anatomy of the anal canal. The Lancet 1934;2:1150-1156

3. Goligher JC, Leacock AG, Brossy JJ. The surgical anatomy of the anal canal. Br J Surg 1955;43: 51-61

4. Oh C, Kark AE. Anatomy of the external anal sphincter. Br J Surg 1972;59:717-723

5. Shafik A. A new concept of the anatomy of the anal sphincter mechanism and the physiology of defecation. The external anal sphincter: a triple-loop system. Invest Urology 1975;12:412-419

6. Ayoub SF. Anatomy of the external anal sphincter in man. Acta anat. 1979:105:25-36

7. Law PJ, Bartram CI. Anal endosonography: technique and normal anatomy. Gastroint Radiol 1989;14:349-353

8. Hussain SM, Stoker J, Kuiper JW, Schouten WR, den Hollander JC, Laméris JS. MR imaging of anal sphincter complex with an endoanal coil: normal anatomy and pathology. Radiology 1994;193(P):445

9. Hussain SM, Stoker J, Laméris JS. Anal sphincter complex: endoanal MR imaging of normal anatomy. Radiology 1995; 197: 671-677

10. Sultan AH, Nicholls RJ, Kamm MA, Hudson CN, Beynon J, Bartram CI. Anal endosonography and correlation with in vitro and in vivo anatomy. Br J Surg 1993;80:508-511

11. Choen S, Burnett S, Bartram CI, Nicholls RJ. Comparison between anal endosonography and digital examination in the evaluation of anal fistulae. Br J Surg 1991;78:445-447.

12. Sultan AH, Kamm MA, Hudson CN, Thomas JM, Bartram CI. Anal-sphincter disruption during vaginal delivery. New Eng J Med 1993;329:1905-1916

Chapter 7

FISTULA-IN-ANO: ENDOANAL SONOGRAPHY vs ENDOANAL MRI

7.1 INTRODUCTION

The perianal fistulae occur in about 10 per 100 000 of the general population[1]. In tertiary referral centres, however, this disease is a common problem. The treatment of fistula-in-ano is surgery. To diminish the postoperative occurrence of faecal incontinence and to keep the recurrence rate as low as possible, understanding of the exact relationship of the fistula to the perianal anatomical structures and spaces is crucial[2]. To characterize this relationship, Parks et al[2] have classified fistula-in-ano into several groups. Each group requires a slightly different operative procedure. The preoperative classification of fistula-in-ano facilitates the determination of the proper surgical procedure.

In this respect, imaging can play an important role. Fistulography[3], which has been used for years, was said to be inaccurate[4]. Computed tomography (CT)[5] and magnetic resonance imaging (MRI)[6-8] have been proposed, though, endoanal sonography[9] is currently the imaging modality of choice in patients with fistula-in-ano. After the initial optimistic reports[9,10], high expectations of endosonography have been tempered[11]. Low soft tissue contrast and occurrence of artifacts may be responsible for the poor results. To overcome the diagnostic problems, MRI with a rigid endoanal coil was introduced[12].

In this chapter, endoanal sonography and endoanal MRI were compared to assess their value in visualization and classification of fistula-in-ano.

7.2 MATERIALS AND METHODS

Between July 1994 and August 1995, forty-two consecutive patients presented with clinically evident fistula-in-ano. Of these patients fourteen, comprised of seven Crohnic fistulae, six ano-vaginal fistulae and one recto-urethral fistula, as being separate entities, were excluded. After an informed consent was obtained, the remaining patients (n=28) were included in the study. On the basis of clinical follow-up, laboratory and endoscopical findings, these patients had no specific underlying disease. The fistulae were characterized as non-specific, crypto-glandular fistulae. There were 19 males and 9 females with a mean age of 43 years (age range 19-70 years). All patients, except four, had undergone one or more operations for fistulae before. Endoanal sonography and endoanal MRI were performed at average six weeks (range: 1-31 weeks) before surgery.

Endoanal sonography

For endoanal sonography, a Brüel & Kjaer (Naerum, Denmark) ultrasound scanner was used with a rotating probe providing a 360° image. A 7 MHz transducer with minimum beam width of 1.1 mm and a focal length of about 3 cm, was used. A hard, sonolucent

---

SM Hussain, J Stoker, WR Schouten, WCJ Hop, JS Laméris. Fistula-in-ano: endoanal sonography versus endoanal MRI. Radiology (in press).

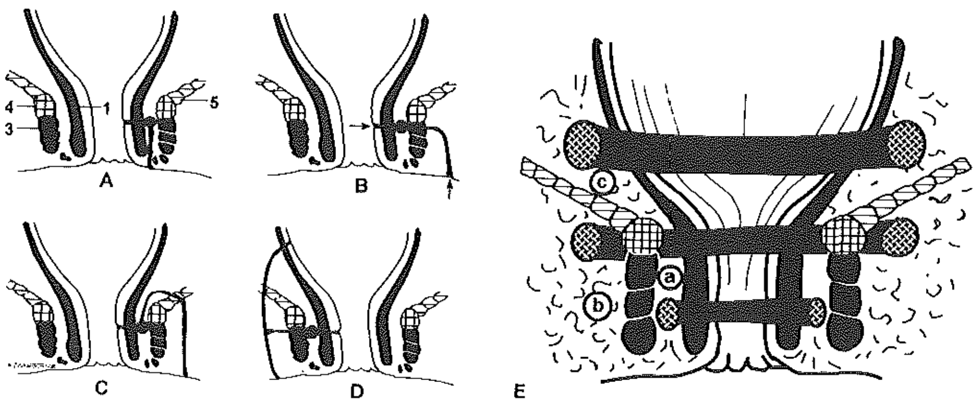

Fig. 7.1. *Parks' classification.* Intersphincteric fistula (A) located between the internal and the external anal sphincter. Transsphincteric fistula (B) crossing these muscles and running in the ischioanal space. The suprasphincteric (C) and extrasphincteric (D) fistulae are rare and show a complex course. Note the horseshoe-shaped spread of inflammation (E).

plastic cone with a diameter of 17 mm covered the transducer and was filled with degassed water for acoustic coupling. The cone was covered with a condom with gel applied to both surfaces. Axial images were performed through the anal canal.

Endoanal MRI

MR imaging was performed at 0.5T (Gyroscan T5-II, Philips Medical Systems, Best, The Netherlands), without bowel preparation. To reduce bowel motion, one ml of butylscopolaminebromide (Buscopan 20 mg/ml, Boehringer Ingelheim KG, Ingelheim, Germany) was injected intramuscularly before scanning. A newly developed endoanal coil with a diameter of 19 mm (Philips Medical Systems, Best, The Netherlands) was used. The coilholder was covered with a condom and gel was applied to the surface. An axial T2-weighted 3D gradient-echo sequence [T2w contrast enhanced fast field echo, acquisition time 6.5 minutes, imaging matrix 205x256, number of signal averages (NSA) 2, repetition time (TR) 30ms, echo time (TE) 13ms, flip angle 60°, field of view (FOV) 140mm, slice thickness 2mm], was placed perpendicular to the long axis of the endoanal coil. For the sagittal and the coronal scans, a T2-weighted turbo spin-echo was performed [acquisition time 5.0 minutes, imaging matrix 186x256, NSA 8, TR 2800, TE 120, turbo factor 10, FOV 120 mm, slice thickness 4.0 mm with an interslice gap of 0.4mm]. The coronal slices were parallel to the long axis of the endoanal coil.

According to Parks et al [2], the non-specific, crypto-glandular fistulae can be divided into several groups (Fig. 7.1A). An intersphincteric fistula passes the internal sphincter and spreads within the intersphincteric space. The transsphincteric fistula crosses the internal sphincter, longitudinal layer and the external sphincter and spreads within the ischioanal space. Any of these fistulae can show horse-shoeing (Fig. 7.1B). When the horse-shoe component predominates, the fistula is called a horse-shoe fistula.

Table 7.1. The assessment of fistula-in-ano with endoanal sonography, endoanal MRI and surgery. Intersphincteric fistulae are almost equally diagnosed with sonography, MRI and surgery. Transsphincteric fistulae are poorly detected with ultrasound. Suprasphincteric and extrasphincteric fistulae were not present in this study. MRI is better in classification of horse-shoe fistulae. Non-classification occurred in the majority of cases with sonography.

	Endoanal US		Endoanal		Surgery	
	N	%	N	%	N	%
Intersphincteric fistula	10	36	12	42	16	57
Transsphincteric fistula	5	18	10	36	9	32
Suprasphincteric fistula	0	0	0	0	0	0
Extrasphincteric fistula	0	0	0	0	0	0
Horseshoe fistula	2	7	3	11	1	4
Non-classification	11	39	3	11	2	7
Total	28	100	28	100	28	100

To classify fistulae and to assess the presence of internal openings, fluid collections and horse-shoeing, endoanal sonography and endoanal MRI were assessed separately by two different workers (SMH and JS). During surgery fistulae were classified, without the knowledge of the imaging findings, by a colo-rectal surgeon (WRS). Percentages were compared by using McNemar's test. Two-sided p-values of <0.05 were considered significant. The agreement between the findings was assessed by calculating kappa-values[13].

7.3 RESULTS

Classification of fistula-in-ano was possible in 61% (17/28) with endoanal sonography, in 89% (25/28) with endoanal MRI and in 93% (26/28) with surgery (Table 7.1).
These percentages were significantly different between endosonography versus MRI and surgery ($p<0.05$), while not significantly different between MRI and surgery. Concordance between the findings was as follows: between endoanal sonography and MRI in 46% (13/28) of the cases (kappa=0.27, indicating poor agreement) (Table 7.2), between sonography and surgery in 36% (10/28) of the cases (kappa=0.09, indicating no agreement) and between MRI and surgery in 64% (18/28) of the cases (kappa=0.43, indicating moderate agreement) (Table 7.3). Intersphincteric fistulae (Fig. 7.2 and 7.4) could almost equally be classified with both imaging modalities as well as surgery (Table 7.1). With sonography, the percentage of cases with transsphincteric fistulae (Fig. 7.3-7.4) was lower as countered with MRI and surgery (Table 7.1). Of the three cases with a horse-shoe fistula (Fig. 7.5-7.6) according to MRI, one was missed by ultrasound (Table

Table 7.2. A comparison of endoanal sonography and endoanal MRI in classification of each type of fistula. Both imaging modalities show agreement in 46% (7+2+2+2 = 13/28) of the cases with a kappa-value of 0.27, indicating a poor agreement. (IS=intersphincteric fistula, TS= transsphincteric fistula, HS=horse-shoe fistula, NC=non-classification)

MRI \ US	IS	TS	HS	NC	Total
IS	7	1	0	4	12
TS	3	2	0	5	10
HS	0	1	2	0	3
NC	0	1	0	2	3
To-	10	5	2	11	28

Table 7.3. A comparison of endoanal MRI and surgery in classification of each type of fistula. MRI and surgery agree in 64% (11+6+1+0 = 18/28) of the cases with a kappa-value of 0.43, indicating a moderate agreement. (IS=intersphincteric fistula, TS=trans- sphincteric fistula, HS=horse-shoe fistula, NC= non-classification)

SURGERY \ MRI	IS	TS	HS	NC	Total
IS	11	2	0	3	16
TS	1	6	2	0	9
HS	0	0	1	0	1
NC	0	2	0	0	2
Total	12	10	3	3	28

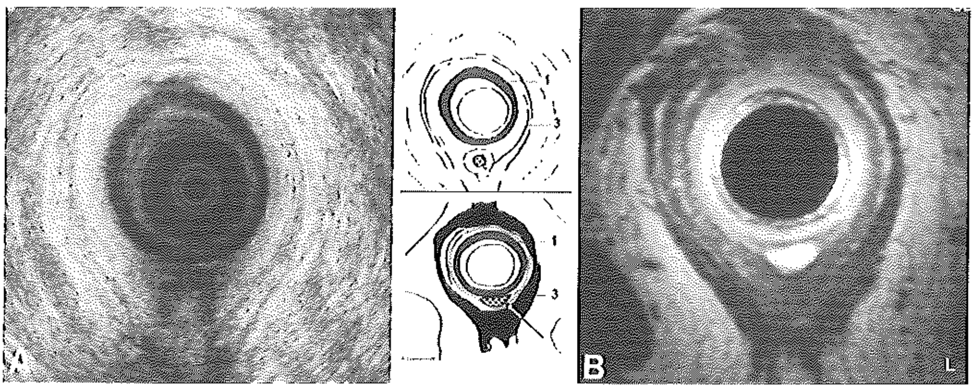

Fig. 7.2. *Intersphincteric fistula.* Axial images. With sonography (A); upper drawing) a hypoechoic fistula (arrow) is visible just outside the internal sphincter (1). With MRI (B); lower drawing) a hyperintense fistula (arrow) is visible within the intersphincteric space. External sphincter (3).

7.2), and two by surgery (Table 7.3). A classification was not possible in 39% (11/28) with endoanal sonography, in 11% (3/28) with endoanal MRI and in 7% (2/28) with surgery. Fluid collections (Fig. 7.7-7.8) were detected with both imaging modalities and surgery in 25% (7/28). Of these seven cases, two supralevatoric and one intersphincteric abscesses were found with both imaging modalities; other three abscesses, in which

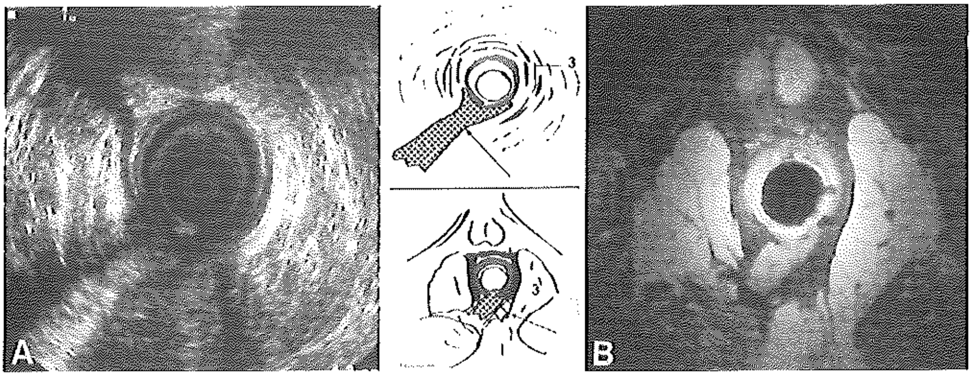

Fig. 7.3. *Transsphincteric fistula.* With sonography (A); upper drawing) an abnormality is visible right dorsolaterally (arrow). Endoanal MRI (B); upper drawing) shows a hyperintense fistula crossing the external sphincter (3).

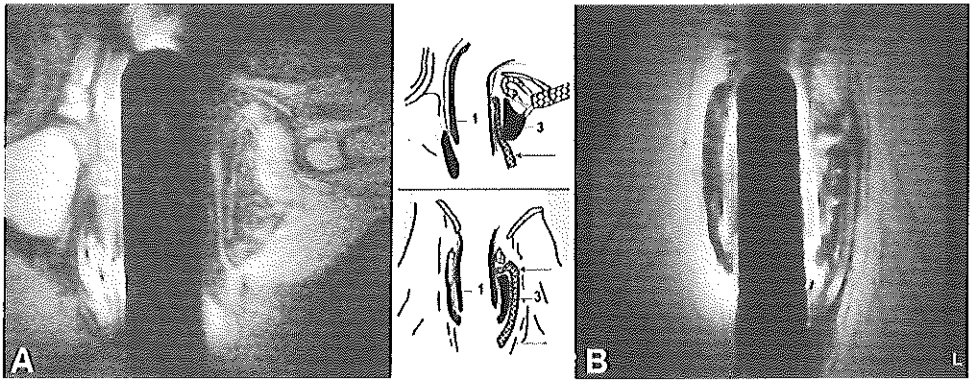

Fig. 7.4. *Intersphincteric versus transsphincteric fistula.* MR images. Intersphincteric fistula(A) (arrow) running between the internal (1) and the external (3) sphincters, whereas the transsphincteric fistula(B) (arrow) runs outside the external sphincter (3).

sonography was inconclusive, appeared to be infralevatoric on MR. In one case, due to scar tissue, the localization of the abscess remained inconclusive with both imaging modalities and surgery. The internal openings were detected in 43% (12/28) with endosonography, in 71% (20/28) with MRI and in 86% (24/28) with surgery.

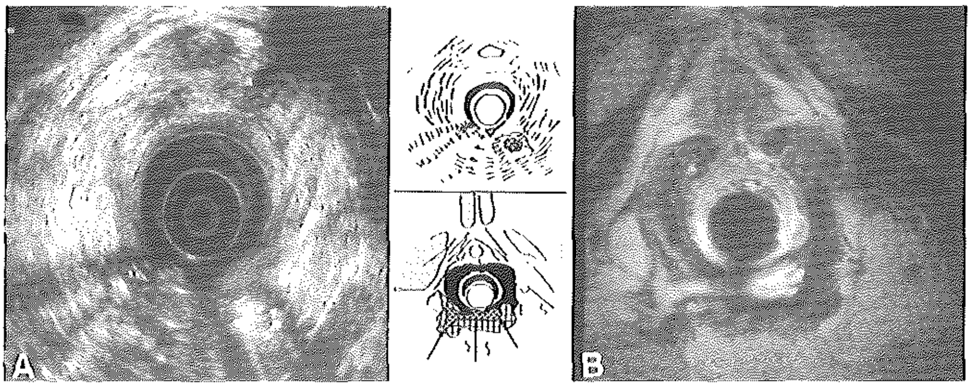

Fig. 7.5. *Horse-shoe fistula.* Axial images. Sonographic image (A); upper drawing) is indistinct. MRI (A); lower drawing) shows the connection between the two fistulae (arrow).

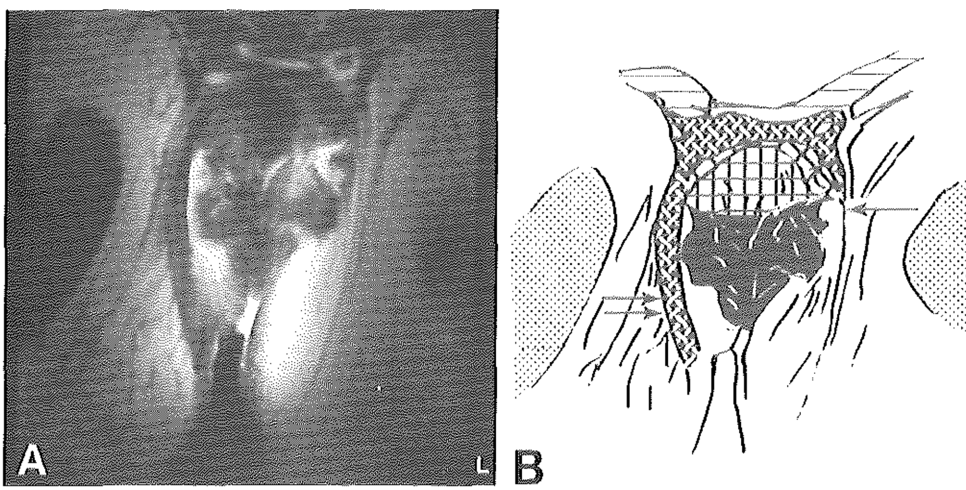

Fig. 7.6. *Horse-shoe fistula.* The same patient as in Fig. 7.5. Coronal MR image (A) with the corresponding drawing on the right (B). Note that the left leg of the fistula is shorter than the right leg.

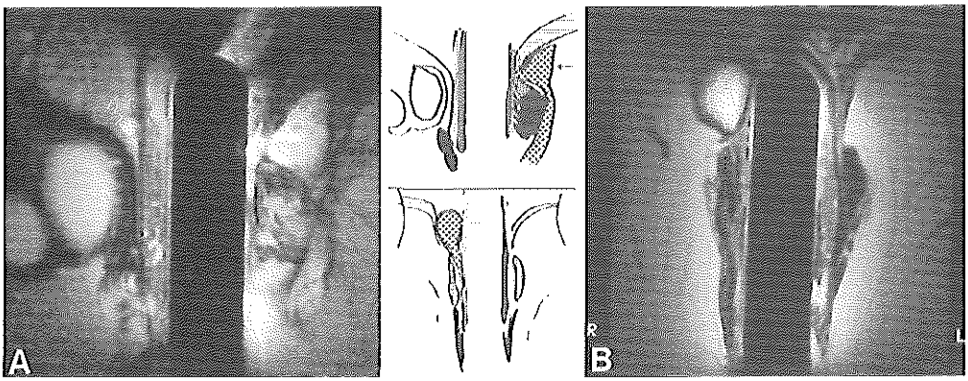

Fig. 7.7. *Infralevator versus supralevator abscess.* Sagittal and coronal MR images. Infralevatoric abscess, due to a transsphincteric fistula, (A); upper drawing) visible in the ischioanal space (arrow). The Supralevatoric abscess (B); lower drawing) is an extension of an intersphincteric fistula.

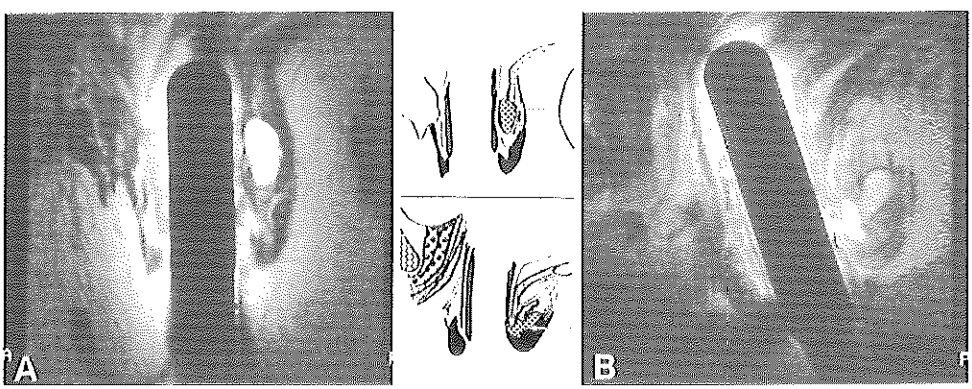

Fig. 7.8. *Intersphincteric versus deep postanal abscess.* Coronal (A) and sagittal (B) MR images. Intersphincteric abscess (A); upper drawing) visible between the internal and the external sphincter. Deep postanal abscess (B); lower drawing) located outside and above the external sphincter.

7.4 DISCUSSION

Inflammation of the anal glands presents as an anorectal abscess in the acute phase, while in the chronic phase, the disease will manifest as fistula-in-ano [2]. Although, Parks et al [2] have divided the fistula-in-ano into several groups, within each group the fistula can be variable in its complexity [2]. The occurrence of horse-shoeing and fluid collections can further complicate the picture. Apart from exact classification, an accurate assessment of such findings is essential for proper surgical management.

Current results show that endoanal MRI is superior to endoanal sonography in visualization and classification of fistula-in-ano. Unlike endoanal sonography, endoanal MRI was in concordance with surgery in the majority of cases. High inherent soft tissue contrast may undoubtedly have played an important role in improved visualization of fistulae with endoanal MRI. The ability of endoanal MRI to display the normal anatomy accurately [14], however, is more significant for classification of fistula-in-ano. Due to high spatial resolution of the endoanal coil, small details, such as the slit-like intersphincteric space, can be visualized [14]. The visualization of intersphincteric space is important because the inflammation within this space is the starting-point of all types of the crypto-glandular fistulae [2].

Currently there was a moderate concordance between endoanal MRI and surgery in the classification of fistulae. Problems in classification of fistulae during operation can occur, particularly, when fistulae have recurred despite one or more previous attempts at treatment [15]. Discrepancies between MRI and surgery in classification of intersphincteric and transsphincteric fistulae occurred in a number cases. Transsphincteric fistulae can track through various levels of the anal canal (Fig. 7.9). In some cases, when a transsphincteric fistula runs through the lower part of the anal canal, only a small amount of the external anal sphincter will be found below the fistulous track. In such cases, fistulae could have been incorrectly classified as intersphincteric fistulae either with MR or with surgery.

Similarly, interssphincteric fistulae may have been confused with low transsphincteric fistulae. Treating a very low transsphincteric fistula as an intersphincteric fistula will result in damage of a small amount of the external sphincter, and is unlikely to cause incontinence. In contrast, the treatment of a horse-shoe fistula as a transsphincteric fistula is more serious [16]. When a horse-shoe fistula has only one external opening, the surgeon will cannulate it, unaware of a blindly ending track on the opposite side, and will classify the fistula as transsphincteric. In fact, both horse-shoe fistulae were classified as transsphincteric at first attempt during surgery (Table 7.3) were of such configuration. They were confirmed as horse-shoe fistulae at a subsequent operation.

Preoperative classification of fistula-in-ano with endoanal MRI and a close cooperation between the radiologist and the colo-rectal surgeon can avoid such problems and may prevent unnecessary errors of interpretation. This may eventually improve the concordance rate between endoanal MRI and surgery. Non-classification could persist in some cases, with extensive scarring of the anal sphincters after multiple surgical procedures or due to technical errors during imaging.

Recently, several reports have been published [6-8], propagating the use of MRI for the assessment of perianal fistula-in-ano. In one of these studies [8], MRI, using an external

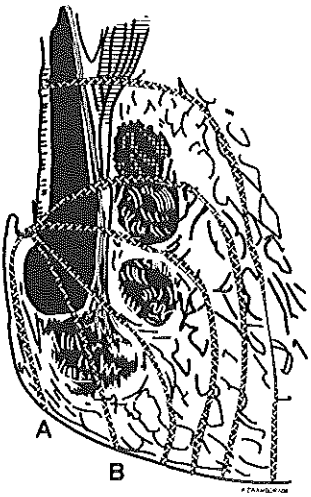

Fig. 7.9. *Intersphincteric versus transsphicteric fistula.* Transsphincteric fistulae can run through different levels of the anal canal. Note the varying amount of muscle below each fistulous track. Compare the intersphincteric fistula (A) to a very low transsphincteric fistula (B).

surface coil or a body coil, high accuracy rate of 89% and concordance between MRI and surgery of 86% was reported. Also the detection of abscesses, horse-shoeing and internal openings was, despite using a slice thickness of 5mm with an interslice gap of 2mm, highly accurate [8]. These results are surprising. With such values of the slice thickness, for instance, the intersphincteric space and the internal anal sphincter, which the authors admitted [8], are not visualized. The visualization of such structures is necessary for accurate classification of fistula-in-ano. Endoanal coil appeared to be superior to the surface coil MRI in a comparative study of ten patients with anal fistulae [17].

The use of saline solution as contrast agent during MR examinations of perianal fistulae has been suggested [7]. Currently no contrast medium or any other solution was necessary to inject into the fistula during MR examination. The majority of fistulae were well recognizable within the fatty connective tissue of the perianal anatomical spaces. In most cases, the fistulae were contained within a fibrotic fistulous canal which was clearly distinguishable from, for instance, the multiple fibrotic septae visible in the anatomical spaces. Only when a fistula is not obvious due to the presence of extensive scarring or destruction of the normal anatomical structures, injection of fluid could be taken into consideration.

This study is limited to a relatively small number of patients with a moderate concordance between MRI and surgery. Preoperative knowledge of the MR imaging findings by the surgeon and the feed-back of the surgical findings to the radiologist could improve the concordance rate. Current results suggest that endoanal MRI should be used in the management of fistula-in-ano.

7.5 ACKNOWLEDGEMENT

Thanks are due to T. Rijsdijk for excellent photography and to AW Zwamborn for preparing the high-quality drawings.

7.6 REFERENCES

1. Sainio P. Fistula-in-ano in defined population. Incidence and epidemiological aspects. Acta Chir Gynaecol 1984;73:219-224

2. Parks AG, Gordon PH, Hardcastle JD. A classification of fistula-in-ano. Br J Surg 1976;63: 1-12

3. Weisman RI, Orsay CP, Pearl RK, Abcarian H. The role of fistulography in fistula-in-ano. Dis Colon Rectum 1991;34:181-184

4. Kuijpers HC, Schulpen T. Fistulography for fistula-in-ano. Dis Colon Rectum 1985;28:103-104

5. Guillaumin E, Jeffrey RB Jr, Shea WJ, Asling CW, Goldberg HI. Perirectal inflammatory disease: CT findings. Radiology 1986;161:153-157

6. Lunniss PJ, Armstrong P, Barker PG, Reznek RH, Phillips RK. Magnetic resonance imaging of anal fistulae. The Lancet 1992;340:394-396

7. Myhr GE, Myrvold HE, Nilsen G, Thoresen JE, Rinck PA. Perianal fistulae: use of MR imaging for diagnosis. Radiology 1994;191:545-549

8. Barker PG, Lunniss PJ, Armstrong P, Reznek RH, Cottam K, Phillips RK. Magnetic resonance imaging of fistula-in-ano: technique, interpretation and accuracy. Clin Radiol 1994;49:7-13

9. Law PJ, Talbot RW, Bartram CI, Northover JMA. Anal endosonography in the evaluation of perianal sepsis and fistula in ano. Br J Surg 1989;76:752-755

10. Tio TL, Mulder CJJ, Wijers OB, Sars PRA, Tytgat GNJ. Endosonography of peri-anal and peri-colorectal fistula and/or abscess in Crohn's disease. Gastroint endoscopy 1990;36:331-336

11. Choen S, Burnett S, Bartram CI, Nicholls RJ. Comparison between anal endosonography and digital examination in the evaluation of anal fistulae. Br J Surg 1991;78:445-447

12. Hussain SM, Stoker J, Kuiper JW, Schouten WR, den Hollander JC, Laméris JS. MR imaging of anal sphincter complex with an endoanal coil: normal anatomy and pathology. Radiology 1994;193(P):445

13. Altman DG. Practical statistics for medical research. Chapman & Hall, London, 1991.

14. Hussain SM, Stoker J, Laméris JS. Anal sphincter complex: endoanal MRI of the normal anatomy. Radiology 1995;197:671-677

15. Choen S, Phillips RKS. Insights gained from the management of problematical anal fistulae at St. Mark's Hospital, 1984-1988. Br J Surg 1991;78:539-541

16. Held D, Khubchandani I, Sheets J, Stasik J, Rosen L, Riether R. Management of anorectal horseshoe abscess and fistula. Dis Colon Rectum 1986;29:793-797

17. Stoker J, Hussain SM, Van Kempen D, Elevelt AJ, Laméris JS. Endoanal coil in MR imaging of anal fistulas. AJR 1996;166:360-362

Chapter 8

FAECAL INCONTINENCE: ENDOANAL SONOGRAPHY versus ENDOANAL MRI

8.1 INTRODUCTION

Faecal incontinence is a common problem in the elderly [1]. The prevalence in the community, which increases with age, has been estimated as 2-13 per 1000 [1]. The most common causes of faecal incontinence are obstetric injury and previous surgical procedures [1]. Childbirth is considered the most common cause of faecal incontinence in women [1-2]. Early studies [3-4] concluded that incontinence resulted from denervation of the anal sphincters, and not from direct muscle damage. Endosonography [5-8] revealed structural damage to the sphincters, which was an important finding, particularly in patients who could be treated surgically. There are several options for treating faecal incontinence [9]. The choice of treatment depends on the severity of incontinence and the presence or absence of sphincter defects.

In this respect, endosonography has become an important technique for identification of patients with sphincter defects [5-7]. Endosonographic findings have been shown to correlate well with manometry and electromyography [5,10]. Endosonography, currently, plays an important role in surgical decision-making in patients with faecal incontinence, and could replace the invasive electromyography [8].

Recently endoanal MRI was introduced [11]. Normal anatomy of the anal sphincter complex appeared to be different from the present-day surgico-anatomical concepts (Chapter 3) [12]. In addition, in a comparison of endoanal sonography and MRI, the normal sonographic appearance of the external sphincter in females did not correlate with the findings of this structure with endoanal MRI (Chapter 4).

In this chapter, endoanal sonography and endoanal MRI were compared in patients with faecal incontinence, to assess their value in characterization of the sphincter damage.

8.2 MATERIALS AND METHODS

Between July 1994 and August 1995, forty-four consecutive patients presented with clinically evident faecal incontinence. Of these, six patients were excluded from the study: three were with congenital anorectal malformations, two showed excessive motion artifacts during MR examination, and in one imaging was impossible due to the extensive scar tissue. After an informed consent was obtained, the remaining patients (n=38) were included in the study. There were 10 males and 28 females with a mean age of 53.1 years (age range 30-73 years). In 28 patients a clinical cause of faecal incontinence was known: obstetric injury (14 patients), fistula surgery (7 patients), manual dilatation (2 patients), hemorrhoidectomy (2 patient), lateral internal sphincterotomy (2 patient), and rape (1 patient). In the remaining 10 patients, who were all women, no particular cause could be identified, though, these patients had had one or more, as far as they could remember uneventful, vaginal deliveries. All patients were examined with endoanal sonography and endoanal MRI.

Submitted for publication as: SM Hussain, J Stoker, WR Schouten, JS Laméris. Faecal incontinence: endoanal sonography vs endoanal MRI.

Endoanal sonography
For endoanal sonography, a Brüel & Kjaer (Naerum, Denmark) ultrasound scanner was used with a rotating probe providing a 360° image. A 7 MHz transducer with minimum beam width of 1.1 mm and a focal length of about 3 cm, was used. A hard, sonolucent plastic cone with a diameter of 17 mm covered the transducer. This cone was filled with degassed water for acoustic coupling and covered with a condom, after gel was applied to both surfaces. Axial images were performed, at least at four different levels, through the anal canal.

Endoanal MRI
MR imaging was performed at 0.5T (Gyroscan T5-II, Philips Medical Systems, Best, The Netherlands). To reduce bowel motion, one ml of butylscopolaminebromide (Buscopan 20 mg/ml, Boehringer Ingelheim KG, Ingelheim, Germany) was injected intramuscularly before scanning. A newly developed endoanal coil with a diameter of 19 mm (Philips Medical Systems, Best, The Netherlands) was used. The coilholder was covered with a condom and gel was applied to the surface. An axial T2-weighted 3D gradient-echo sequence [T2w contrast enhanced fast field echo, acquisition time 6.5 minutes, imaging matrix 205x256, number of signal averages (NSA) 2, repetition time (TR) 30ms, echo time (TE) 13ms, flip angle 60°, field of view (FOV) 140mm, slice thickness 2mm], was placed perpendicular to the long axis of the endoanal coil. For the sagittal and the coronal scans, a T2-weighted turbo spin-echo was performed [acquisition time 5.0 minutes, imaging matrix 186x256, NSA 8, TR 2800, TE 120, turbo factor 10, FOV 120mm, slice thickness 4.0mm with an interslice gap of 0.4mm]. The coronal slices were parallel to the long axis of the endoanal coil.

Two workers evaluated endoanal sonography (SMH) and MRI (JS), separately. To assess the sphincter damage with sonography, the previous criteria for sphincter damage [4] were used. The internal anal sphincter defect is defined as an interruption of the hypoechoic ring. The external anal sphincter defect is defined as a change in the band of mixed echogenicity located just outside the external sphincter. To determine sphincter damage with endoanal MRI, as no criteria exist, the normal endoanal MR findings (Chapter 3) were used as a reference [12]. Any change in the appearance of muscles, the presence of scar tissue or interruption of the muscular rings was recorded. To understand the discrepancies, the two techniques were compared side by side as well (SMH).

8.3 RESULTS

The sphincter damage was detected in 84% (32/38) with endoanal sonography and in 79% (30/38) with endoanal MRI. In detection of the sphincter damage, both techniques were in agreement in 63% (24/38) of the cases. Particularly, with endoanal MRI clear distinction of all muscle layers, the detection of scar tissue, and defects were possible. Due to this ability of MRI, the sphincter damage could be subdivided into: 1) localized defects, 2) localized scarring, 3) generalized scarring, 4) fragmentation, and 5) atrophy.

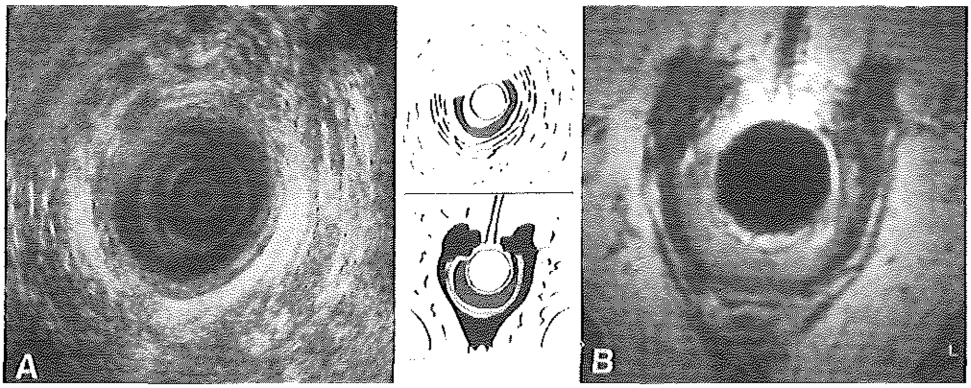

Fig. 8.1 *Localized defect.* A female (40) with a total rupture after delivery. With sonography (A), upper drawing), the internal sphincter (1) defect is well visible. Abnormal echogenicity anteriorly indicates an external sphincter (3) defect. With endoanal MRI (B),lower drawing), all layers show a defect anteriorly.

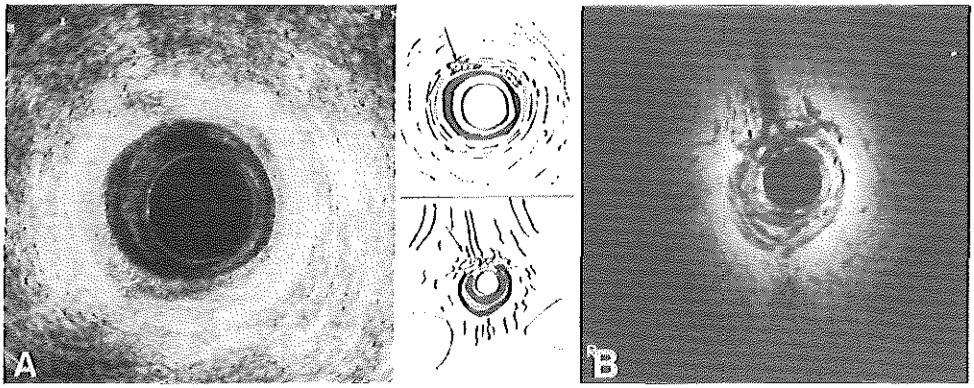

Fig. 8.2 *Localized defect with scarring.* A female (36) became incontinent after an obstetric injury. Note the scar tissue and the defects anteriorly with sonography (A),upper drawing) and MRI (B),lower drawing). Internal sphincter (1). External sphincter (3). Scar tissue (arrow).

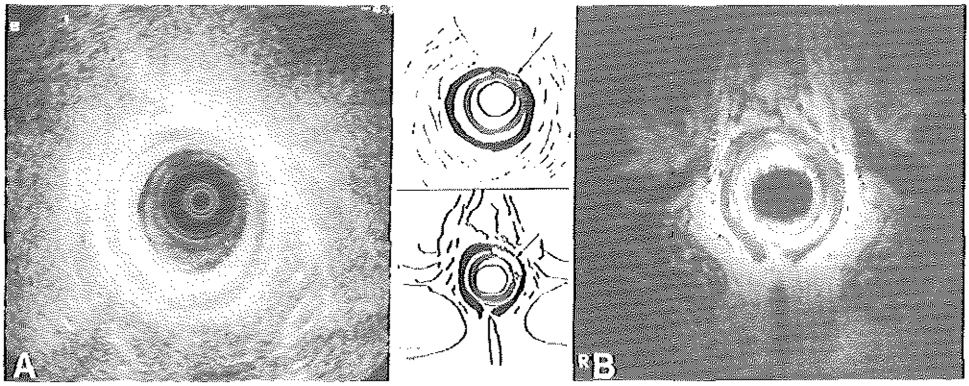

Fig. 8.3 *Localized scarring.* Axial sonography (A) and MRI (B) in a male (37) with faecal incontinence after hemorrhoidectomy. Note the deformation of the external sphincter (arrow) left anteriorly due to the presence of scar tissue.

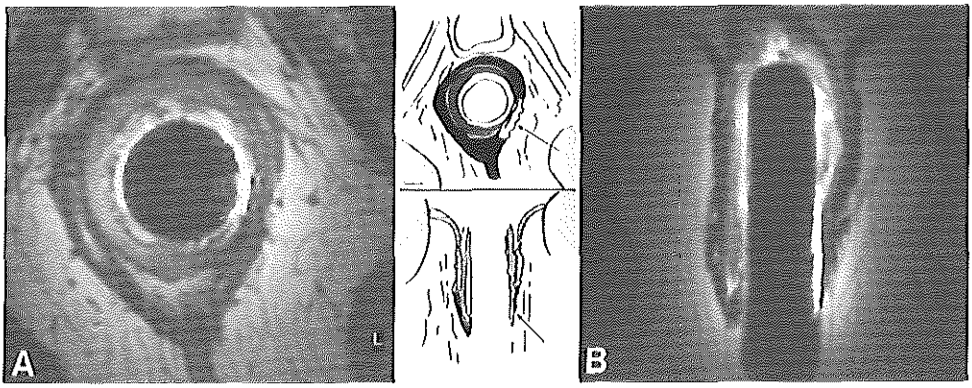

Fig. 8.4 *Localized scarring.* Axial (A) and coronal MRI (B) in a male (31) with faecal incontinence after fistulectomy. On the right, normal muscle layers are present. On the left, there is a localized scarring (arrow) of all layers.

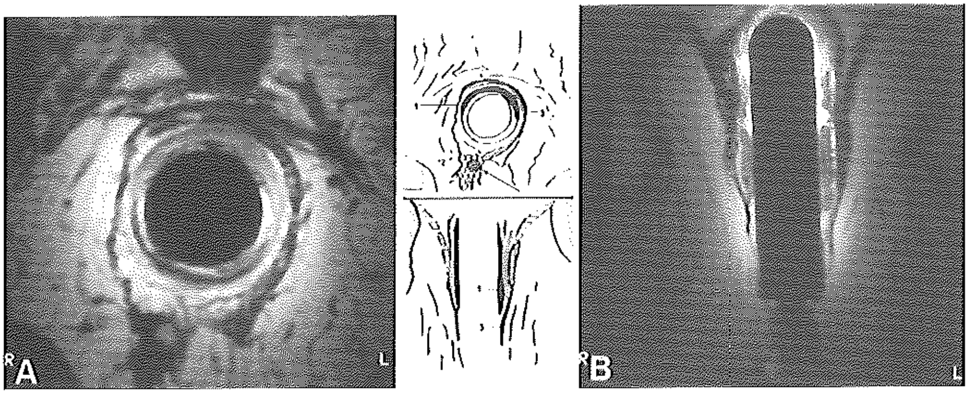

Fig. 8.5 *Generalized scarring*. Axial (A) and coronal MRI (B) in a male (45) with faecal incontinence after multiple operations for fistula-in-ano. The external (3) and a part of the internal sphincters (1) are replaced by scar tissue. Fistula (arrow) is still present.

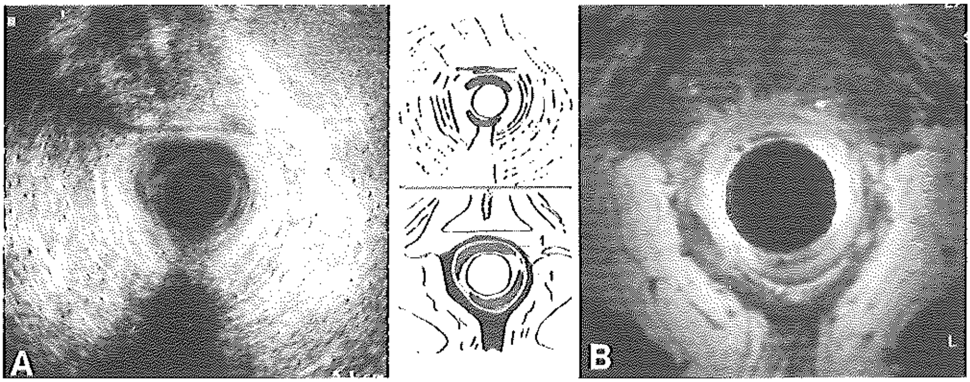

Fig. 8.6 *Fragmentation*. Axial sonography (A) and MRI (B) in a female (29) with incontinence after an unwanted anal penetration. The internal sphincter (1) is divided into at least two fragments.

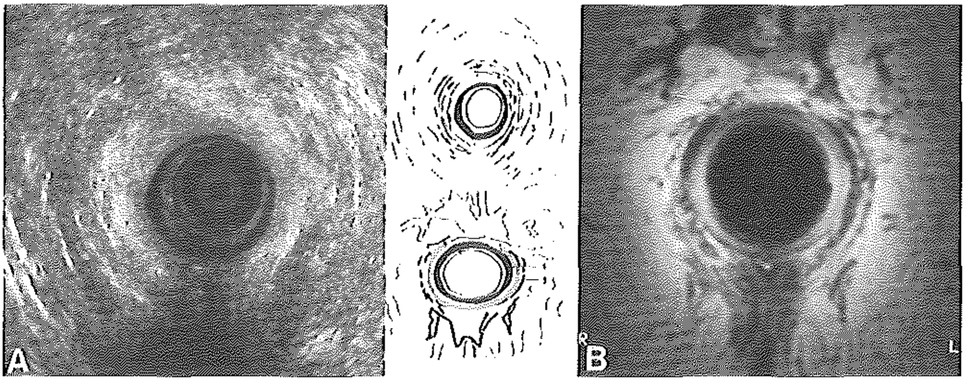

Fig. 8.7 *Atrophy.* Axial sonography (A) and MRI (B) in a female (67) who gradually became incontinent during recent years. With sonography there is a defect anteriorly whereas with MRI an extreme thinning of the external sphincter (3) is visible. The internal anal sphincter (1) is normal.

Table 8.1. The distribution of the number of cases in each type of sphincter damage. (IS = internal sphincter, ES = external sphincter, US = ultrasound, MR = magnetic resonance)

	IS damage only		ES damage only		IS + ES damage	
	US	MR	US	MR	US	MR
Loc. defect	4	1	11	6	7	3
Loc. scarring	2	0	1	0	3	6
Gen. scarring	0	0	0	0	2	2
Fragmentation	2	2	0	0	0	0
Atrophy	0	0	0	6	0	2
Total	8	3	12	12	12	13

With both techniques, a localized defect was visible as a discontinuity of the muscle ring of either the internal, the external sphincter or both (Fig. 8.1). With MRI, the localized defects were also seen in combination with scar tissue at the level of the defect (Fig. 8.2). Localized scarring was visible as a deformation of the normal configuration of the muscle layer which was often due to replacement of the muscle fibres by scar tissue (Fig. 8.3 - 8.4). Generalized scarring was visible as a destruction of more than half of the diameter of the anal sphincter muscle. In such cases, with sonography, the external sphincter was inhomogeneous whereas with MRI, the muscle fibres were seen to be replaced by extensive scar tissue (Fig. 8.5). Both techniques showed fragmentation as two or more

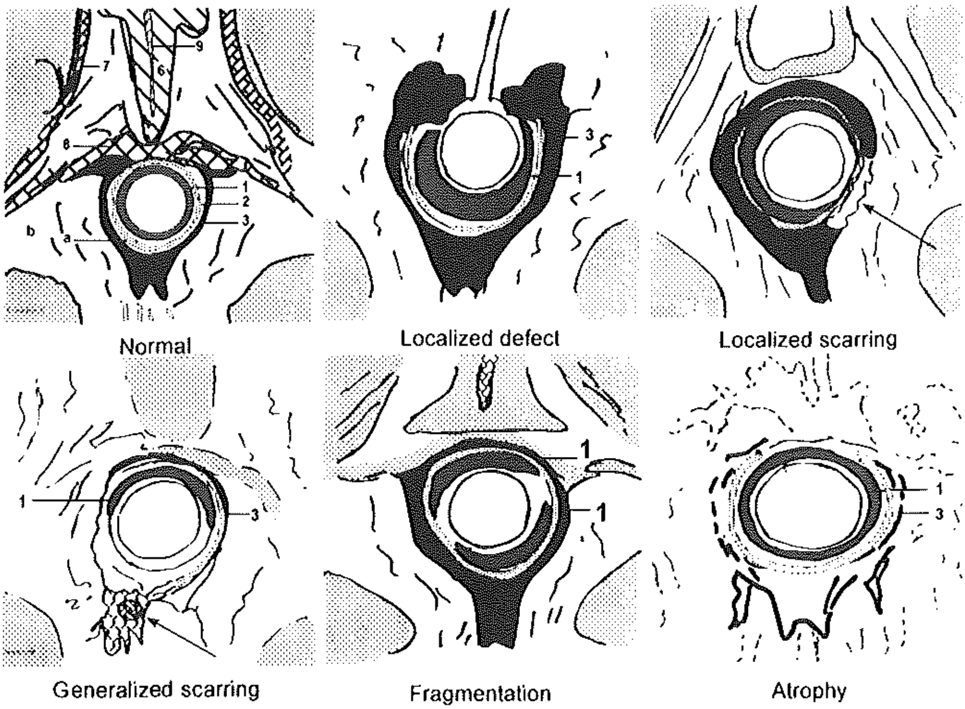

Fig. 8.8 *Schematic representation.* Normal appearance and types of anal sphincter damage as visible with endoanal MRI.

fragments of the anal sphincter visible in the axial plane, due to the longitudinal tears of the sphincter (Fig. 8.6). Atrophy was only visible with MRI as an extreme thinning of sphincter fibres (Fig. 8.7). The different kinds of sphincter damage is presented, schematically, in Fig. 8.8. The number of cases with sphincter damage and the specification of the abnormalities is shown in Table 1.

The damage to the internal anal sphincter only, was visible in 8 cases with endoanal sonography and in 3 cases with endoanal MRI (Table 1). A localized defect was seen in 4 cases with endoanal sonography, whereas in 1 case with MRI. Localized scarring was visible in two cases with sonography; this was confirmed with MRI, though, with endoanal MRI, the external sphincter was damaged as well (Table 1). Fragmentation of the internal anal sphincter was seen in 2 cases (Table 1), one was a women after rape and another a male patient with a history of anal dilatation.

The damage to the external anal sphincter only, was visible in 12 cases with endoanal sonography as well as with MRI (Table 1). In detection of the damage, both techniques were in agreement in 11 cases; in one case, unlike ultrasound, MRI showed no external sphincter defect; in stead, a normal anal sphincter complex with a very short anal canal was visible with sagittal MR images. With sonography, a localized defect was seen in 11 cases and a localized scarring in 1 case (Table 1). With MRI, a localized defect was confirmed in 6 cases, though, the defect was often present in combination with scar tissue (Fig. 8.2). In the remaining 6 cases, in stead of a defect, atrophy of the external sphincter was visible (Fig. 8.7).

The damage to the internal and the external anal sphincter was visible in 12 cases with endoanal sonography and in 13 cases with endoanal MRI (Table 1). In detection of the damage, both technique were in agreement in 10 cases. With endoanal sonography, a localized defect was seen in 7 cases, localized scarring in 3 cases and inhomogeneous echogenicity of almost entire sphincter, interpreted as scarring, in 2 cases. With endoanal MRI, a localized defect was seen in 3 cases, localized scarring in 6 cases, generalized scarring in 2 cases, and atrophy of the external sphincter in combination with an internal sphincter defect, in the remaining 2 cases.

In addition, in all women with an external anal sphincter defect anteriorly, there was also disruption of the anchoring fibres of longitudinal muscle layer and the shield-like extension of the perineal muscles, visible with endoanal MRI. In four male patients with a history of fistula surgery, MRI showed additional partial defects of the puborectal muscle. In 6 out of 8 patients with atrophy of the external sphincter, the puborectal muscle was visible prominently. In two case with atrophy of the external sphincter scar tissue was present anteriorly and in another one atrophy was seen in combination with a small defect. No defects of the levator ani muscle were encountered in this study.

8.4 DISCUSSION

Faecal incontinence is a complex problem from the clinical as well as from the surgical point of view. Clinically, the severity of the problem can vary from "minor" to "severe" incontinence [9]. It can take months or perhaps years before a patient will present with the problem. Hence, the patient-delay can often be very long [4]. The physician will try to objectify the problem with a number of tests, i.e. digital rectal examination, manometry, electromyography, and since recently also, with endosonography. In the most severe cases, sphincter repair will be successful [9]. In the current clinical practice, though, several methods of treatment are available. The physicians have a choice among constipating agents, exercise and electrical therapy, anterior sphincter repair, postanal repair, and indirect repair with circumanal slings of skeletal muscles [9,12].

The choice of a certain method of treatment may be influenced by the type of the sphincter damage. As a consequence, the mere detection of the sphincter disruption will not quite suffice. Further characterization of sphincter abnormalities may facilitate the identification of patients who would benefit most from a certain treatment. In this respect, the current subdivision of the sphincter damage into different types, particularly with endoanal MRI, could be of significance for surgical decision-making.

Currently, the detection of sphincter damage was not significantly different with two techniques. The detection rate of sphincter damage with endoanal sonography was comparable to the previous findings [8]. In characterization of sphincter damage, though, endoanal MRI was superior to endoanal sonography. Previously, the sphincter damage was subdivided into simple and complex lesions by using electromyography [9]. The simple lesions were more successfully treated with sphincter repair as compared to the complex lesions. The simple lesions were often found in patients with a history of fistula surgery, childbirth caused both types of lesions, and sexual trauma resulted into complex sphincter damage. In the current study, a different distribution was found.

A localized sphincter defect, with or without the presence of scar tissue, was often found in patients with a history of an obstetric injury. The preoperative information about the presence and the extent of the scar tissue, which had either to be excised or could be used for overlapping sphincteroplasty [4,9]. Localized scarring occurred in patients with hemorrhoidectomy and fistula operation. In such patients, a sphincter repair is not considered but the detection of the lesion provides an explanation for the occurrence of incontinence. Generalized scarring, which can be considered as a complex lesions, was seen in patients with a history of multiple fistula operations. In such patients, when restoration of incontinence is considered, an indirect sphincter repair, such as with a circumanal sling of gracilis muscle [13], would be more successful than a direct repair. Fragmentation of the internal anal sphincter occurred in one patient with a sexual trauma and in one patient with a history of anal dilatation. From the legal point of view, in patients with sexual trauma, the detection and the extent of the lesions can be important.

In the current study, the findings of atrophy of the external sphincter, only detectable with endoanal MRI, were remarkable. This lesion occurred in a majority of women in which no particular cause of incontinence could be found. The combination of an atrophic external sphincter and a prominent puborectal muscle was also remarkable. In this respect, it is interesting to know that Parks [4] took biopsies during postanal repair in patients with idiopathic incontinence and found atrophy of the external sphincter, a hypertrophy of the puborectal muscle and a normal levator ani muscle. The term "idiopathic incontinence" is reserved for patients with a slow conduction of the pudendal nerve due to the damage of this nerve [3]. Since the nerve supply to the puborectal muscle and the external sphincter is considered different [3], current findings of the atrophy of the external sphincter could have resulted from an injury to its nerve. The puborectal muscle, perhaps, tried to compensate the sphincter function and became reactively hypertrophic. According to others [2], idiopathic incontinence has multifactorial etiology. To validate the current considerations and the previous findings, further investigation is necessary.

With endoanal sonography the characterization of sphincter damage into different types is difficult. The muscle layers, except the internal sphincter, are not recognizable in each patient separately (Chapter 4). In addition, the defects of the external sphincter are defined as a change in the echogenicity. The localized defects could be recognised, though, this criterium is highly subjective and can cause difficulty in recognition of damage that is extensive or diffuse.

Due to the various possibilities of treatment available, it is difficult to validate the current imaging findings with another standard method. This is the important limitation of this study. Generally, only patients with an external sphincter are considered for sphincter repair; others receive often a non-surgical treatment. Currently seven patients with at least an external sphincter defect were operated with sphincter repair; in these patients, the imaging findings were confirmed during surgery. A comparison of the imaging findings with other physiologic test, which was beyond the scope of this study, should be considered in the near future. Other non-surgical methods, for instance a muscle biopsy which could be technically possible, have important ethical implications.

Despite its limitations, the current study displays the possibility of characterization of sphincter damage which can have implications for the choice of treatment. Future studies will be necessary to evaluate the impact of MRI in different groups of patients with faecal incontinence. To evaluate, which imaging modality should be used in the future, separate studies in different groups of patients should be carried out.

8.5 ACKNOWLEDGEMENT

Thanks are due to T. Rijsdijk for excellent photography and to AW Zwamborn for preparing the high-quality drawings.

8.6 REFERENCES

1. Gordon PH, Nivatvongs S. Principles and practice of surgery for the colon, rectum, and anus. St. Louis: Quality Medical Publishing Inc., 1992

2. Womack NR, Morrison JFB, Williams NS. The role of pelvic floor denervation in the aetiology of idiopathic faecal incontinence. Br J Surg 1986;73:404-407

3. Kiff ES, Swash M. Slowed conduction in the pudendal nerves in idiopathic (neurogenic) faecal incontinence. Br J Surg 1984;71:614-616

4. Parks AG. Anorectal incontinence. Proc R Soc Med 1975;68:681-690

5. Law PJ, Kamm MA, Bartram CI. Anal endosonography in the investigation of faecal incontinence. Br J Surg 1991;78:312-314

6. Cuesta MA, Meijer S, Derksen EJ, Boutkan, Meuwissen SGM. Anal sphincter imaging in fecal incontinence using endosonography. Dis Colon Rectum 1992;35:59-63

7. Sultan AH, Kamm MA, Hudson CN, Bartram CI. Anal sphincter disruption during vaginal delivery. New Eng J Med 1993;329:1905-1911

8. Nielsen MB, Hauge C, Pedersen JF, Christiansen J. Endosonographic evaluation of patients with anal incontinence:findings and influence on surgical management. AJR 1993;160:771-775

9. Keighley MRR, Fielding JWL. Management of faecal incontinence and results of surgical treatment. Br J Surg 1983;70:463-468

10. Emblem R, Dhaenens G, Stien R, Mokrid L, Aasen AO, Bergan A. The importance of anal endosonography in the evaluation of idiopathic fecal incontinence. Dis Colon Rectum 1994;37:42-48

11. Hussain SM, Stoker J, Kuiper JW, Schouten WR, den Hollander JC, Laméris JS. MR imaging of anal sphincter complex with an endoanal coil: normal anatomy and pathology. Radiology 1994;193(P):445

12. Hussain SM, Stoker J, Laméris JS. Anal sphincter complex: endoanal MR of normal anatomy. Radiology 1995;197:671-677

13. Browning GGP, Motson RW. Anal sphincter injury. Management and results of Parks sphincter repair. Ann Surg 1984;199:351-357

Chapter 9

ANORECTAL TUMOURS: EVALUATION OF TUMOUR INVASION OF THE ANAL SPHINCTER COMPLEX WITH US AND MRI

9.1 INTRODUCTION

Classification of anorectal tumours is essential for planning treatment as well as predicting the prognosis [1]. For staging the anorectal tumours, the visualization of the tumour infiltration of the layers of the bowel wall and the regional lymph nodes is important [2,3]. In addition to staging of the rectal tumours, the evaluation of the tumour invasion of the anal sphincter complex is, in our opinion, relevant in deciding between abdominoperineal resection and a sphincter saving procedure. For staging the tumours at the level of the anal canal, the size of the tumour and invasion of the adjacent anatomical structures [3], including the anal sphincter complex, are important.

In this respect, imaging can play an important role. Transrectal ultrasound [2] and transrectal MRI with the endorectal surface coil, which was originally used to examine the prostate [4], have been used for staging the rectal tumours [5,6]. The endorectal coil is placed within the rectum and has to be inflated with air in order to make imaging possible. For imaging the anal canal tumours, endoanal sonography has been used for the assessment of the extent of the tumour in our Hospital. Recently, a rigid endoanal MR coil was introduced to study the anal sphincter complex [7,8]. Soon it was realized that this rigid MR coil could also be used for transrectal MRI, particularly in the assessment of the malignancy at or near the anorectal junction.

In this chapter, the tumour invasion of the anal sphincter complex was evaluated with endosonography and MRI using the rigid coil, and correlated with pathology.

9.2 MATERIALS AND METHODS

Between June 1994 and September 1995, twenty-three consecutive patients presented with anorectal tumours. Of these, three patients were excluded: one because of a too high location of the rectal tumour and the two due to excessive motion artifacts during MR examination. The remaining twenty patients (11 males and 9 females; mean age 57.5 years; age range of 27-81 years) with histologically proven anorectal tumours entered the study after an informed consent was obtained. There were 16 adenocarcinomas of the rectum, 3 squamous cell carcinomas of the anal canal and 1 metastasis from a coloncarcinoma in the rectovaginal septum. All patients were examined with transrectal and endoanal ultrasound and MRI. Pathological correlation was obtained in all patients who underwent resection of the tumour.

Submitted for publication as: SM Hussain, J Stoker, JC den Hollander, WR Schouten, JS Laméris. Anorectal tumours: evaluation of tumour invasion of the anal sphincter complex with US and MRI.

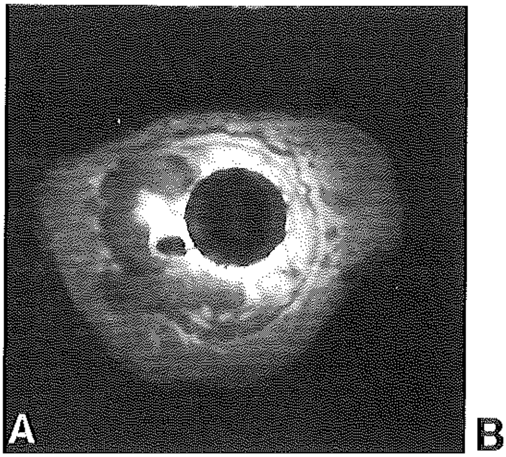

Fig. 9.1. *Rectal pT3 tumour. In vitro MRI using the rigid endoanal coil (A), with the drawing (B).* Note the layer of the rectal wall. The tumour (arrow) invades the perirectal fat.

Transrectal and endoanal sonography
For sonography, a Brüel & Kjaer (Naerum, Denmark) ultrasound scanner was used with a rotating probe providing a 360° image. A 5-7 MHz transducer with minimum beam width of 1.1 mm and a focal length of about 3 cm, was used. For transrectal ultrasound, a water-filled balloon, which covered the rotating ultrasound probe, was used for the imaging of rectal tumours. For endoanal sonography the balloon was replaced by a hard, sonolucent plastic cone with a diameter of 17 mm covered the transducer and was filled with degassed water for acoustic coupling. The cone was covered with a condom with gel applied to both surfaces. Axial images were obtained through the anorectum during the retraction of the probe. The transrectal and the endoanal probes were retracted with a constant speed during examination and the images were taken at every half centimeter.

Transrectal and endoanal MRI
Before MRI study in vivo, the rigid endoanal coil, which had been used to image the anal canal [7,8], was tested in four tumour specimens in vitro, and the findings were correlated with pathology.

In vivo MR imaging was performed at 0.5T (Gyroscan T5-II, Philips Medical Systems, Best, The Netherlands). To reduce bowel motion, one ml of butylscopolamine bromide (Buscopan 20 mg/ml, Boehringer Ingelheim KG, Ingelheim, Germany) was injected intramuscularly before scanning. For transrectal and endoanal MRI, the rigid coil (Philips Medical Systems) was used. The coilholder was covered with a condom and gel and the coil was placed at the level of the tumour. Axial, coronal, and sagittal T2-weighted turbo spin-echo sequences were performed [acquisition time 5.0 minutes, imaging matrix 186x256, number of signal averages 8, TR 2800, TE 120, turbo factor 10, field of view 120mm, slice thickness 4.0mm with an interslice gap of 0.4mm]. The coronal slices were parallel to the long axis of the endoanal coil. In addition, an axial

Table 9.1. This table shows the number of rectal tumours located above the level of the levator ani muscle (+1 to +4), at the level of the levator ani muscle (zero), and below the levator ani muscle (-1 to -2) with transrectal ultrasound (US), transrectal MR (MR), and pathology (PA). Note that in five cases, transrectal ultrasound was inconclusive.

Tumour-levator distance	US	MR	PA
+ 4 cm	2	0	0
+ 3 cm	1	2	2
+ 2 cm	3	1	2
+ 1 cm	1	3	2
0	4	5	5
- 1 cm	0	4	3
- 2 cm	0	1	2
Inconclusive	5	0	0
Total	16	16	16

turbo spin-echo was performed using a surface coil. The same parameters were used as for the sequences with the intracavitory coil, except a larger field of view of 250mm.

The tumour invasion of the anal sphincter complex was evaluated by the following parameters: 1) the distance between the tumour and the attachment of the levator ani muscle to the rectum, i.e. the deepest point of the pelvis; 2) the direct invasion of any component of the anal sphincter complex, i.e. the internal anal sphincter, the longitudinal layer, the external anal sphincter, the puborectal muscle, and the levator ani muscle; 3) the relationship of the T-component of the tumour stage, according to TNM classification[9], and spread towards the anal sphincter complex.

9.3 RESULTS

In vitro MRI of the tumour specimens showed all layers of the rectal wall, comprised of the mucosa, the submucosa, the inner circular layer and the outer longitudinal layer of the muscularis propria, as hypointense structures with great accuracy. The rectal layers were surrounded by the perirectal fat. Also the tumour and its relationship to the rectal layers was well displayed (Fig. 9.1). The findings correlated well with pathology.

In all patients, ultrasound probe and MRI coil were well tolerated. In two cases, it was somewhat difficult to introduce the probe because of the large size of the tumour. In four patients, there were slight motion artifacts during MR examination.

Table 9.2. The results of tumour staging with transrectal ultrasound (US) versus MRI using the rigid coil. Concordance between ultrasound and MR was present in 15 out of 16 (94%) cases.
Abbreviation: T=TNM Tumour stage

US / MR	T1	T2	T3	T4	Total
T1	0	0	0	0	0
T2	0	7	1	0	8
T3	0	0	7	0	7
T4	0	0	0	1	1
Total	0	7	8	1	16

Table 9.3. The results of tumour staging with transrectal ultrasound versus pathology. The accuracy of transrectal ultrasound (US) was 13/16 (81%). Note the overstaging in two cases and understaging in one case.
Abbreviation: T=TNM Tumour stage

US / Pathology	T1	T2	T3	T4	Total
T1	0	0	0	0	0
T2	0	6	1	0	7
T3	0	1	7	1	9
T4	0	0	0	0	0
Total	0	7	8	1	16

Table 9.4. The results of tumour staging with MRI using the rigid coil versus pathology. The accuracy of this technique was 12/16 (75%). Note the overstaging in two cases and understaging in two cases as well.
Abbrevation: T=TNM Tumor stage

MR / Pathology	T1	T2	T3	T4	Total
T1	0	0	0	0	0
T2	0	6	1	0	7
T3	0	2	6	1	9
T4	0	0	0	0	0
Total	0	8	7	1	16

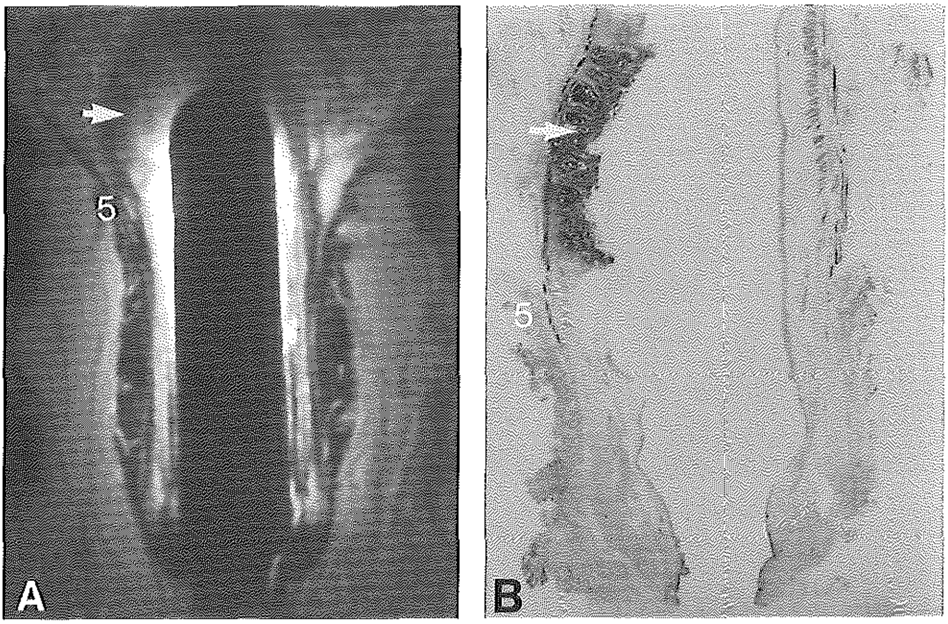

Fig. 9.2. *Tumor in relation to the sphincter complex.* MRI (A) vs. histology (B). Rectal tumor (arrow) located just above the level of the levator ani muscle (5).

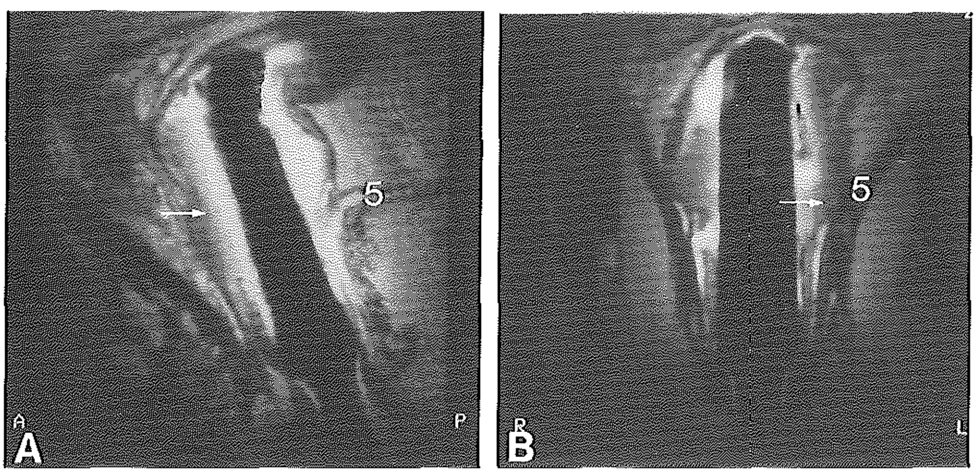

Fig. 9.3. Sagittal (A) and coronal (B) endoanal MRI. Note the tumor (arrow) reaching below the level of the levator ani muscle (5).

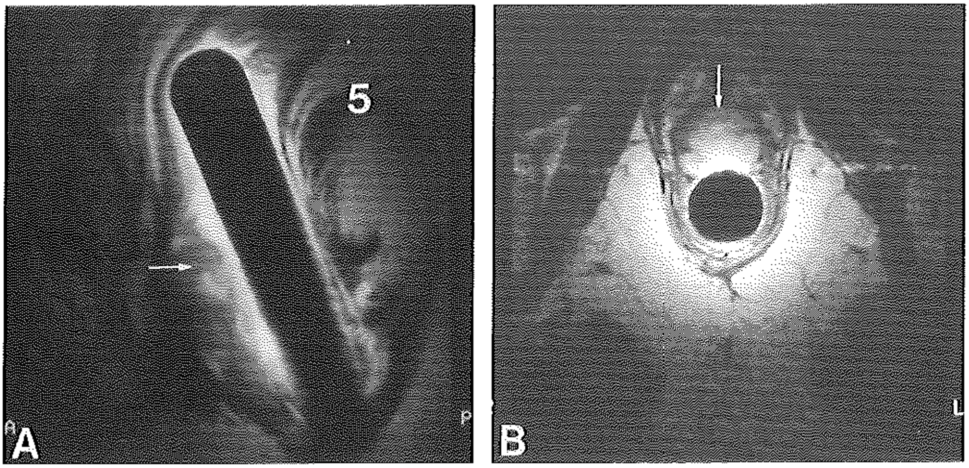

Fig. 9.4. Sagittal (A) and axial (B) endoanal MRI. The tumor (arrow) is located entirely below the level of the levator ani (5).

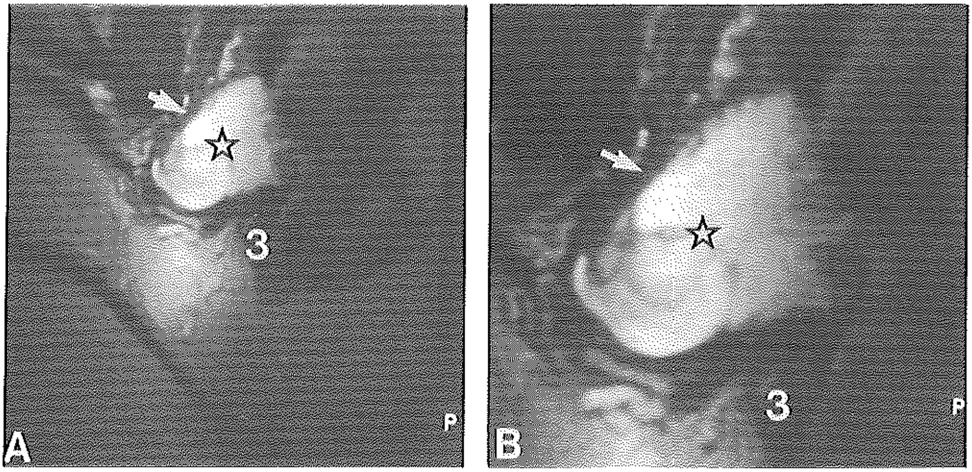

Fig. 9.5. Metastasis (✱) in the recto-vaginal septum invading the anterior part of the external sphincter (3) and the vagina (arrow).

Tumour-levator distance and direct tumour invasion
In the rectal tumours (n=16), the distance between the lower margin of the tumour and the attachment of the levator ani is presented in Table 9.1. With transrectal ultrasound, the distance had to be estimated. In contrast, with transrectal MRI the distance could be measured directly from the coronal or sagittal images (Fig. 9.2 and 9.3). In 5 out of 16 (31%) cases, endoMRI accurately showed the rectal tumour reaching 1 to 2 centimeters below the level of the attachment of the levator ani muscle. In these cases, with transrectal ultrasound the tumour was said to be reaching at or below the deepest point of the pelvis though exact measurement of the distance was not possible. In another 5 out of 16 (31%) cases, the lower margin of the tumour was located at the level of the levator ani (Table 9.1). In both groups with the tumour at or below the level of the levator ani muscle, there was, in six cases, evidence of direct tumour invasion of the internal anal sphincter and the longitudinal layer of the anal canal. The tumour-levator distances found with the imaging techniques, correlated well with the findings of the pathology (Table 9.1). With transrectal MRI, 6 out of 16 (38%) and with transrectal ultrasound 7 out of 16 (44%) cases were found to be located 1-4 cm above the level of the levator ani muscle (Table 9.1). Fourteen out of 16 patients with rectal tumours underwent abdominoperineal resection and the remaining two were subjected to a sphincter saving procedure. In patients with an abdominoperineal resection, there was an excellent MR-pathologic correlation for the distance between the lower margin of the tumours and the levator ani muscle. In two patients with a sphincter saving procedure, the tumour-levator distance was at least three centimetres with MR (Table 9.1).

In the anal canal tumours (n=4), the lesions were located entirely below the level of the levator ani muscle (Fig. 9.4). In the three cases of squamous cell carcinomas, because of non-surgical treatment, no pathological correlation was possible. One patient, with metastasis in the rectovaginal septum, underwent abdominoperineal resection. In this patient, endoanal MRI showed evidence of direct tumour invasion and destruction of the internal anal sphincter, the longitudinal layer of the anal canal, and the anterior part of the external anal sphincter (Fig. 9.5). The MR findings correlated well with the histopathological findings.

T-component of the tumour and the relationship to the anal sphincter complex
Staging of the T-component of the rectal tumours is shown in Tables 9.2-9.4. Between transrectal ultrasound and MRI, there was a concordance in 94% (15/16) of the cases (Table 9.2 and Fig. 9.6). The accuracy in staging the T-component was 81% (13/16) with sonography (Table 9.3), whereas 75% (12/16) with MRI (Table 9.4). Overstaging occurred in two cases with ultrasound while in three cases with MRI. Understaging was observed in one case with sonography whereas in two cases with MRI. In cases with overstaging, the tumour specimens showed peritumoral inflammatory reaction with pathology. In cases with understaging, technical problems, such as large tumour mass and slight mispositioning of the probe or coil, were encountered during imaging.

There was no direct relationship between the T-component of the tumour stage and the downward tumour spread towards the anal sphincter complex. Of the ten cases in which the tumour was seen located at or below the level of the levator ani muscle with

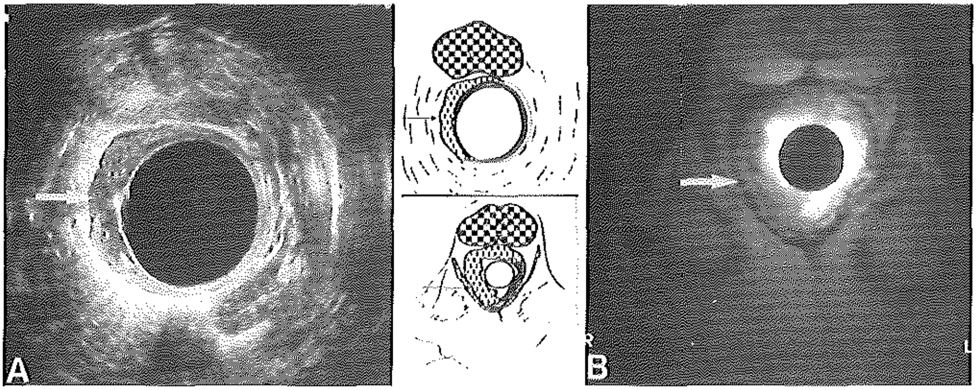

Fig. 9.6. *Rectal pT2 tumor. Transrectal ultrasound (A) versus transrectal MRI (B).* Axial images showing the tumor (arrow) limited to the muscularis propria. Correct staging with both imaging techniques.

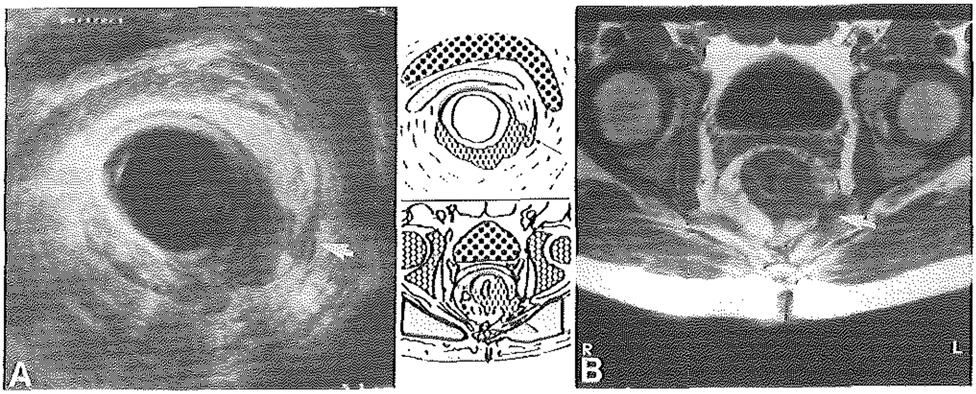

Fig. 9.7. *Rectal pT2 tumor. Transrectal ultrasound(A) versus surface coil MRI (B).* Overstaging, with both imaging modalities. Due to the thickening of perirectal septae (arrow), the tumor was staged as T3 with both imaging modalities.

MRI, five appeared to be pT3-tumours and four were pT2-tumours with invasion of mainly the internal anal sphincter. In some instances the longitudinal layer of the anal canal was also invaded. None of the cases showed invasion of the external anal sphincter or puborectal muscle. The remaining one case, staged as a T4-tumour with ultrasound and MR because of suspicion of infiltration of the levator ani muscle, appeared to be a T3-tumour with pathology (Table 9.4). The tumour was overstaged because of thickened perirectal septae extending from the tumour towards the levator ani muscle (Fig. 9.7).

The three primary tumours of the anal canal were staged as T2-tumours with ultrasound and MR. One tumour was located anteriorly, the second one laterally and the third was seen posteriorly. The extent of the tumour and its relationship to the anal sphincter complex were better appreciated with endoanal MRI as compared to endoanal sonography.

9.4 DISCUSSION

Preoperative evaluation of the tumour invasion of the anal sphincter complex can have implications for surgical management. The recent developments in surgical techniques such as colo-anal anastomosis and stapling devices has made it possible to restore gastrointestinal continuity in patients with low rectal cancer [3,10]. In addition, for many years it was believed that for the preservation of continence 6-8 cm of anorectum had to remain after rectal excision [11]. Faecal continence though remains preserved even after excision of the rectum [12]. Social and psychological problems experienced by the patients with colostomy are considerable, while the overall survival rate is not significantly different from patients with colo-anal anastomosis [10]. Damage to pelvic autonomic nerves, which can result in sexual and bladder dysfunction, is less likely to occur during sphincter saving operations [13]. Such findings have encouraged the surgeons to perform sphincter saving procedures [10].

For proper patient selection for the various treatments of rectal tumours, recent developments in imaging techniques, particularly transrectal ultrasound [14] and MRI using an endorectal coil [5-6], are important. Classically the rectal tumours spread in three directions: upwards, downwards and laterally [10]. Previous imaging studies of rectal tumours have concentrated on the evaluation of the upward and lateral spread, i.e. the transmural tumour spread and nodal metastases [2,6]. To our knowledge, the downward spread and the relationship of the rectal tumour to the anal sphincter complex, important for proper surgical management, have not been addressed in an imaging study before.

Current study shows that MRI using a rigid intracavitory coil is excellent in imaging the different layers of rectal wall and rectal tumours in vitro. Our results confirm the previous findings of MR study of colorectal tumours in vitro, using very small surface coils [5]. MRI using the rigid endoanal coil produces superb images of rectal tumours in patients as well. In addition, the relationship of the tumour to the anal sphincter complex can be assessed accurately. Such findings are difficult to evaluate with transrectal ultrasound and MRI using an inflatable balloon around the the probe and the coil respectively. With both techniques the balloon will prevent the imaging of structures located at or below the pelvic diaphragm, i.e. the level of the levator ani muscle. In contrast the rigid coil, used for imaging the anal sphincter complex [7,8], can be used for the rectum as well as the anorectal junction. The results indicate that MR using the rigid coil can reliably determine the tumour invasion of the components of the anal sphincter complex and is superior to transrectal ultrasound.

In addition, with transrectal ultrasound, miscalculation of the tumour-levator distance can occur either during introduction or retraction of the ultrasound probe. Underestimation of the tumour-levator distance can occur during the introduction of the ultrasound probe: the anal canal is likely to be pushed towards the tumour. Overestimation of the distance can result from pulling the transducer away from the tumour which can occur during retraction of the transducer.

In contrast to the assessment of tumour invasion, the staging of rectal tumours was not significantly different with transrectal ultrasound and MRI in the current study. The accuracy of both techniques is in agreement with the previous findings [2,6]. In a majority of the cases with overstaging, there was histological evidence of the reactive inflammatory changes on the outer border of the tumours, which has also been described before [15]. Understaging resulted from errors of interpretation in patients with either very large or very small rectal tumours.

The primary tumours of the anal canal are well displayed with endoanal sonography and MRI. These tumours, located relatively near the sonographic probe or MR coil, cause no problems during imaging. Though a lesion located out of the focal range of the sonographic probe may poorly be visualized. Due to its superiority in visualizing the normal anatomy of the anal sphincter complex [8], endoanal MR is better in showing the relationship of the tumour and the components of the anal sphincter complex.

Current results, though based on a relatively small number of patients, show that MRI using a rigid coil is excellent in evaluating the tumour invasion of the anal sphincter complex. This is an important finding from the surgical point of view. In the current clinical practice, the digital rectal examination is the only method to determine the relationship of the tumour to the pelvic floor. MRI using the rigid coil could be of value in substantiating the surgeon's decision of performing either an abdominoperineal resection or a sphincter saving procedure. MR imaging of rectal tumours should be aimed on staging as well as the relationship of the tumour to the anal sphincter complex.

9.5 ACKNOWLEDGEMENT

Thanks are due to AW Zwamborn and T Rijsdijk for preparation of the drawings and the photographs.

9.6 REFERENCES

1. Dukes CE, Bussy HJR. The spread of rectal cancer and its effect on prognosis. Br J Cancer 1958;12:309-320

2. Tio TL, Coene PPLO, Van Delden OM, Tytgat GNJ. Colorectal carcinoma: preoperative TNM classification with endosonography. Radiology 1991; 179:165-170

3. Nivatvongs S.: in Gordon PH, Nivatvongs S. Principles and practice of surgery for colon, rectum, and anus. Quality Medical Publishing, Inc. St. Louis, Missouri, 1992; p 407-417

4. Mirowitz SA, Brown JJ, Heiken JP. Evaluation of the prostate and prostate carcinoma with gadolinium-enhanced endorectal coil imaging. Radiology 1993;186:153-157

5. Imai Y, Kressel HY, Saul SH, Chan PW, Schnall MD, Lenkinski RE, Listerud JM, Daly JM. Colorectal tumors: an in vitro study of high-resolution MR imaging. Radiology 1990;177:695-701

6. Schnall MD, Furth EE, Rosato E, Kressel HY. Rectal tumor stage: correlation of endorectal MR imaging and pathologic findings. Radiology 1994;190:709-714

7. Hussain SM, Stoker J, Kuiper JW, Schouten WR, den Hollander JC, Laméris JS. MR imaging of anal sphincter complex with an endoanal coil: normal anatomy and pathology. Radiology 1994;193(P):445

8. Hussain SM, Stoker J, Laméris JS. Anal sphincter complex: endoanal MR imaging of normal anatomy. Radiology 1995;197:671-677

9. Spiessl B, Beahrs OH, Hermanek P, Hutter RVP, Scheibe O, Sobin LH, Wagner G, editors. UICC TNM atlas, 3rd edition. Springer-Verlag, New York, 1992

10. Williams NS. The rationale for preservation of the anal sphincter in patients with low rectal cancer. Br J Surg 1984;71:575-581

11. Goligher JC, Hughes ESR. Sensibility of the rectum and colon: its role in the mechanism of anal continence. Lancet 1951;i:543-548

12. Scharli AF, Kieswater WB. Defaecation and continence: some new concepts. Dis Col Rect 1970;13:81-107

13. Kirkegaard P, Hjartrup A, Sanders S. Bladder dysfunction after low anterior resection for mid rectal carcinoma. Am J Surg 1981;141:266-268

14. Beynon J, Mortensen NJM, Rigby HS. Rectal endosonography, a new technique for the preoperative staging of rectal carcinoma. Eur J Surg Oncol 1988;14:297-309

15. Hulsmans FJH, Tio TL, Fockens P, Bosma A, Tytgat GNJ. Assessment of tumor infiltration depth in rectal cancer with transrectal sonography: caution is necessary. Radiology 1994;190:715-720

Chapter 10

DISCUSSION

In this section, the findings of the separate studies will be briefly discussed. The readers interested in lengthy discussion of various aspects of the study are kindly referred to the discussion sections of the separate chapters.

The anatomy of the anorectum has been controversial for a number of reasons. The relationship of the muscles of the pelvic floor and adjacent structures is complex. In addition, this region is relatively inaccessible. The organs which play an important role in sexual intercourse and defecation are located in this area, making this region guilt-ridden and relatively difficult to investigate in living subjects.

The introduction of anal endosonography [1] was an important milestone. For the first time, the anal sphincter complex could be visualized and studied in vivo. Because of the controversies about the in the surgical and anatomical literature [2], flaws have occurred during the interpretation of the endosonographic images. This is the main reason that the controversies, particularly about the sonographic appearance of the external anal sphincter, still exist.

The introduction of endoanal and transrectal MRI with a rigid coil [3], has improved the imaging of the ano-rectal diseases. The new MRI anatomic concept of the anal sphincter complex, emerging from the endoanal MRI data, is in many aspects different from the previous views (Chapter 3) [4]. In this respect, it is interesting to note, that very recently other workers [5,6] using a similar endoanal MRI coil, have described the anal sphincter anatomy by considering the laminar concepts of the sphincter anatomy[Dally] as the standard of reference. According to these workers [5,6], the different parts of the external anal sphincter could be identified with endoanal MR images. In our opinion, these investigators failed to exploit the multi-planar capability of MRI. In chapter 3, we have described the anal sphincter anatomy as it is visible with MRI in all its details in three dimensions. Afterwards, the MRI findings were compared to the previous concepts, in order to understand the controversies. In addition, the endoanal MRI concept has been validated by a correlation with cross-sectional anatomy and histology (chapter 6). According to us, the concept of the sphincter anatomy described in chapter 3, will certainly have consequences for our view of the anatomy of the anal sphincter complex in particular, and perhaps also for the concept of the anatomy of the pelvic region in general.

In patients with fistula-in-ano, endoanal MRI seems to be superior to endoanal ultrasound in classification of the fistulae. To improve the concordance between MRI and surgery, though, close cooperation between the radiologist and the surgeon will be necessary. In the near future, in our opinion, additional studies should be carried out to determine the additional value of MRI in classification of fistulae as compared to surgery. The improved preoperative classification can provide the surgeon a road-map during fistula surgery. This could reduce the risks of procedure-dependent incontinence. In addition, the more accurate preoperative imaging data could be used to inform the patient about the complexity of the problem and the risks concerning the treatment.

In patients with faecal incontinence, the detection of the sphincter damage was similar with endoanal sonography as well as MRI. The characterization of the sphincter damage, though, was better with endoanal MRI. Due to its ability to visualize all layers of the anal canal wall, including the external anal sphincter, endoanal MRI, in contrast to ultrasound, led to further characterization of the sphincter damage into the localized defects, localized scarring, generalized scarring, fragmentation and atrophy. These findings will need validation by other techniques, perhaps by performing small needle biopsies of the sphincter muscles. This could raise important ethical questions. In addition, in the near future, it will become necessary to determine which imaging modality should be used in specific groups of patients suffering from faecal incontinence.

In patients with anorectal tumours, sonography and MRI were comparable for staging the tumor. However, transrectal MRI appeared to be superior in displaying the relationship of the rectal tumours to the anal sphincters. The direct invasion of different components of the anal sphincter complex are well displayed with endoanal and transrectal MRI. In this respect, MRI could be of value in substantiating the surgeon's decision of performing either an abdominoperineal resection or a sphincter saving procedure.

Currently, the emphasis has been on the description and understanding the structural anatomy and disease in the anorectal region. Accurate knowledge of the structural anatomy of the anorectum could facilitate the understanding of the relationship of the anorectum to the pelvic diaphragm. In addition, this could also result in studies of the functional anatomy and may be helpful in solving complex problems related to the pelvic floor.

To accomplish such tasks in the near future, a consensus about the structural anatomy of the anal sphincter complex is most welcome. Therefore every effort should be made in this direction. This will benefit all who are interested in solving the patient-related as well as research-related problems of this area.

The new cross-sectional imaging techniques, ultrasound and MRI, with dedicated probes and coils provide a different way of looking at the anorectum and its relation to the pelvic region. These powerful imaging modalities open new doors for understanding the anatomy and disease of this region and provide us with new opportunities for further research in this area.

REFERENCES

1. Law PJ, Bartram CI. Anal endosonography: technique and normal anatomy. Gastroint Radiol 1989;14:349-353

2. Dally AF II. The riddle of the sphincters. The morphophysiology of the anorectal mechanism reviewed. Am Surg 1987;53:298-306

3. Hussain SM, Stoker J, Kuiper JW, Schouten WR, den Hollander JC, Laméris JS. MR imaging of the anal sphincter complex with an endoanal coil: normal anatomy and pathology. Radiology 1994;193(P):445

4. Hussain SM, Stoker J, Laméris JS. Anal sphincter complex: endoanal MR imaging of normal anatomy. Radiology 1995;197:671-677

5. DeSouza NM, Puni R, Gilderdale DJ, Bydder GM. Magnetic resonance imaging of the anal sphincter using an internal coil. Mag Res Quart 1995;11:45-56

6. DeSouza NM, Puni R, Kmiot WA, Bartram CI, Hall AS, Bydder GM. MRI of the anal sphincter. J Comp Assist Tomogr 1995;19:745-751

SUMMARY

The purpose of this study was to improve the imaging of the normal anal sphincter complex and to apply the new data in order to enhance the insight in the normal anatomy and the anorectal diseases.

Chapter 1. After the introductory remarks about the history of the anorectal anatomy, the recent developments in imaging techniques are described and the importance of imaging the anorectal diseases is stressed. In addition, the aims and the outline of the study are described.

Chapter 2 describes the basic principles of the two imaging techniques, used in the current study. For MRI, a recently developed rigid MRI coil was used. This coil can be placed at the anal canal and the rectal level, and provides us with new possibilities for imaging the anatomy and pathology of this region.

Chapter 3 provides a description of the normal MR anatomy of the anal sphincter complex using a rigid endoanal coil in ten healthy volunteers. The muscle layers of the lower and the upper part of the anal canal are different. The lower part is surrounded by the internal anal sphincter, the longitudinal layer, and the external anal sphincter. The upper part of the anal canal contains the internal anal sphincter, the longitudinal layer, and the sling of the puborectalis muscle.
Between the internal anal sphincter, and the external anal sphincter and the puborectalis, the intersphincteric space is well visible. The whole sphincter apparatus is embedded within the ischioanal space. At its upper end the puborectalis muscle is attached to the levator ani muscle. The anatomy of the internal anal sphincter and the longitudinal layer of the anal canal was not substantially different from the previous studies. In contrast, the anatomy of the external anal sphincter and its relationship to the puborectalis is quite different than previously mentioned.

Chapter 4 compares the anatomy of the anal sphincter complex with endoanal sonography and MRI in order to explain the controversies existing in the sonographic literature. The findings of the internal anal sphincter correlate well in the two imaging techniques. The longitudinal layer is better visualised with MRI. There are two sonographic patterns of the external anal sphincter: a hyperechoic band, often found in females, and a relatively hypoechoic thin structure, often seen in the male. The echogenic band does not correspond to the external anal sphincter visible with endoanal MRI, and may be an artifactual finding. The hypoecoic structure correlates quite well with the MRI findings. Such findings could have consequences for endoanal sonography which is currently the modality of choice to identify patients with anal sphincter defects.

Chapter 5 compares, in detail, the sex-dependent anatomy of the anterior part of the anal sphincter complex and related structures. In men, the anterior part of the external anal sphincter is oblong and shows muscular connections to the bulbocavernous muscle in the midline anteriorly. In women, the anterior part of the external sphincter is oval in shape and shows no muscular connections in the midline. In addition, in the female, a shield-like, downward extension of the transverse perineal muscles just anterior to the anal sphincter complex can be seen. In both sexes, no perineal body could be identified with

endoanal MR images. In the female, perhaps the connective tissue in front of the anterior part of the external sphincter and parts of the shield-like muscle have been misconceived as the perineal body previously. This study shows that there are more sex-dependent differences in the anatomy of the anal sphincter complex than mentioned previously. The knowledge of the exact anatomy of this region will certainly benefit the colo-rectal surgeon as well as the gynaecologist.

Chapter 6 describes the correlation between the endoanal MRI findings of the anal sphincter complex and the cross-sectional anatomy and histology. After an informed consent was obtained, fourteen patients with rectal tumours, who underwent abdominoperineal resection, were examined with endoanal MRI before operation. An informed consent was obtained in all patients. The resected rectal preparations were used to obtain anatomical and histological slices. In addition, to obtain also a correlation of the structures surrounding the anal canal, twelve cadavers were sectioned. There was an excellent correlation between the endoanal MRI findings and the cross-sectional anatomy and histology of the anal sphincter complex.

Chapter 7 presents a comparative study between endoanal sonography, endoanal MRI and surgery in 28 patients with perianal fistulae. Classification of fistulae, using the Parks' method of classifying perianal fistulae, was possible in 61%(17/28) with endoanal sonography, in 89%(25/28) with endoanal MRI and in 93%(26/28) with surgery. The concordance among the three techniques was as follows: between sonography and MRI in 46%(13/28) of the cases (kappa=0.27, indicating poor agreement), between sonography and surgery in 36%(10/28) of the cases (kappa=0.09, indicating no agreement) and between MRI and surgery in 64%(18/28) of the cases (kappa=0.43, indicating moderate agreement). The relatively poor results of concordance were mainly caused by the differences in classification of the transsphincteric and the horse-shoe fistulae. The concordance rate between MRI and surgery could be improved by the preoperative knowledge of the imaging findings by the surgeon and the feed-back of the surgical findings to the radiologist. In this respect, the preoperative endoanal MRI findings could serve as a road-map for fistula surgery.

Chapter 8 provides a comparison of endoanal sonography and endoanal MRI in patients with faecal incontinence. The incontinence was caused by obstetric injury, fistula surgery, haemorrhoidectomy, anal dilatation or rape. In a number of patients the cause was unknown. In detection of the lesion, there was no significant difference between the two techniques. Endoanal MRI, though, provided better characterization of the lesion into localized defects, localized scarring, generalized scarring, and atrophy. Such subdivision of the sphincter damage could facilitate the choice among the various possibilities of treatment.

Chapter 9 presents the results of a study of the anorectal tumours with an evaluation of tumour invasion of the anal sphincter complex. Ultrasound (US) and MRI were compared in 20 patients with tumours, comprised of 16 adenocarcinomas of the rectum, 3 squamous cell carcinomas of the anal canal and 1 metastasis in the rectovaginal septum. Pathological correlation was obtained in all patients who underwent resection of the tumour. The tumour invasion of the anal sphincter complex was evaluated on the basis of the tumour-levator distance, the direct invasion and the stage of the tumour and its relationship to the spread of the tumour towards the anal sphincter complex. In the assessment of the tumour-levator distance and the direct tumour invasion, MRI was superior to US. In staging the rectal tumours, there was no difference between ultrasound and MRI. The stage of the tumour was not related to the spread of the tumour towards the sphincter complex. MR imaging of rectal tumours should be aimed on staging as well as the relationship of the tumour to the anal sphincter complex which could substantiate the surgeon's decision of performing either an abdominoperineal resection or a sphincter saving operation .

Chapter 10 provides the discussion.

SAMENVATTING

Het doel van deze studie was het verbeteren van de afbeelding van de anatomie van het anale sfincter complex en het toepassen van de nieuwe inzichten om de anorectale afwijkingen beter te interpreteren.

Hoofdstuk 1. Na een overzicht van de bekende anorectale anatomie, worden de recente ontwikkelingen in de afbeeldingstechnieken beschreven en het belang van de afbeelding van de anorectale afwijkingen benadrukt. Voorts, worden de doelen en de opbouw van de studie gedefinieerd.

Hoofdstuk 2 beschrijft de basale principes van de twee gebruikte afbeeldingstechnieken in deze studie. Voor MRI werd een recent ontwikkelde starre spoel gebruikt. Deze spoel kan zowel ter hoogte van het anaal kanaal als ter hoogte van het rectum geplaatst worden, en geeft ons nieuwe mogelijkheden om de anatomie en de pathologie van dit gebied beter af te beelden.

Hoofdstuk 3 geeft een beschrijving van de normale MR anatomie van het anale sfincter complex in tien gezonde vrijwilligers. De spierlagen van de onderste en de bovenste helft bleken te verschillen. De onderste helft van het anaal kanaal is omgeven door de interne anale sfincter, de longitudinale laag en de externe anale sfincter. De bovenste helft van het anaal kanaal bevat de interne anale sfincter, de longitudinale laag en de musculus puborectalis. Tussen de interne anale sfincter, en de externe anale sfincter en de m. puborectalis, is de intersfincterische ruimte goed zichtbaar. Het gehele sfincterapparaat is ingebed in de ischioanale ruimte. Aan zijn bovenste uiteinde zit de m. puborectalis vast aan de m. levator ani. De anatomie van de interne sfincter en de longitudinale laag verschilt in essentie niet van die in de literatuur. Daarentegen vertoont de anatomie van de externe sfincter en zijn relatie met de m. puborectalis en de m. levator ani wel grote verschillen in vergelijking met de eerdere opvattingen. Endoanale MRI geeft nauwkeurig de normale anatomie van het anale sfincter complex weer.

Hoofdstuk 4 vergelijkt de anatomie van het anale sfincter complex met endoanale echografie en MRI om de controverses die in de echografische literatuur bestaan te verklaren. De bevindingen van de interne anale sfincter correleren goed in beide afbeeldingstechnieken. De longitudinale laag is beter zichtbaar met MRI. Er zijn twee echografische patronen van de externe anale sfincter: echogene band, vaker te zien bij vrouwen, en een relatieve echoarme dunne structuur, vaker voorkomend bij mannen. De echogene band correspondeert niet met de externe sfincter zichtbaar met MRI, en zou kunnen berusten op een soort artefact. De echoarme structuur correleert wel goed met de MRI bevindingen. Zulke bevindingen kunnen gevolgen hebben voor endoanale echografie wat op dit moment afbeeldingstechniek van keuze is om de patiënten met een sfincter defect te detecteren.

Hoofdstuk 5 vergelijkt, in detail, de sexe-afhankelijke anatomie van het voorste deel van het anale sfincter complex en gerelateerde structuren. In mannen, is het voorste deel van de externe anale sfincter langwerpig en heeft musculaire connecties met de musculus bulbocavernosus in de mediaan lijn. In vrouwen, is het voorste deel van de externe anale sfincter ovaalvormig en heeft geen musculaire connecties. Voorts is, bij de vrouw, een schildvormige uitbreiding van de perineale spieren naar caudaal, vlak voor de externe sfincter te zien. In geen van de sexen werd een perineaal lichaampje waargenomen. Bij de vrouw, is mogelijkerwijs in het verleden, het bindweefsel anterieur van de externe sfincter en delen van de schildvormige uitloper ten onrechte aangenomen als perineaal lichaampje. Deze studie toont aan dat er meer sexe-afhankelijke verschillen zijn in de anatomie van het anale sfincter complex dan tot dusver bekend. De kennis van de exacte anatomie van deze regio zal zeker ten goede komen van de colo-rectale chirurg en de gynaecoloog.

Hoofdstuk 6 beschrijft de correlatie tussen de endoanale MRI bevindingen van het anale sfincter complex en de anatomie en histologie. Na toestemming werden veertien patiënten met een rectumtumor, die een abdominoperineale resectie ondergingen, onderzocht met endoanale MRI voor de operatie. De resectiepreparaten werden gebruikt voor de histologische en de anatomische coupes. Daarnaast, om ook de correlatie om het anaal kanaal heen liggende structuren te verkrijgen, werden twaalf cadavers doorgezaagd. Er was een goede correlatie tussen de MRI bevindingen en de anatomische en de histologische coupes van het anaal sfincter complex.

Hoofdstuk 7 presenteert een vergelijkende studie tussen endoanale echografie, endoanale MRI en chirurgie in 28 patiënten met perianale fistels. Classificatie van de fistels, door gebruik van de methode van Parks om de perianale fistels te classificeren, was mogelijk in 61%(17/28) met endoanale echografie, in 89%(25/28) met endoanale MRI en in 93%(26/28) met chirurgie. De concordantie tussen de drie technieken was als volgt: tussen echografie en MRI in 46%(13/28) van de gevallen (kappa=0.27, betekent een slechte overeenkomst), tussen echografie en chirurgie 36%(10/28) van de gevallen (kappa=0.09, betekent geen overeenkomst) en tussen MRI en chirurgie in 64%(18/28) van de gevallen (kappa=0.43, betekent een matige overeenkomst). De relatief slechte resultaten van de concordantie worden voornamelijk veroorzaakt door de verschillen in de classificatie van de transsfincterische en de hoefijzer fistels. De mate van concordantie tussen MRI en chirurgie zou verbeterd kunnen worden als de chirurg de preoperatieve MRI bevindingen kent en er goede feed-back is voor de radioloog. In dit opzicht kunnen de preoperatieve endoanale MRI bevindingen als een leidraad dienen bij fistel operaties.

Hoofdstuk 8 beschrijft een vergelijking van endoanal echografie en MRI in patiënten met faecale incontinentie. De incontinentie werd veroorzaakt door obstetrische letsel, fistel operaties, hemorrhoidectomie, Lords procedure en verkrachting. In een aantal patiënten was de oorzaak onbekend. De schade aan de sfincters werd met beide technieken goed gedetecteerd. Voor verdere karakterisatie van de sfincterschade in lokale defect, lokale verlittekening, gegeneraliseerde verlittekening, fragmentatie en atrofie, is MRI echter beter dan echografie. Deze onderverdeling van de sfincterschade zou gevolgen kunnen hebben voor het kiezen van een therapie uit een scala van mogelijkheden.

Hoofdstuk 9 presenteert de resultaten van een studie van de anorectale tumoren met een evaluatie van de tumor invasie van het anaal sfincter complex. Echografie en MRI werd vergeleken in 20 patiënten met tumoren, bestaande uit 16 adenocarcinomas van het rectum, 3 plaveiselcelcarcinomas van het anaal kanaal en 1 metastase in het septum rectovaginale. Pathologische correlatie werd verkregen in alle patiënten die een tumorresectie ondergingen. De tumor invasie van het anaal sfincter complex werd geëvalueerd op basis van de tumor-levator afstand, de directe invasie en het stadium van de tumor en zijn relatie met de uitbreiding van de tumor in de richting van het anaal sfincter complex. Voor de bepaling van de tumor-levator afstand en de directe tumor invasie, was MRI superieur aan echografie. Voor de stagering van de rectumtumoren was er geen verschil tussen echografie en MRI. Het stadium van de tumor toonde geen relatie met de uitbreiding van de tumor in de richting van het anaal sfincter complex. MRI van de rectumtumoren zou behalve op de stagering ook gericht moeten worden ter bepaling van de relatie van de tumor met het anaal sfincter complex hetgeen de beslissing van de chirurg om wel of geen sfinctersparende ingreep te doen, zou kunnen ondersteunen.

Hoofdstuk 10 geeft een nabeschouwing weer. Dit hoofdstuk bespreekt in het kort de resultaten. Voor een uitgebreide discussie wordt de geinteresseerde lezer vriendelijk verwezen naar de aparte hoofdstukken.

DANKWOORD

Dit proefschrift is niet het werk van één individu, doch een resultaat van de inspanning van velen. Dit werk was mogelijk dankzij de goede samenwerking tussen de afdeling Radiologie en de afdelingen Algemene Heelkunde, Pathologische Anatomie en Anatomie. Met name ben ik dankbaar:

Prof. Dr. J.S. Laméris, die mij enkele jaren geleden wees op het belang van endoechografie en mij de mogelijkheid gaf om, in combinatie met MRI, een wetenschappelijk onderzoek op te zetten.

Prof. Dr. H.E. Schütte voor het vertrouwen dat hij in mij stelde en die mij de tijd en de gelegenheid gaf om dit proefschrift af te ronden.

Prof. Dr. J. Jeekel, Prof. Dr. Th. H. van de Kwast en Prof. Dr. A.C. Drogendijk voor het zitting nemen in de promotiecommissie.

Dr. J. Stoker voor zijn begeleiding van en bijdrage aan dit onderzoek.

Dr. W.R. Schouten voor het mogelijk maken van de patiëntgebonden studies.

Drs. J.C. den Hollander voor de hulp bij het interpreteren van vele preparaten.

Drs. H. Pieterman met name voor zijn hulp bij het opstarten van de studie.

Drs. J.W. Kuiper en Drs. H.W. Slis voor het helpen opzetten van de MRI-studie van de vrijwilligers.

Dr. C. van Kuijk voor zijn steun en waardevolle adviezen.

Drs. R. van Rijn voor het kritisch lezen van het manuscript en voor zijn waardevolle opmerkingen.

Andries Zwamborn voor de lay-out en voor het maken van de grafische tekeningen, die onmisbaar zijn bij de interpretatie van met name de MR beelden.

Teun Rijsdijk voor de foto's van hoge kwaliteit, die voor dit onderzoek essentieel zijn.

Dick van Kempen (Philips Medical Systems) voor het vervaardigen van de MRI spoel.

Frank van der Panne voor het fotograferen van de PA-preparaten.

Kees Entius en Jan Vellekens voor het vervaardigen van de anatomische coupes.

Alle MRI laboranten, met name Olga de Boer, Conny Planken, Bert van Heerebeek en Hanneke Kamminga, voor het helpen opzetten van het MRI-protocol en de hulp bij de onderzoeken.

Alle medewerkers van de afdeling Radiologie voor hun steun.

CURRICULUM VITAE

De schrijver van dit proefschrift werd geboren op 2 april 1962 te Guliana, Pakistan. Sinds 1977 is hij woonachtig in Nederland. Na het behalen van het VWO diploma aan het scholengemeenschap Johan de Witt te Scheveningen, werd in 1984 gestart met de studie Geneeskunde aan de Erasmus Universiteit Rotterdam. In 1990 werd het arts-examen behaald.

Hierna werd voor enkele maanden gewerkt als arts-assistent op de afdeling Chirurgie in het Schieland Ziekenhuis te Schiedam. In 1991 werd gestart met de opleiding tot radioloog op de afdeling Radiologie in het Academisch Ziekenhuis Rotterdam-Dijkzigt (Hoofd: Prof. Dr. H.E. Schütte). De opleiding tot radioloog zal in september 1996 worden afgerond.